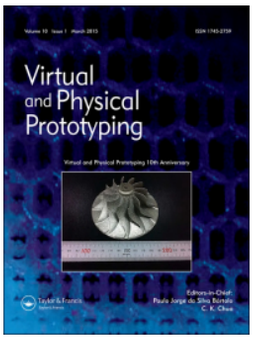

Virtual and Physical Prototyping

ISSN: 1745-2759 (Print) 1745-2767 (Online) Journal homepage: www.tandfonline.com/journals/nvpp20

A review of direct ink writing of polymer derived ceramics

Victoria Bishop, Saket Chand Mathur, Nhu Nguyen, Bhisham Sharma, Mary Drouin, Bin Li, Cheol Park & Wei Wei

To cite this article: Victoria Bishop, Saket Chand Mathur, Nhu Nguyen, Bhisham Sharma, Mary Drouin, Bin Li, Cheol Park & Wei Wei (2025) A review of direct ink writing of polymer derived ceramics, Virtual and Physical Prototyping, 20:1, 2499938, DOI: 10.1080/17452759.2025.2499938

To link to this article: https://doi.org/10.1080/17452759.2025.2499938

Published online: 18 May 2025.

VIRTUAL AND PHYSICAL PROTOTYPING
2025, VOL. 20, NO. 1, 2499938 (45 pages)
https://doi.org/10.1080/17452759.2025.2499938

Taylor & Francis
Taylor & Francis Group

REVIEW ARTICLE

OPEN ACCESS Check for updates

A review of direct ink writing of polymer derived ceramics

Victoria Bishop[a], Saket Chand Mathur[b], Nhu Nguyen[b], Bhisham Sharma[a], Mary Drouin[c], Bin Li[b], Cheol Park[d] and Wei Wei[a]

[a]Mechanical and Aerospace Engineering Department, Michigan Technological University, Houghton, MI, USA; [b]Mechanical Engineering Department, Wichita State University, Wichita, KS, USA; [c]Spirit AeroSystem, Wichita, KS, USA; [d]Advanced Materials and Processing Branch, NASA Langley Research Centre, Hampton, VA, USA

ABSTRACT

With the growing demand for materials capable of withstanding extreme temperatures and pressures, ceramic components with exceptional corrosion resistance and reliable mechanical properties have experienced a significant surge in demand. However, traditional ceramic forming methods involve high-temperatures and energy-intensive processes that often struggle to produce complex parts or composites efficiently. Polymer-Derived Ceramics (PDCs) offer a transformative solution by using polymeric precursors that can be converted into a wide variety of silicon-based and non-silicon-based ceramics through heat treatment. The polymeric nature of PDC precursors enables the fabrication of geometrically intricate components using conventional polymer-forming techniques at significantly lower processing temperatures. Furthermore, PDCs are well-suited for additive manufacturing (AM), allowing the production of complex structural and functional components through cost-effective, low-temperature processes. By leveraging the diverse properties of PDC materials – each with unique advantages and limitations – manufacturers can optimise performance for specific applications. This review provides an overview of the types of PDCs developed to date and their broad range of applications. Specifically, it delves into the Direct Ink Writing (DIW) process, exploring its rheological requirements and the critical role of fillers in tailoring the rheological properties of polymeric precursors to meet the specific demands of DIW.

ARTICLE HISTORY
Received 24 February 2025
Accepted 11 April 2025

KEYWORDS
Polymer-derived ceramics; additive manufacture; direct ink writing

1. Introduction

1.1. What are polymer-derived ceramics?

Polymer-derived ceramics (PDCs) represent an innovative class of materials characterised by exceptional high-temperature stability, distinctive semiconductive, electrical, and optical properties, superior corrosion and oxidation resistance, and robust mechanical strength [1]. PDCs are designed to simplify the production of silicon- and non-silicon-based ceramics by eliminating the need for high-temperature sintering methods. This approach enables greater flexibility in the geometry, composition, and functionality of components, allowing for the use of polymer-forming techniques in their fabrication [2]. All PDCs follow a similar four-step process as outlined in Figure 1 polymer synthesis, the forming or shaping of the precursor, a crosslinking reaction to form a green body, and the pyrolysis of the green body [2,3].

Polymer precursors for PDCs encompass a diverse range of organosilicon and non-organosilicon polymers, synthesised through various chemical reactions tailored to their specific structures. Hydrosilylation of unsaturated polymers is a widely used method for producing silane and siloxane polymers, which are commonly employed as preceramic materials [6,7]. Customised polymers can also be designed to produce precise microstructures, controlled porosities, and tailored properties [2,8]. A variety of commercial polymer precursors are now available, spurring extensive research into their influence on ceramic structures and potential applications. These precursors can be synthesised using techniques suitable for both liquid and solid polymers, offering a significant advantage over traditional ceramic manufacturing methods. Liquid precursors, in particular, are compatible with conventional plastic-forming techniques such as thin film production, template moulding, injection moulding, and blowing processes [3]. The development of liquid precursors was primarily motivated by the need for ceramic fibres manufactured through melt spinning, dry spinning or electrospinning; today these fibres are sought after for their reinforcement capabilities in composites and felts [9,10]. Recently, liquid precursors

CONTACT Wei Wei wwei4@mtu.edu Mechanical and Aerospace Engineering Department, Michigan Technological University, 1400 Townsend Drive, Houghton, MI 49931, USA

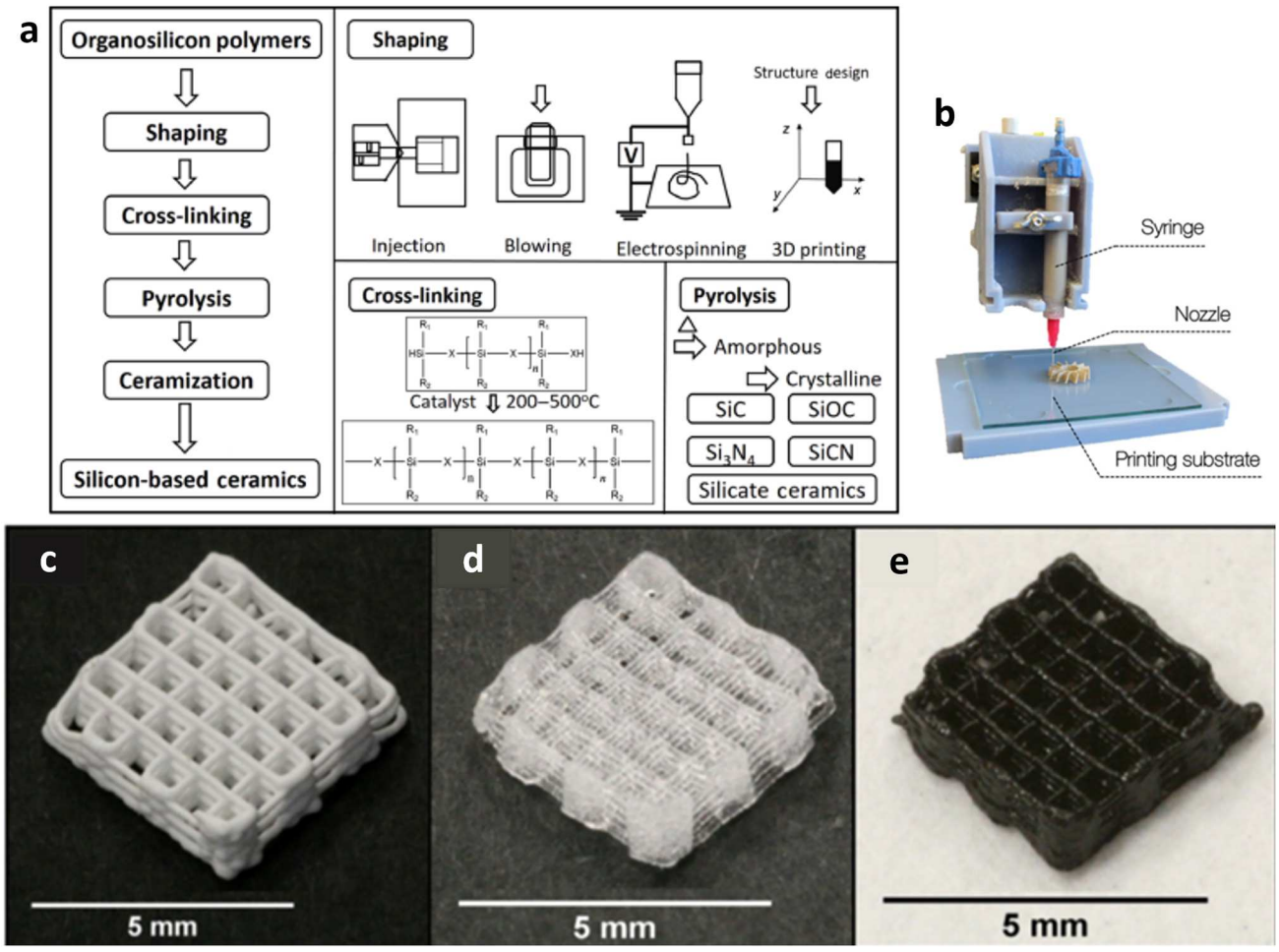

Figure 1. Polymer Derived Ceramic manufacture process involving Direct Ink Writing (DIW). (a) An overview of the manufacturing process and the four steps involved. Reproduced under terms of the CC-BY license [3]. (b) An example of the DIW shaping process for PDCs. Reproduced with permission [4]. Copyright 2015, Wiley. (c) A body as printed from the DIW process, (d) A crosslinked or green body, and (e) A pyrolyzed ceramic body. Reproduced with permission [5]. Copyright 2016, Journal of the European Ceramic Society.

have been integrated into additive manufacturing (AM) techniques for vat polymerisation methods such as stereolithography and digital light processing, and additionally for fused deposition modelling, direct ink writing, and binder jetting. These methods enable the fabrication of complex structures that would otherwise be unattainable, making this a key area of ongoing and future research [11,12].

Once the structure is formed, the preceramic polymer precursor undergoes a curing process, which typically involves heat treatment to establish crosslinking bonds, transforming the material into a rigid green body. In cases where the material is sufficiently transparent, UV light can also be employed to induce crosslinking, a step that can be integrated into the forming process in certain AM techniques [13–16]. The thermal curing process generally occurs below the polymer's degradation temperature and can be accelerated with the use of a catalyst [17]. Pyrolysis, or ceramization, transforms the preceramic polymer into a ceramic by subjecting the green body to elevated temperatures – typically between 800°C and 1800°C – under an active or inert atmosphere. During this process, volatile components such as -CH_3 and -H are released as gaseous byproducts, leaving behind an inorganic ceramic structure. However, the removal of these volatiles can introduce challenges, including shrinkage, thermal stresses that may lead to cracking, and occasionally, undesired porosity in the final ceramic [18–20]. Minimising these effects is essential to ensure the production of precise, high-quality structures that meet the requirements of their intended applications. Such applications have included structural components in the form of ceramic fibres for use as reinforcement of composites [9,21,22]; ceramic matrix composites for the automotive and aerospace industries [23–25]; coatings [18,26]; joints [27,28];biomedical devices [29]; and as

components in sensors [3,13,30], batteries [31–35], and electromagnetic wave absorbers [36–38].

1.2. What is direct ink writing (DIW)?

Owing to their numerous advantages, PDCs have emerged as a highly promising material system for AM applications [39]. AM utilises digital 3D design data to build components layer by layer, facilitating the creation of customised functional architectures with adjustable chemical compositions at the micro- and molecular scales [11,40]. The AM processes applied to PDCs encompass a range of techniques, including Direct Ink Writing (DIW).

DIW, also referred to as robocasting, involves the extrusion and deposition of a viscous ink or paste containing fine solid particles onto a substrate under applied pressure, enabling the fabrication of three-dimensional structures. DIW offers several advantages, including cost-effectiveness, faster printing speeds compared to vat-polymerisation methods such as stereolithography and two-photon polymerisation of materials with similar material loading compositions, a wide printing area, and a simple printing setup, making it a highly appealing choice for diverse applications [11,41]. However, the successful fabrication of desired shapes using DIW is highly dependent on the rheological properties of the ceramic ink. These properties must meet specific criteria, including appropriate yield stress, storage modulus, viscosity, and elasticity, to ensure optimal performance during the printing process [11,39]. Despite these challenges, DIW has gained increasing popularity in the field of ceramic printing. Its versatility has been demonstrated through the production of a wide array of structures, such as magnetic separation tools [13], electrodes [42], composite structures [43], bioengineering constructs [44], and components resistant to high temperatures and corrosion [45]. PDC components fabricated through DIW are utilised across a wide range of sectors, including aerospace, electronics, biomedical engineering, chemical processing, and environmental engineering. This integration offers remarkable opportunities for the additive manufacturing of ceramic-based components, characterised by their tailored properties, complex geometries, and superior performance. Such advancements are driving innovation and fostering technological progress across numerous industries [11,13,39,42–45].

1.3. Methods for direct ink writing of polymer-derived ceramics

Optimising the rheological properties of PDC-derived inks for DIW presents a considerable challenge. PDC precursors frequently lack the rheological characteristics required to maintain shape fidelity after extrusion in the DIW process. Additionally, in some instances, they may fail to meet the specific mechanical, electronic, or thermal performance criteria needed for particular applications [46]. To overcome these challenges, the incorporation of rheological modifiers, or 'fillers', plays a vital role in maintaining the shape fidelity of extruded inks. The choice of these modifiers is carefully tailored to the desired composition and application of the final ceramic product, ranging from solid ceramic materials for mechanical reinforcement [47,48] to polymers for biologically-inspired materials [49].

The behaviour of individual filler materials can significantly vary during heat treatment, impacting the final properties of the printed part. Some fillers remain chemically inert, while others may react with PDC precursors or decompose, leaving the ceramic composition unchanged. These effects are influenced by the selected PDC precursor, heat treatment parameters, and the process duration and atmosphere. Furthermore, fillers can impart beneficial functional properties to the final ceramic that are not inherent to the original PDC. For instance, Shibuya et al. demonstrated that incorporating vapour-grown carbon fibres enhances the electrical conductivity of porous silicon oxycarbide ceramics while simultaneously providing mechanical reinforcement [50]. Alternatively, functional properties can be achieved through the chemical modification of PDCs during heat treatment, facilitating the production of ceramics with enhanced high-temperature stability [51]. The wide range of applications, techniques for modifying PDCs, and the variety of fillers constitute a dynamic area of research that has been extensively explored in the existing literature [51–53].

1.4. Contents of this review

This review is intended to provide an overview of the state of the art in the field of DIW as a manufacturing method for precursor-based ceramics. To this end, the fundamental aspects of PDCs will be highlighted, including an overview of the types of ceramics that have been produced through precursor methods, crosslinking methods for these materials, the importance and effect of pyrolysis on the ceramic product, and an overview of the current applications for PDCs, independent of manufacturing method. Following this section, the current status of DIW will be analyzed, providing a comparison of this AM method to other existing methods specifically used for shaping PDCs, and explaining the fundamental properties that are critical for developing PDC feedstock inks. Finally, the current state-of-the-art

in DIW of PDCs utilising fillers as modifiers to achieve printability will be discussed, including the different types of fillers that can be added and the effect of these fillers on the printability and ceramic product. Finally, the future work in this field will be summarised.

2. Polymer-derived ceramics

Although a relatively recent innovation, PDCs offer distinct advantages over traditional metals in several critical areas. One of their standout benefits is exceptional design flexibility, enabling the fabrication of complex geometries that are unattainable with conventional metals or ceramic sintering techniques. This flexibility extends to their properties, which can be precisely tailored to meet specific application requirements. PDCs also feature a significantly lower density and weight than their metallic counterparts, making them highly desirable for applications where weight reduction is a priority. Furthermore, their production, particularly for intricate shapes and small-scale manufacturing, is more cost-effective than traditional metal fabrication, providing an economically attractive alternative. In addition to these benefits, PDCs exhibit excellent chemical resistance and biocompatibility, making them well-suited for sensitive applications across a range of industries [54].

2.1. Types of PDCs

PDCs can be classified based on their precursors and the desired composition following pyrolysis, with increasing specificity as additional criteria are applied. At the broadest level, PDC precursors are categorised into silicon-containing polymers and non-silicon-containing polymers [55]. Silicon-containing polymers – organosilicon polymers illustrated in Figure 2 – are further classified based on their compositional elements and the resulting structures formed after pyrolysis. The resulting polymer-derived ceramics are categorised as binary, ternary, quaternary, or higher-order systems, depending on the number of constituent elements incorporated [3]. Non-silicon-based ceramics, such as AlN, BN, and Ti-ceramics, just to name a few, have also been fabricated in binary and ternary forms using polymer precursors, employing a variety of specialised processing techniques [56].

2.1.1. Binary ceramics

Binary PDCs produce ceramics composed of two elemental components, most commonly silicon paired with carbon or nitrogen, although binary non-silicon ceramics are not restricted to these elements. Prominent examples of silicon-based PDCs include silicon carbide (SiC) and silicon nitride (Si_3N_4). SiC is commonly synthesised from polysilanes or polycarbosilanes (PCSs) with the basic structure shown in Figure 3(a), with the choice of precursor determined by the specific manufacturing process and the desired properties of the final product [9]. Recent advancements in commercial polycarbosilanes have significantly improved the feasibility of fabricating near-stoichiometric SiC ceramics using PDC methods [57]. The desirable properties of SiC ceramics, such as exceptional wear resistance and thermal stability, make them highly attractive for manufacturing [11,58]. Precursor polymers for SiC were first developed in the 1970s to produce high-quality SiC fibres for use as reinforcing materials in composites. Polycarbosilanes synthesised from dimethylchlorosilane historically yielded a viscous liquid that could be spun and dried to form SiC fibres, in a form pictured in Figure 3(b) [9]. Zunjarrao et al. observed that bulk SiC fabricated from commercially available PCS exhibits an amorphous structure upon initial pyrolysis at temperatures of at least 900°C, even after a 4-hour hold, with only a few small crystalline SiC domains present. The crystallinity of the bulk SiC structures increased with increasing pyrolysis temperatures. Intermediate microstructures annealed at elevated temperatures displayed amorphous regions surrounding crystalline SiC tetrahedral structures, which expanded further at annealing temperatures up to 1650°C, generating large and distinct crystalline domains appearing in Figure 3(e). Under optimised pyrolysis conditions – 1150°C with a 1-hour hold – the average crystalline size was approximately 3 nm [57]. Thin layers, such as coatings applied through spin or dip coating methods, exhibit microstructures similar to those of bulk SiC. At low pyrolysis temperatures, the microstructure consists predominantly of amorphous SiC, with occasional domains of free silicon. These silicon domains result from the rapid effusion of gaseous organic compounds during initial pyrolysis, which diminishes as the process progresses [59]. The microstructure of fibrous SiC produced through the melt-spinning of preceramic polymers is influenced by the precursor type and grade. Ceramic-grade Nicalon fibres, derived from melt-spun polymer precursors, exhibit a significant presence of β-SiC, along with some α-SiC domains and crystalline regions concentrated on the fibre surface. Heat treatment promotes growth in the size of the α-SiC particles. In contrast, standard-grade SiC fibres produced using the same process contain lower amounts of β-SiC and transition to nearly pure α-SiC upon heat treatment [60]. Innovative heating methods for curing and pyrolysis have been explored to reduce the lengthy production times associated with SiC ceramics. Microwave heating has demonstrated the ability to uniformly increase the

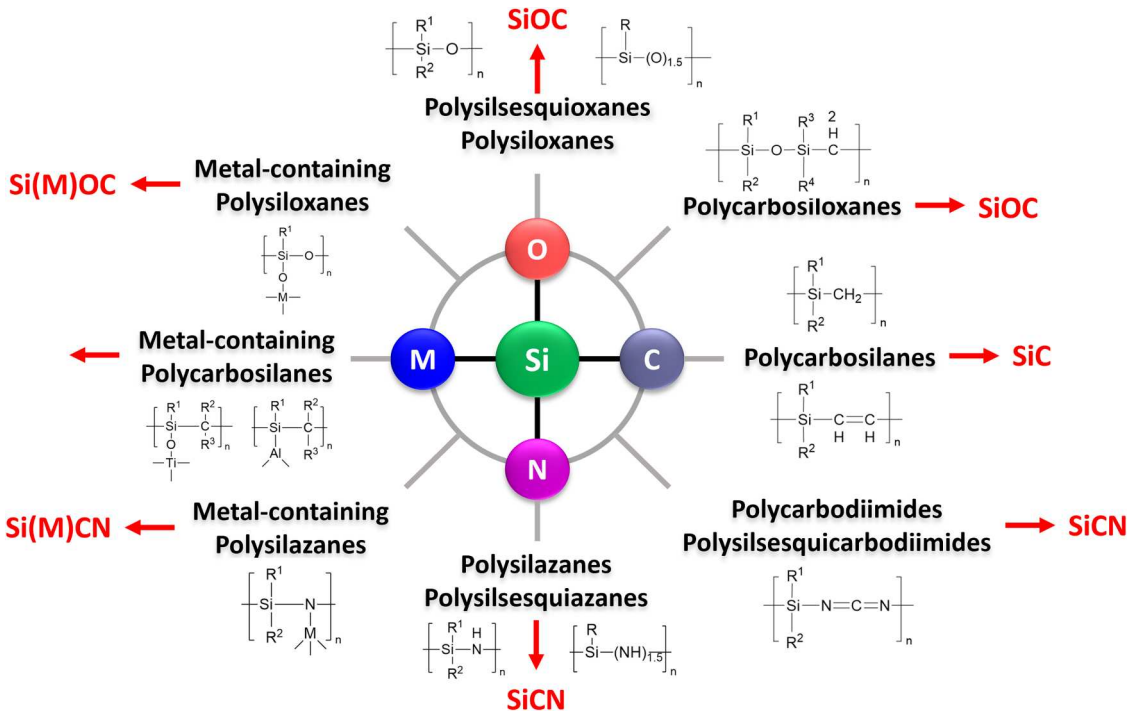

Figure 2. The classes and basic structures of organosilicon polymers that have been used as preceramic precursors. The typical binary, ternary, and quaternary ceramics are shown, based on the precursor organosilicon that generated them. Reproduced under terms of the CC-BY license [2]. Copyright 2015, Mera, G. et al, MDPI.

temperature of preceramic materials, ensuring complete curing and resulting in reduced mass loss during pyrolysis. However, this approach requires the incorporation of microwave absorbers, such as carbon nanotubes, which have been shown to be highly effective when used with the commercial polycarbosilane precursor SMP-10 [61]. Photothermal heating using a Xenon flash lamp was employed to heat a cured commercial preceramic in incremental stages. Following the initial exposure, the absorbed energy raised the material's temperature to 1100°C, which then cooled to 75°C within a minute through conduction to the substrate. Subsequent exposures progressively increased the temperature, reaching a peak of 1360°C, with reduced temperature decay after each cycle. These brief, high-intensity exposures facilitated the transformation of the polymer into SiC ceramics with crystalline domains while minimising oxidation due to the short heating durations, resulting in purer ceramic materials [62].

Si_3N_4 is synthesised from polysilazanes or other low-carbon organosilicon polymers under inert nitrogen or ammonia atmospheres – conditions that promote the removal of carbon and oxygen from the polymer and enable its conversion into Si_3N_4 crystalline structures. In contrast, this transformation does not occur in argon atmospheres, which instead causes the formation of silicon carbonitride (SiCN) [63–65]. An alternative approach to producing Si_3N_4 from polymer precursors involves the decomposition and crystallization of SiCN at elevated temperatures, resulting in a more thermally stable and crystalline form of Si_3N_4. Bao et al. investigated several types of polycyclodisilazane as precursor polymers for this process, employing three distinct reaction methods to achieve variations in the polymer structure and molecular weight. The pyrolytic yield from these methods was significantly affected by the molecular weight and the presence of Si-H and N-H reactive groups. Polymers with higher molecular weights and a higher number of reactive groups exhibited increased ceramic yields and produced greater amounts of Si_3N_4 [66]. Structurally, Si_3N_4 exhibits trends similar to those of SiC ceramics. At low pyrolysis temperatures, Si_3N_4 remains predominantly amorphous, with only small crystalline Si-N domains present. The amorphous structure typically persists up to approximately 1200°C, after which crystalline Si_3N_4 domains begin to form in greater quantities and continue to grow until the temperature reaches 1600–1700°C. At these elevated temperatures, the structure transitions entirely to crystalline Si_3N_4, with no amorphous phase remaining. However, the complete removal of carbon is challenging, leading to the retention of small amounts of β-SiC in crystalline form within the structure, even after further heat treatments [63,66]. This residual carbon complicates the

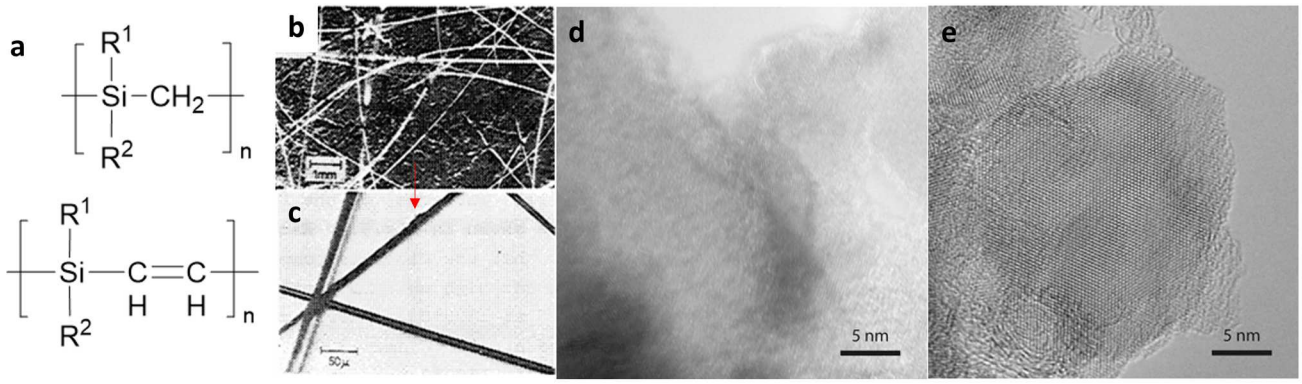

Figure 3. (a) Structure of polymers that generate SiC. (b) Organosilicon fibres in spun form. (c) SiC fibres as pyrolyzed from spun organosilicon. Reproduced with permission [9]. Copyright 1975, The Chemical Society of Japan. (d) TEM image of microstructure of SiC pyrolyzed at 900°C revealing amorphous regions, (e) TEM image of microstructure of SiC pyrolyzed at 1650°C revealing large crystalline regions. Reproduced with permission [57]. Copyright 2013, The American Ceramic Society.

production of pure, homogeneous Si_3N_4. However, its exceptional oxidation resistance and ability to maintain high mechanical performance at elevated temperatures make it a highly desirable material for manufacturing applications [66].

2.1.2. Ternary ceramics

Ternary PDCs produce ceramics composed of three primary elements, with silicon as the dominant component, typically combined with oxygen, carbon, or nitrogen. Various polymer precursors have been developed in stoichiometric or near-stoichiometric ratios to fabricate silicon oxycarbide (SiOC) and silicon carbonitride (SiCN) ceramics. SiOC ceramics can be synthesised using a wide range of silicon-based polymers, including polysiloxanes, polysilsesquioxanes, and polycarbosilanes, many of which are commercially available and have been extensively evaluated. The phases present in the resulting SiOC ceramics remain consistent across different polymer types, depending solely on the Si-O-C ratio in the precursor [67]. The optimal phase structure for SiOC and other ternary ceramics consists of tetrahedral silicon ions bonded exclusively to the constituent elements – carbon and oxygen – while excluding Si-Si, C-C, and O-O bonds. Experimentally, however, this ideal crystalline structure has not been achieved, as SiOC remains amorphous when pyrolyzed below 1100°C. Consequently, two alternative approaches to define the phase diagram have been proposed [68,69]. The first defined structure consists of $SiC_xO_{2(1-x)}$ domains, based on a combination of SiO_2 and SiC tetrahedra. The second and more widely observed phase domain consists of amorphous SiO_xC_{4-x} where $x = 1–3$, resulting in mixed $SiOC_3$ SiO_2C_2, SiO_3C, and free carbon sp^2 bonds that depend on the amount of carbon in the precursor and the pyrolysis conditions; this amorphous

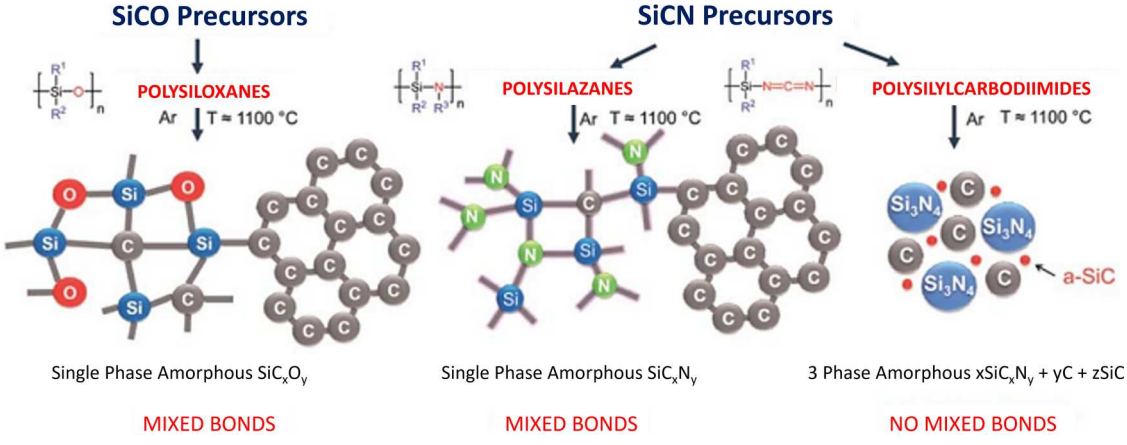

Figure 4. Structure of SiOC and SiCN PDCs based on the precursor type. SiCO precursors are typically polysiloxanes, generating single-phase amorphous SiC_xO_y with mixed bonds. SiCN precursors include polysilazanes which generate single phase amorphous SiC_xN_y with mixed bonds, and polysilylcarbodiimides that generate 3-phase amorphous $Si_3N_4 + yC + zSiC$ without mixed bonds. Reproduced with permission [67]. Copyright 2013, Royal Society of Chemistry.

structure is demonstrated in Figure 4 [69,70]. The carbon composition and phase play critical roles in determining the thermal and electrical properties of SiOC ceramics, which are directly influenced by the choice of polymer precursor. An increase in the sp^2-bonded carbon content enhances the thermal stability by improving the resistance to crystallization and suppressing the carbothermal reactions that lead to oxidation. Additionally, it modifies the viscoelastic behaviour of the material and increases the specific surface area of the carbon-rich regions [68,71]. An increase in the free carbon content, caused by changes in the environment or the precursor, also decreases the electrical resistivity of the ceramic, producing more conductive materials that could have unique applications in electronics [72]. Upon crystallization, SiOC ceramics split into distinct phases consisting of β-SiC embedded in amorphous SiO_2 domains. This crystallization effect occurs at lower annealing temperatures as compared to other ternary and quaternary ceramics, but also serves to increase the number of conductive domains [72,73]. Photothermal heating significantly reduces the pyrolysis time and produces samples lacking SiO_2 domains, suggesting diminished oxidation that enhances thermal resistance. This reduction in oxidation positively affects the electrical properties, making this pyrolysis approach beneficial for enhancing SiOC ceramics' electrical characteristics for supercapacitors and improving thermal properties for coatings [62].

SiCN ceramics are produced using Si-based polymers that include silicon (Si), carbon (C), nitrogen (N), and hydrogen (H) in diverse structural forms. Predominantly, these polymers are polyvinylsilazanes, along with their cyclic or linear variants, or polysilylcarbodiimides. The pyrolysis of these polymer species yields SiCN ceramics; however, the resulting microstructure varies depending on the specific type of polymer used [8,65,67]. Polyvinylsilazanes are one of the most commercialised polymer precursors for producing SiCN ceramics, with a wide range of options available that typically differ in the ratio of Si-vinyl and $Si\text{-}CH_3$ bonding that is in the compound [74,75]. Vinyl-precursors yield a distinct microstructure within the SiCN ceramics that favours the creation of single-phase amorphous SiC_xN_y where $x + y = 4$ and Si atoms are bonded to C, N, and free carbon that is sp^2 bonded [8,67,76,77]. As compared to vinyl-precursors, polysilylcarbodiimides form a different, three-phase amorphous system due to the nature of the C-N bonds in the polymer, although they are still considered as SiCN precursors. The three-phase system formed by polysilylcarbodiimides is composed of mostly Si_3N_4 clusters, dispersed with α-SiC and free carbon clusters that do not contain any mixed bonds [67,68]. These two different phase structures are compared in Figure 4. The impact of differing phase structures on the properties of SiCN ceramics has not been extensively explored in direct comparisons, largely due to the challenge of correlating properties with phase composition due to its complexity. The formation of crystalline structures in the pyrolyzed ceramic, along with its thermal stability and electrical properties, are significantly influenced by the phase composition, making these characteristics most susceptible to alteration [68]. The crystallization of SiCN ceramics by pyrolysis at higher temperatures results in greater phase separation and increases the amount of β-SiC as the major crystalline phase. Crystallization of these ceramics leads to higher electrical conductivity, an effect that is shared with carbon-rich SiC ceramics [78]. The mechanical properties and thermal stability of SiCN ceramics are improved by the presence of fillers, which can reinforce the microstructure and has the additional effect of allowing several different manufacturing methods, including additive manufacturing [56,79–82].

2.1.3. Quaternary ceramics

Quaternary PDCs produce Si-based ceramics composed of four elemental components, typically including silicon along with boron, carbon, nitrogen, oxygen, or aluminum, although other elements may also be incorporated. Ceramics with the general structure SiMCN or SiMCO, where M represents boron, aluminum, or a transition metal, are particularly desirable for their exceptional performance under extreme conditions and their distinctive electrical and magnetic properties [11,58,82].

The production of silicon oxycarbonitride (SiCNO) ceramics is relatively straightforward among quaternary ceramics, as they do not require any extra elements beyond those found in commonly accessible precursors. Historically, SiCNO has been formed by curing polycarbosilazane precursors under oxygen or water vapour to introduce oxygen into the cured body, then pyrolyzed them under inert atmospheres into bulk or fibre forms. The microstructure from this process is amorphous when pyrolyzed below 1400°C under both nitrogen and argon atmospheres. Crystallization of this precursor was noted to begin between 1400 and 1600°C, depending on the atmosphere type, with the mechanical and semiconductive properties heavily dependent on the crystalline state of the product [83]. Ryu et al. extended this work, determining that the N/O ratio had the largest effect on the resistivity of SiCNO manufactured with a polysilazane precursor, and confirmed that the amorphous ceramic is a semiconductor until 1300°C [84]. Yang et al. developed a method to produce SiCNO 1D nanofibers using a composite polysiloxane precursor

with urea acting as both the nitrogen source and a critical component in fibre formation, producing fibres with an amorphous microstructure and high surface area [85]. Polysilazane precursors have also been used to yield amorphous SiCNO nanoparticles with mixed structures containing Si_3N_4, SiO_2, and graphitic carbon with a chemical and electrical properties acceptable for use in energy storage devices [31]. In bulk structures, the mixed bonding present in SiN_xC_{4-x} and SiO_xC_{4-x} has been noted to enhance structural stabilisation as compared to SiOC ternary ceramics. Despite this, the anticipated temperature stability of these quaternary ceramics is comparable to that of SiOC and SiCN ceramics, likely due to the mixed microstructure they exhibit [75]. Copolymer processes using polysilazane and polysiloxane precursors have also been recently developed to modify the N/O ratios to determine specific properties and tailor the viscosity more effectively for 3D printing processes, albeit with a low ceramic yield [41].

Silicon boron oxycarbide (SiBCO) and silicon boron carbonitride (SiBCN) stand out as particularly promising silicon-based PDCs for high-temperature applications. They are capable of performing without decomposition, serving as environmental protection materials at temperatures up to 2000°C [23,77,82,86,87]. The manufacturing of PDCs that contain boron has traditionally been achieved through two primary methods: the first method involves the copolymerisation of monomers that already contain the necessary boron element; the second method uses single-source precursors to develop specialised compounds such as borazines, polyborosilazanes, and polyborosilylcarbodiimides [86,88]. The copolymerisation of monomers that contain the necessary components for the desired ceramic is a simple method to obtain the necessary precursors; however, precursors developed in this way tend to decompose into binary parts from the mixed monomers, lowering the performance at high temperatures [88]. The concept of modifying established polysiloxanes and polysilazanes to create polyborosiloxanes or polyborosilazanes has gained traction, particularly given the availability of commercial precursors. The process yields more homogenous microstructures with improved thermal stability and associated properties, as outlined in existing studies [86,88,89]. The structure of the SiBCO/SiBCN(O) ceramics generally remains amorphous until heat treatment at 1400°C, at which point β-SiC and SiO_2 begin to form. Prior to the onset of crystallization, the structure contains mixed tetrahedral units of SiC_xN_{4-x} and SiC_xO_{4-x} accompanied by mixed B-N-O and B-N bonding, with the amount of O_2 in the system decreasing above 1600°C due to the carbothermal reaction resulting in crystallization. This system is still incredibly stable, showing little to no decomposition in air or argon when exposed to temperatures of 1580°C [87]. Ideal SiBCN ceramics that do not contain elemental oxygen defects are more thermally stable when they are composed of mixed SiC-C-BN phases, but realistically, the microstructure falls within the potential four-phase domain illustrated in Figure 5. These phases are most likely organised into amorphous Si-C-N domains that have similar structures to those of the SiCN phases, with inclusions of B-C-N domains of intercalating carbon and boron nitride that impede the decomposition of the Si-N component [77,86]. The onset of the crystalline structures in SiBCN is counteracted by the incorporation of boron, increasing the stability of the structure in air and the resistance to oxidation at high temperature, like emphasised in Figure 5 [86]. The incorporation of boron acts to restrict the mobility of the grain boundaries, thereby suppressing crystallization. The effectiveness of this process is dependent on the concentration of boron within the material [90].

Silicon aluminum oxycarbide (SiAlCO) and silicon aluminum carbonitride (SiAlCN) share many similarities in terms of their synthesis to boron-containing quaternary ceramics. The inclusion of aluminum in SiAlCN enhances its corrosion and oxidation resistance compared to SiCN and SiBCN by reducing oxygen diffusion under oxidative conditions, thereby limiting the formation of SiO_2 inclusions. These inclusions can also cause the growth of Al_2O_3 phases that increase the thermal stability of the ceramic [91,92]. SiAlCN has excellent electrical properties at high temperature, and has been shown to maintain semiconductive properties between 650 and 900°C [93]. Liu et al. have demonstrated that the material exhibits elevated dielectric constants at increased temperatures, noting that both the AC conductivity and dielectric constant rise in conjunction with the pyrolysis temperature and as the free carbon content diminishes [94]. SiAlCN and SiAlCO ceramics can be manufactured by employing analogous methods used for quaternary materials containing boron, typically through the synthesis of polyaluminasilazanes or polyaluminasiloxanes. This is often achieved by reacting an existing polymer with an aluminum-containing compound [69,95]. Initially pyrolyzed into an amorphous state, SiAlCN contains mixed SiC_xN_{x-4} bonds, with increasing Al content favouring nitrogen rich $SiCN_3$ units, interacting with AlN_y ($y = 4,6$) units and reduced free carbon phases [95]. The SiAlCO structures are similar in that they contain mixed SiC_xO_{4-x} phases, but Al shows increased bonding to Si-O structures and thermally favourable AlO_4 units. Bik et al. reported that Al^{3+} cations also influence phase evolution

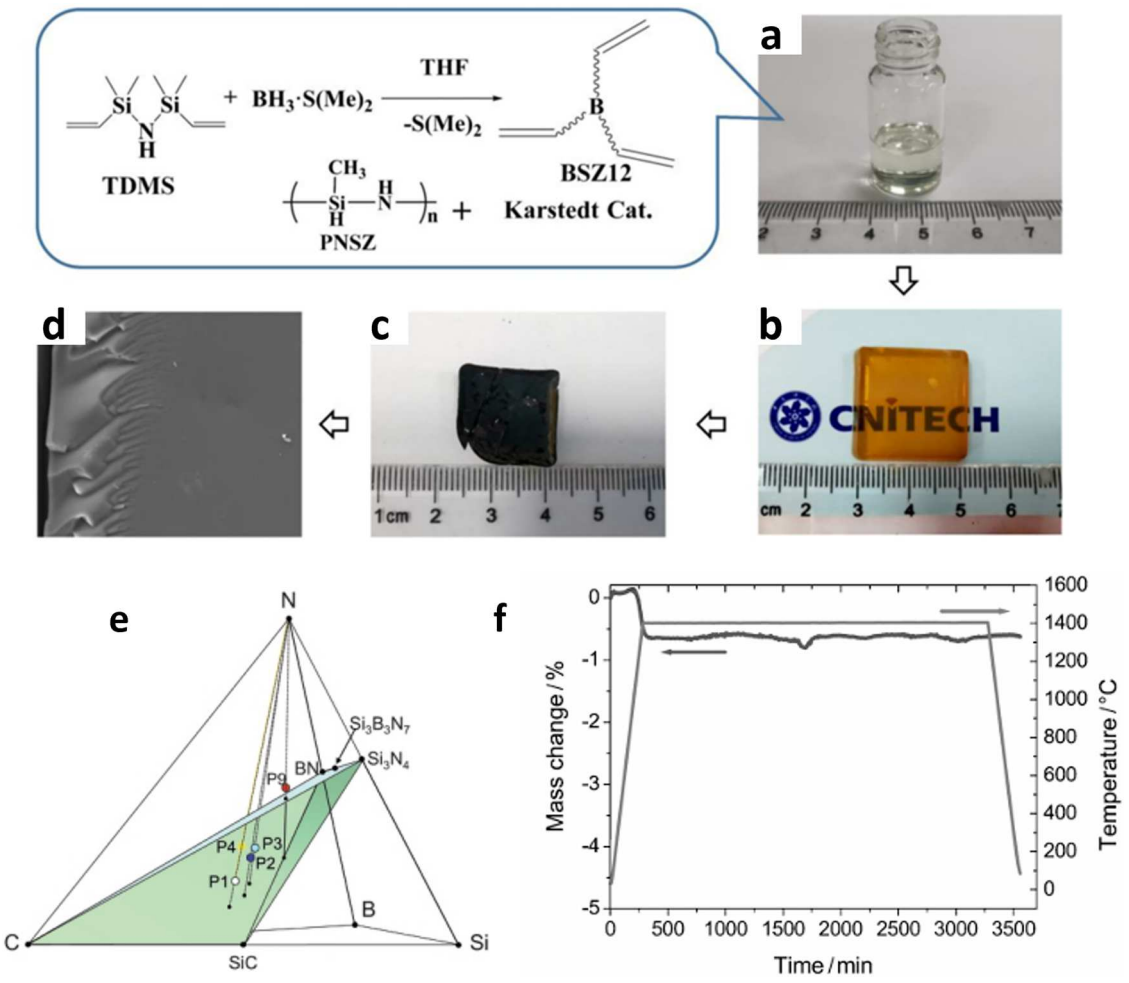

Figure 5. Composition, structure, and oxidation resistance of SiBCN ceramics. (a–d) manufacture of SiBCN ceramics, (a) Composition of preceramic polymer for generating SiBCN, (b) Cured body, (c) Pyrolyzed body showing shrinkage, and (d) SEM image of surface structure. Reproduced with permission [87]. Copyright 2022, Elsevier Ltd. (e) Phase separation in SiBCN ceramics under 0.1 MPa N_2 pyrolysis conditions where points P1–P4 and P9 represent the compositions of SiBCN derived from alternate polyborosilazanes. (f) Oxidation behaviour of SiBCN at 1400°C in air over 50 h. Reproduced with permission [86]. Copyright 2006, The Ceramic Society of Japan.

during the pyrolysis of SiAlCO. The polymer was observed to have less violent mass loss during pyrolysis, which resulted in homogenous structures with a reduced carbon content that is otherwise present in the SiOC and improved the thermal behaviour in the intermediate stages [69].

2.1.4. Non-silicon-based ceramics

PDCs have also been manufactured with non-silicon-based polymers, yielding a range of ceramic structures that include boron-nitride and aluminum nitride binary ceramics, as well as transition metal nitrides, carbides, and borides [26,56]. Boron Nitride (BN) ceramics have been developed from preceramic polymers based on borazine/polyborazylene and B-trichloro-/B-tri(methylamino)-Borazine/Poly[B-tri(methylamino)borazine] precursors. Generally, polymers derived from borazine, i.e. polyborazylene, are useful for creating monolithic structures using polymer forming methods that have a high ceramic yield but have a turbostratic morphology that results in brittle monoliths, although it can also be useful for infiltration methods that generate composites and nanotubes as highlighted in Figure 6(a). In contrast, poly[B-tri(methylamino)borazine] precursors, and their related polymers like poly(alkylamino)borazine, are excellent for melt spinning BN fibres due to their melt-processability [96–98]. Polyborazine is a highly adaptable polymer that can be manufactured from the reaction between ammonium sulphate ($(NH_4)_2SO_4$) and sodium borohydride ($NaBH_4$) following distillation and polycondensation. Matsoso et al. evaluated three different methods of processing for this product with the goal of obtaining hexagonal-BN (h-BN). Polyborazine can be pyrolyzed directly under inert atmosphere at 1400°C to yield amorphous BN structures, or with the addition of a crystallization agent, Li_3N, it can yield a

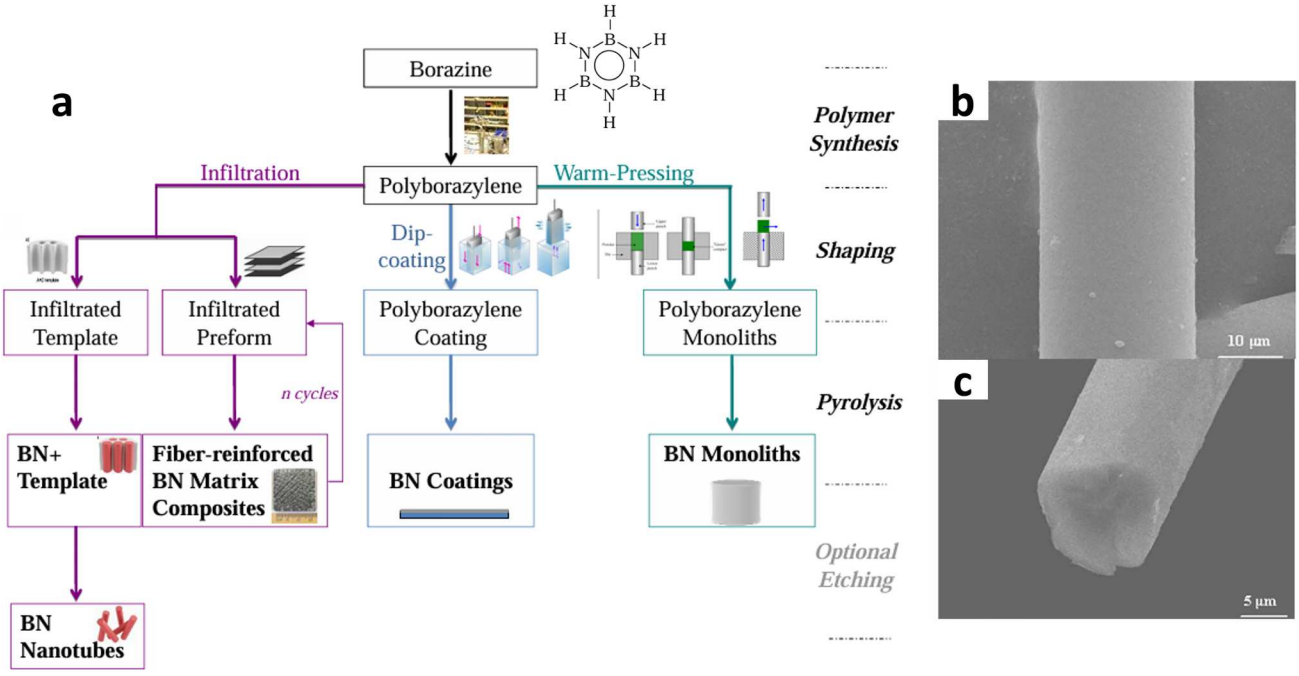

Figure 6. Potential structures manufactured from Borazine based precursors. (a) BN ceramics manufactured from borazine-based precursors, separated based on the shaping method. Reproduced under terms of the CC-BY license [96]. 2014, Samuel Bernard and Philippe Miele, published by MDPI. (b) polyborazylene polymer fibre prior to pyrolysis, and (c) BN ceramic fibre structure following pyrolysis. Reproduced with permission [97]. Copyright 2011, Elsevier.

mixture of h-BN and rhombohedral BN. Preference to produce h-BN can be increased by combining the preceramic precursor with gas pressure sintering methods, yielding a significant amount of h-BN that can be manufactured into BN nanosheets. The last approach involves atomic layer deposition (ALD), a straightforward technique that entails depositing a preceramic polymer followed by its transformation into dense boron nitride (BN) via thermal processing. ALD results in amorphous, turbostratic, or h-BN films depending on the substrate material, with the potential for use with templates to generate complex structures [21]. Recently, BN fibres have been manufactured from poly[tris(methylamino)borane] (PTMB) to yield BN fibres with mixed amorphous and unaligned h-BN microstructures following melt-spinning and pyrolysis with microstructures displayed in Figure 6(b and c). The alignment of the h-BN grains to radial microstructures through thermal treatment and stretching increased the Young's modulus and the tensile strength of the fibres [63]. BN ceramics manufactured with preceramic polymers are electrical insulators with low wettability and are capable of acting as high hardness coatings, being the second hardest material behind diamond, and in fibre form as reinforcing materials in composites due to high young's modulus and tensile strength [63,96,99,100].

Aluminum Nitride (AlN) ceramics obtained through precursor methods were initially developed during the second world war through the reaction of trimethyl aluminum with ammonia, creating an intermediate polymer material that was converted to AlN during heating [101]. Traditional methods of manufacturing AlN include high temperature and high-pressure powder sintering, carbothermal reduction reactions, and chemical vapour deposition [101,102]. More advanced precursor methods are required to produce high purity AlN due to its favourable properties; AlN is a chemically resistant ceramic with a large bandgap, high thermal conductivity, and piezoresistivity, which make it appropriate for a range of structural and electrical applications [101–104]. Current research has focused on developing polymer precursors that result in high purity AlN with few carbon and oxygen inclusions and defects. Liquid or solid precursors for AlN ceramics include poly[N-(alkylimino)alanes] or poly[N-(methylamino)alanes] which are manufactured using different processes. Liquid precursors such as poly[N-(alkylimino)alanes] are useful for dip coating substrates, although the ceramic yield of this polymer can be low depending on the alkyl chain length. For example, liquid poly[N-(isopropylimino)alane] was used to prepare 1D AlN nanostructures by infiltrating a template, the resulting 1D ceramic formed w-AlN nanorods pictured in Figure 7(a) as defined by the template [104]. Shimokawa et al. developed a liquid precursor from the reaction of

bis(trimethylsilyl)carbodiimide and aluminum tri-chloride. The pyrolyzed product had an amorphous microstructure until 800°C, after which point the hexagonal AlN diffraction peaks were observed under XRD, although with a ceramic yield of only ~20%. The ceramic yield and purity of the sample were improved by increasing the synthesis temperature of the polymer and increasing the amount of crosslinking, raising the ceramic yield to ~35%. Heat treatments up to 1800°C improved the purity of the sample and increased the AlN crystallinity [105]. Recently, researchers have attempted to simplify the reaction components, identifying the reaction between metal chlorides and hexamethyldisilazane (HMDS) as a sufficient precursor source for not only AlN, but also other transition metal nitride precursors through the pathways outlined in Figure 7(b). The products of this reaction and pyrolysis at temperatures between 800 and 1200°C yielded amorphous ceramics with mixed α-Al_2O_3 regions; at higher pyrolysis temperatures (~1600°C) the ceramic was a mixture of α-Al_2O_3 and AlN phases. Other metal chlorides reacted with HMDS, yielding precursors that could potentially be applied for gas phase deposition processes [106].

Titanium nitride (TiN), carbide (TiC), boride (TiB_2), and carbonitride (TiCN) are also among the non-silicon ceramics that can be produced from polymer precursors. Traditional methods for producing Ti-based ceramics typically involve high-temperature processes. These methods, while effective for creating limited but thermally stable and hard ceramics, are generally not favourable for producing fibrous materials [107,108]. The most straightforward methods of producing transition metal ceramics rely on well-developed reactions, such as the reduction of transition metal oxides with boron carbide (BC) and carbon, where the transition metal compound acts as an active filler to produce the desired ceramics. Utilising a precursor for BC, mixed with some amount of a transition metal oxide, high purity TiB_2 or ZrB_2 could be produced, potentially as a protective coating, albeit with low ceramic yield and formability [109]. A similar reaction also allows for the production of transition metal carbides and nitrides. Keller et al. utilised a carbon-based polymer, 1,2,4,5-tetrakis(phenylethnyl)benzene (TPEB), and TiH_2 mixture that could be pyrolyzed to form TiC or TiN nanoparticles. In this process, the polymer precursor acts a matrix and as a carbon source for the Ti to form TiC. Under nitrogen atmospheres, TiN is preferentially produced, although this method only produces nanoparticles regardless of the reactant ratios [107]. This method has also been used to produce a significant number of other Ti-based ceramics, that are not as formable as single source precursors, but are simplistic and have interesting electrical properties [110,111]. Single source precursors are also being developed to allow for the formation of more structures such as fibres and dense monoliths. The simplest single source polymers that can be decomposed into TiN are titanium amides, which provide TiN and organic products with low ceramic yields. Titanium nitride precursors with higher molecular weights derived from diamines produce high ceramic yields and, in the case of precursors containing more elemental carbon, potentially TiCN ceramics [112]. Polytitanosilazanes, synthesised through the reaction of polysilazanes and titanium amides, are desirable because they can be processed through melt spinning into fibrous forms or made into dense monoliths, yielding TiN/Si_3N_4 composites. The ceramic yield of mixed composites, although no longer pure, is higher than that of other single source precursors, but further work is required to develop improved precursors and ceramic products [113].

Further non-silicon ceramics that have been generated through polymer-precursor methods have included other high-entropy or ultra-high temperature ceramics (UHTCs) based on zirconium, hafnium, and niobium precursors [114,115]. Fabricating UHTCs through the polymer precursor method is attractive due to the reduced temperatures that are required, the polymer forming methods that are available, and the high control over the composition [115,116]. In particular, UHTCs are desired for their mechanical, chemical, and thermal properties; UHTCs have high melting points, high hardness, resistance to ablation, corrosion, and wear, thermal and electrical conductivity, and very good thermos-mechanical and thermos-chemical properties [116,117]. A common synthesis reaction utilised to obtain high-entropy carbides such as ZrC, HfC, and NiC is the polymerisation of MCl (M = Zr, Hf, Ni, etc) with a carbon source and chelating agent, involving a replacement reaction, a chelation reaction, and polycondensation [114,116,118–120]. This type of reaction is favourable due to the ability to electrospin the product into fibres, or to use as a component in composites [119]. The ceramic yield of such precursors, however, is very low, and high heat treatment temperatures are required to obtain crystalline products [116]. Further work is required to increase the yield of these precursors and to integrate them with AM methods.

2.2. Crosslinking and pyrolysis

2.2.1. Crosslinking of precursors

The crosslinking reaction during the curing process dictates many properties in the pyrolyzed ceramic such as

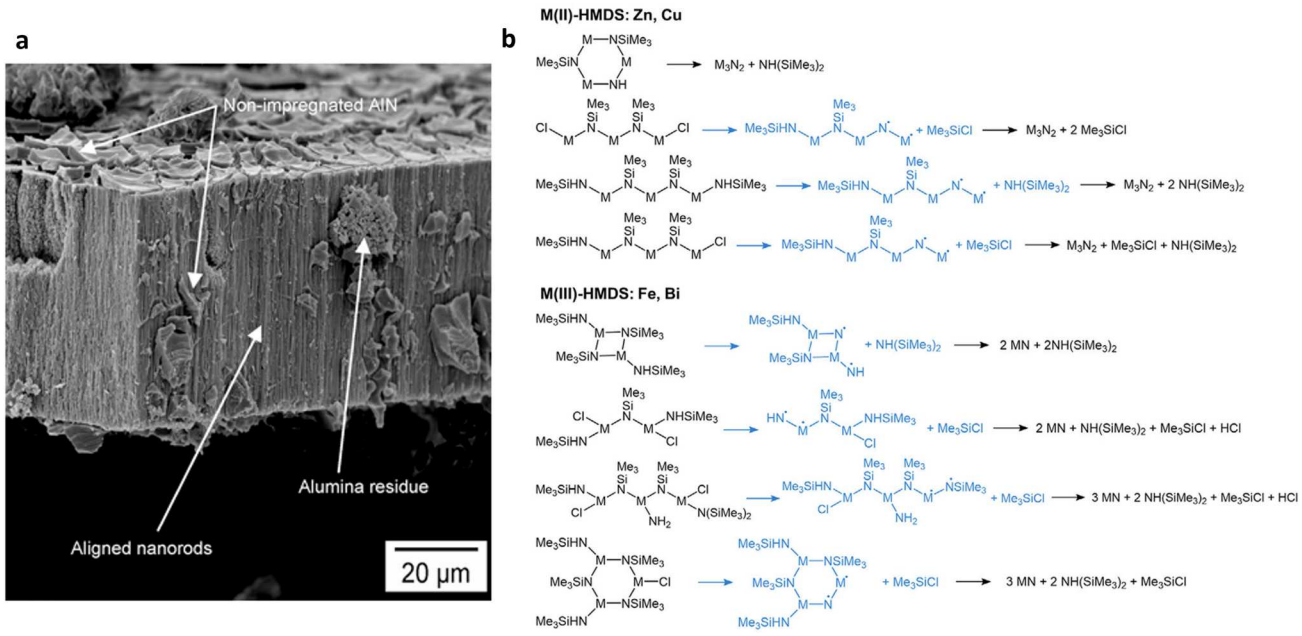

Figure 7. Potential of AlN ceramic through precursor or PDC methods. (a) AlN aligned nanorods generated by infiltration of template with poly[N-(isopropylimino)alane]. Reproduced with permission [104]. Copyright 2009, Elsevier. (b) Thermal decomposition pathways for transition metal PDC precursors. Reproduced with permission [106]. Copyright 2021, Wiley.

the converted mass and density, and higher degrees of crosslinking can also reduce the amount of fracture following pyrolysis [56,121]. These reactions vary depending on the polymer base and chain structure, altering for ring-like molecules versus chains [19]. The mechanisms for this process can be analyzed using a battery of tests that include combined Thermogravimetric-Fourier Infrared Transform (TG-FTIR) and Nuclear Magnetic Resonance (NMR) that reveal the types of bonds in the crosslinked polymer, and the groups released during the process [122]. The crosslinked polymer itself can be suitable for many applications depending on the mechanical properties, which are dependent on the crosslink density (the number of cross-links per unit volume in a polymer network).

2.2.1.1. Catalysts. To accelerate the crosslinking process, catalysts are frequently added to the formulations. When curing preceramic polymers such as polymethylhydrosiloxane (PMHS) and polymethylvinylsiloxane (PMVS), metallic catalysts such as Karstedt's catalyst and non-metallic catalysts in the form of peroxides are generally used. The cured product, a silicone rubber can have visual mechanical defects such as bubbles and cracks when Karstedt's catalyst is used. To reduce these defects, Derbin et al. provides an alternative, cis-[$PtCl_2(BnCN)_2$] [123]. The same group also worked on alternative non-metal catalysts, since peroxide-based catalysts such as dicumyl peroxide (DCP) require high temperatures for the crosslinking to begin. These catalysts also induce the formation of gaseous byproducts during the reaction, which can lead to change in dimension when used in additive manufacturing applications. They reported catalysts based on diazo compounds such azobisisobutyronitrile (AIBN) for the crosslinking of PMHS and PMVS [124].

Reschke and colleagues investigated the rheological properties and crosslinking dynamics of a low-viscosity SiOC preceramic polymer blend, comprising poly(-methoxymethyl)siloxane, a low-chain-length hydroxy-terminated linear polysiloxane (silicone oil) with a comparable viscosity, and a tin catalyst (bis-2-ethylhexanoatetin). The rheological behaviour of this preceramic polymer is significantly influenced by the concentration of the tin catalyst. At lower catalyst concentrations, the system exhibits Newtonian flow behaviour, transitioning to shear-thinning flow behaviour at higher catalyst concentrations. This transition is attributed to the formation of crosslinks between poly(methoxymethyl)siloxane and hydroxy-terminated linear polysiloxane, which increases the system's viscosity and makes it more prone to shear. The crosslinking process in the preceramic polymer system is catalyzed by the tin catalyst. The reaction proceeds through the hydrolysis of methoxymethyl groups on poly(methoxymethyl)siloxane, followed by the condensation of resulting hydroxyl groups with those on hydroxy-terminated linear polysiloxane. As a result, viscosity increases and gelation time decreases. The system viscosity increases proportionally with increasing

catalyst concentration, indicating increased crosslink formation between poly(methoxymethyl)siloxane and hydroxy-terminated linear polysiloxane. Ultimately, fine-tuning the tin catalyst concentration has emerged as a pivotal strategy for manipulating the rheological attributes and crosslinking tendencies of this low-viscosity SiOC preceramic polymer system [17].

UV sensitive catalysts result in polymers that can crosslink under exposure to UV light, as opposed to thermal conditions. The use of UV catalysts results in highly selective, nearly instantaneous curing of the appropriate polymer, which can be appropriate for coatings or microelectromechanical systems (MEMS) devices [125]. These catalysts promote crosslinking through two mechanisms: radical polymerisation and cationic polymerisation, which are separated on the basis of which polymer or catalyst is exposed to UV light [126]. These catalysts have been used extensively in vat polymerisation printing methods, such as digital light processing and stereolithography of PDCs, as well as for direct ink writing thin films, and bulk precursors [11,31,58]. Wei et al. paired with UV curing with DIW processes, discovering that UV curing can be used with reduced fillers to print inks that lack the appropriate shear-thinning properties by near-instantaneously curing the printed structure into shape. The resulting polymer and ceramic were highly dense and had few defects but experiences 25% line shrinkage and 30% mass loss [127]. Co-polymerisation with UV active polymers results in photoinitiated crosslinking without the introduction of catalysts, useful for developing flexible polymers that yield hierarchically porous ceramics with low thermal conductivity [13]. Fillers influence the UV curing process independent of the catalyst or copolymerisation initiators. Fillers are known to have positive effects on the mechanical properties of the ceramic in controlled amounts, however, fillers can also inhibit the absorption of UV light to activate the curing process [16,128].

2.2.2. Pyrolysis

Following the pyrolysis process, the green body is transformed into a ceramic with a degree or yield of composition on the basis of the mass or volume of the resulting structure called the ceramic or char yield. The ceramic yield is measured on the basis of the mass or volume of the structure before and after ceramization, with all mass loss occurring as the escape of volatile gases and appearing as the shrinkage in the ceramic [129]. The reactions that occur during heat treatment are dependent on the degree of crosslinking in the polymer and the composition of the precursor, typically occurring as a 4-phase procedure, outlined in Figure 8. The first phase is the crosslinking of the material, occurring between room temperature and 300–400°C depending on when the decomposition of the thermoset polymer begins. The second phase is the organic/inorganic transition during the decomposition process between the onset temperature of decomposition to 700–800°C when decomposition is complete. In this phase, significant off gassing of volatile or organic components results in the largest change in mass and volume of the sample. The third phase occurs after all volatile components have been removed, resulting in a reorganisation of the remaining inorganic structure and the development of the ceramic phases, as well as the off gassing of remaining hydrogen, typically between 800 and 1200°C. The fourth and final phase is the decomposition of the amorphous ceramic phases yielding ordered crystalline phases that depend on the composition of the remaining components [18,122,130]. The actual onset temperatures for each of these phases and the overall degree to which they are formed depend on the type of precursor and the desired composition and microstructure. To alter the degree of formation and composition of the ceramic, the pyrolysis temperature, hold duration, heating and cooling rates, and the atmospheric conditions can be finely tuned, and an overview of those effects is given herein.

2.2.2.1. Effect of pyrolysis conditions. The pyrolysis temperature and hold duration affect the phase development of the ceramic structures within the final product, and thus influence the physical properties of the ceramic [20,57,68,131]. Performing heat-treatments prior to crosslinking and pyrolysis of the precursor can improve the mass yield of the ceramic by a significant degree as illustrated for the polycarbosilane (SMP-10) and polysilazane (Ceraset® PSZ20) precursors in Figure 9. Although also found to decrease the cure enthalpy, the mass yield of pre-treated polymers increases due to the increased molecular weight of the crosslinked polymer and the decreased thermally induced volatilisation of the polymer. The overall effect is a potential improvement in the handling ability of the precursor prior to part manufacture, and an increased mass yield of the final ceramic product [132]. An increased ceramic yield can improve the density of the product and decrease the cracking that occurs in certain types of geometries, such as coatings and composites [133].

Increasing the pyrolysis temperature and duration during the process has several general effects that are independent of the type of precursor used. Higher pyrolysis and sintering temperatures have been noted to increase the crystallinity and phase distribution of the ceramic material, generally making the phases more

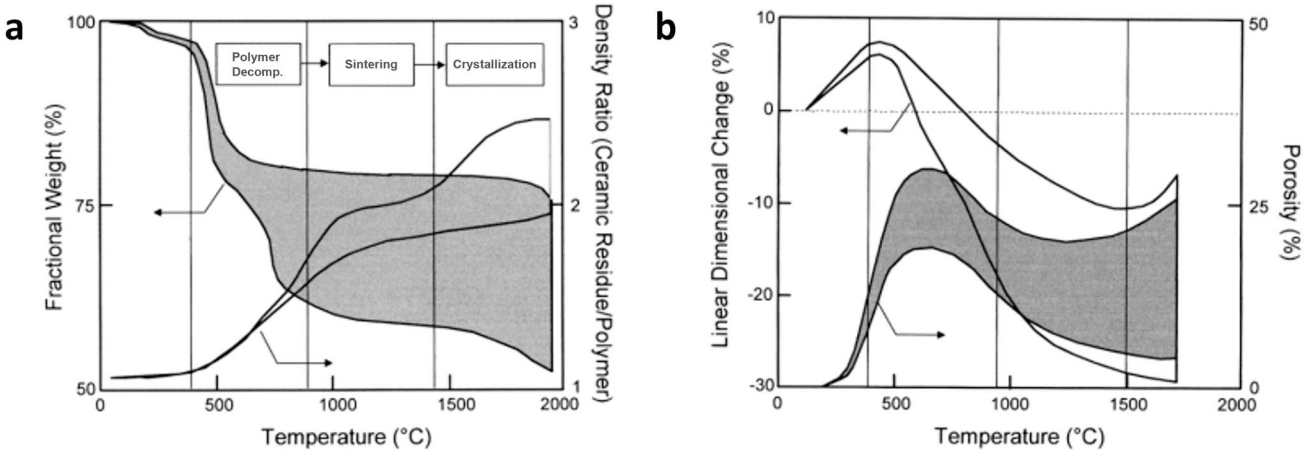

Figure 8. (a) Weight and density changes and (b) linear dimension and porosity changes as a function of pyrolysis temperature in an inert atmosphere. Reproduced with permission [18]. Copyright 2000, Wiley.

distinct while reducing the number of grain boundary defects [22,24,134]. The degree of crystallinity and phase size influences the amount of free carbon in the structure, which has proven to have a large effect on the physical and electrical properties of the ceramic; increased temperatures have also led to increased oxidation, lowered glass transition temperatures, increase in the dielectric loss of the ceramic, and increased activation energy of the final product [68,135–138]. For SiOC ceramics in particular, higher sintering temperatures lead to increased thermal stability due to the growth in more crystalline and thermally stable β-SiC domains through carbothermal reduction [75]. Similarly, increasing the sintering temperature for bulk and layered SiC increased the domain size of crystalline β-SiC from the amorphous state [57,59]. Heating at greatly increased temperatures can induce the opening of pores within the structure as decomposition occurs, allowing for channels to use polymer impregnation and pyrolysis to generate complex composites and densify the structure [139]. The duration of the pyrolysis and heat treatment can affect the size of the phases generated, which typically increases in size as the pyrolysis or post-treatment duration is increased. Larger phases can serve to increase the density of the structure, which has been shown to have a large effect on all properties of the ceramic [122]. Overall, the duration of the pyrolysis any subsequent post-processes are among the most influential variables on the resultant properties of the material. However, the specific effects of these variables are precursor and ceramic dependant, making these effects unique for each PDC, going well beyond the scope of this review.

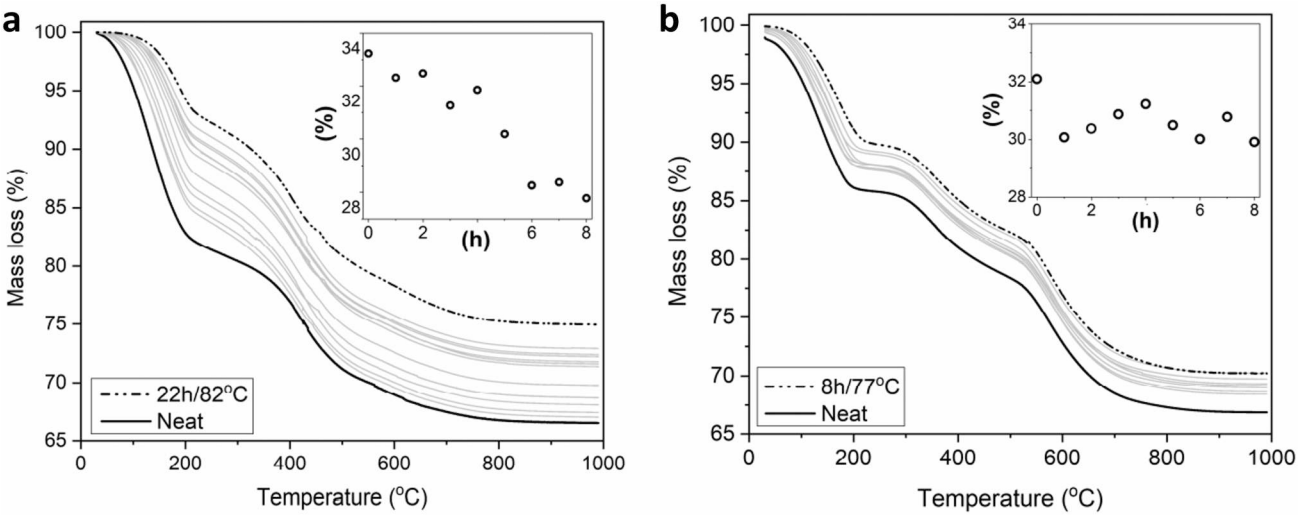

Figure 9. Thermogravimetric analysis of pre-treated preceramic polymers. The inset graph shows the decreasing weight loss over longer heat treatment durations up to 8 h. (a) Data for polycarbosilane SMP-10. (b) Data for Ceraset® PSZ20. Reproduced with permission [132]. Copyright 2020, Elsevier.

The heating and cooling rates affect the onset and physical state of the ceramic following pyrolysis. Lower heating rates typically result in earlier onset temperatures for the mass loss phases during the pyrolysis process, and decreases the peak mass loss during transformation [121]. When comparing the poly(methylsilsesquioxane) and oxycarbide samples at heating rates of 1, 5, and 10°C min^{-1}, the slowest heating rate of 1°C min^{-1} resulted in the completion of the transformation to ceramic at a point 100°C, which was lower than the fastest heating rate at 10°C min^{-1}. However, the changed heating rate did not affect the ceramic yield to a large degree [133]. The heating and cooling rates have a much greater effect on the physical state of the ceramic or composite. For example, a mismatch in the heating and cooling rates of ceramics and fillers can result in the variations in thermal expansion and shrinkage, causing increased thermal stresses in product that yield cracks and defects that weaken the overall structure. Increasing the heating and cooling rate can exaggerate these effects, leading to more defects [140,141]. Heating at extremely fast rates, such as through microwave heating can lead to an increase in volume due to rapid outgassing of volatile gases during the decomposition and transformation. The benefit of high heating rates due to microwave heating is an increase in yield and a uniform temperature distribution, however, only certain fillers can be used with this type of heating [61].

The pyrolysis atmosphere has the greatest effect on the elemental composition of the resulting ceramic as compared to the temperature and heating rates. The atmosphere largely affects the amount and state of free carbon that is generated as part of ceramic structure and thus affects the properties that depend on this phase, which include mechanical and electrical properties [22]. Oxidative atmospheres like air, containing water, oxygen, or CO_2 result in an increase in O- containing phases such as silica, which act as the matrix of the ceramic instead of Si-C or Si-N bonds. The increase in silica phases reduces the amount of free carbon in the structure, by removing it from the final composition during heating as an outgas product after combination reactions [22,58,142]. Dense or microporous samples of SiOC with reduced carbon content can be made specifically using an atmosphere that contains water vapour from polysiloxanes [143,144]. The degree of porosity and colour change of this microstructure depends on the amount of water vapour added. Oxidative atmospheres also generally result in less volume shrinkage, a higher ceramic yield, and less density due to the inclusion of SiO_2 and SiO_4 phases that are much less dense than SiC phases that would otherwise result from the transformation [145]. Oxidative atmospheres are typically avoided except when specific porosities are desired due to the inclusion of oxygen defects that lead to the onset of crystallization and degradation; defects such as SiO_2 growths are also brittle, and reduce the mechanical properties under high temperature conditions [8,19]. Pyrolysis in pure hydrogen also reduces the amount of free carbon in the product by suppressing the evolution of H_2 from the precursor and facilitating the removal of larger carbon containing groups such as alkyls and aryls. Effectively, this can act as a control for the carbon content in the precursor, especially for polycarbosilanes during the development of high purity SiC fibres [22,146].

Inert atmospheres are the most common type used to prevent any kind of oxidation and develop specifically tuned compositions with many studies preferring nitrogen or argon depending on their purpose, ammonia is also used in certain cases. Ammonia (NH_3) atmospheres result in unique compositions that lack free carbon. The carbon in the precursor becomes converted to hydrocarbons and is thus removed from the ceramic during transformation, yielding carbon-free microstructures that are appropriate for ultra-high temperature Si-based ceramics [22,56]. Nitrogen is also added to the final composition when transformed under NH_3 by nitridation, as noted for polysiloxane precursors which can result in oxynitride glasses [147]. The atmosphere also affects the nitrogen composition in binary Si_3N_4 and the oxygen composition in all polymer-derived ceramics, shifting the composition between carbon-rich and nitrogen-rich [23]. For non-silicon-based ceramics manufactured from titanium containing polymers, the type of inert atmosphere has significant influence on the composition of the final product. Polymers reacted under ammonia atmospheres will readily generate TiN or TiCN ceramics, while pyrolysis under argon or nitrogen will generate TiC ceramics from the same base polymer [107,110,112,148,149].

Unlike NH_3 and N_2 atmospheres, argon is unreactive and does not readily add components such as N or O through chemical reactions to the composition of the final ceramic, instead, it shifts the ceramic to be more carbon-rich, and devoid of oxide phases, except in the case of pyrolyzed siloxanes [19,23]. Owing to this effect, polymers under Ar often experience greater shrinkage and lower ceramic yield depending on the number of hydrocarbons in the mixture, with greater hydrocarbon content leading to lower ceramic yield [134,145]. Despite the removal of the hydrocarbons, due to the lack of H_2, free carbon from the Si-C backbone can form in increased amounts alongside Si-C bonds [68,142,147]. An increased free carbon content has shown a positive effect on the electrical conductivity

of PDCs [22,36,73]. The oxygen content and porosity can also be controlled under Ar through the injection of H_2 or H_2O during treatment, specifically, studies have analysed this effect for developing highly porous SiOC ceramics. The addition of H_2O to the Ar atmosphere shifts the phase composition toward SiO/C, through the growth of SiO_2 phases, the porosity and ceramic yield are increased, fundamentally altering the surface area that is available [143–145].

2.3. Applications of polymer-derived ceramics

The applications of PDCs span a broad spectrum, ranging from structural designs to functional materials [22,58]. In structural applications, PDCs are utilised for their excellent mechanical properties, often in the form of fibres and coatings [24]. These designs are particularly valuable for specialised uses under extreme service conditions, such as high-temperature environments [32,55,135]. On the other hand, functional materials leverage the unique thermal, electrical, chemical, and magnetic properties inherent in PDCs [11,13,30,32]. However, the scope of these applications is currently limited by the natural drawbacks of ceramics, including their inherent brittleness and low resistance to crack propagation [150].

2.3.1. Structural applications

The structural applications of PDCs include ceramic fibres, composites, coatings, and adhesives. Ceramic fibres, among the earliest structural designs of PDCs, were first fabricated in the 1970s [9,21,22]. These fibres are valued for their heat resistance and high strength, both as standalone materials and as reinforcement components in composites. PDC-containing composites find extensive use in the automotive, aerospace, and space industries. They have been evaluated for applications such as thermal protection systems, high thrust-to-weight ratio engine hot structures, aircraft brakes, and exit cones of liquid rocket engines [23–25,150]. In spacecraft, surfaces exposed to atmospheric re-entry endure complex thermal and aerodynamic environments that cause rapid oxidation. PDCs, including quaternary ceramics and binary ZrB_2-based composites, offer a promising solution for these surfaces. These materials are notable for their high melting points, improved thermal insulation, and low weight, making them ideal for such demanding conditions [151].

Coatings manufactured from PDCs typically act as thermal (TBC) or environmental barriers (EBC) that protect the coated material from wear, oxidation, or other environmental effects. These coatings can be easily applied using simple liquid phase methods such as dip, spin, or spray coating [13,18,25,26,32]. Thickness is the largest limiting factor for the use of PDCs as coatings, because extensive shrinkage can occur during pyrolysis, resulting in a critical thickness that can be used without failure and evaluated experimentally. This critical thickness can be a function of heat treatment temperature, as with higher temperatures more volatiles are removed, leading to greater shrinkage [20]. The use of fillers and multi-layer applications of the coating have opened new avenues for coating PDCs on surfaces with desirable properties and structures [13,32]. In applications where high-temperature corrosion is the greatest consideration, SiOC is often considered for environmental coatings on metals. Metals coated with SiOC ceramics are reported to withstand temperatures above 800°C with minimal degradation [152]. To improve the quality of SiOC coatings, they are often paired with active fillers such as Cr, Fe, and $TiSi_2$ powders which enhance bonding to the substrate and oxidative resistance, while reducing the amount of shrinkage [133,153]. $TiSi_2$ has been used extensively in several studies as an expansion agent in SiOC ceramics, increasing the volume of the end ceramic after heat treatment. This volume change occurs due to the formation of oxides which are complementary to SiOC and improve the mechanical properties of the surface, resulting in a structure that is highly chemical resistant to oxidative attack, and does not decrease in the thickness of the substrate-coating interface [133,152,154]. SiOC is particularly effective as an EBC because it can form a silicon oxide-rich surface layer that is oxidation resistant and chemically inert. Depending on the polymer precursor used, this layer can also facilitate the growth of Cr-rich oxides on stainless-steel surfaces during the heat treatment of the coating that further increase the oxidation protection of stainless steels [26]. In addition to chemical attack resistance, PDC coatings can also serve to protect the surface from wear and act as lubricants with enhanced tribological properties [155]. Coatings for multi-stress environments require more complex layering that can withstand both environmental and mechanical stresses. This can be achieved by using multiple compatible layers of PDCs or physical vapour deposited ceramics. Precursors to SiCN can be easily applied in coatings of varying thickness and treated and then layered with hard materials such as TiN, which serve to improve not only the thermal protection offered by the SiCN layer, but lend the surface scratch resistance, which would be useful in a wider range of environments [156]. Quaternary ceramics are investigated as well for their functional properties when applied as coatings, such as SiAlCO ceramics for solid oxide fuel cells. SiAlCO ceramics are ideal for this

environment because of the formation of several layers, as illustrated in Figure 10, which import environmental protection, increased adhesion through the interaction of the SiAlCO ceramic and the chromium within the steel, and electrical conductivity at the bond site where carbon is present [157].

The ability to act as a joint or adhesive is one of the most unique aspects that is possible when manufacturing ceramics with a polymer precursor. Chemical joining through PDCs can reduce the number of stress concentrators that are present in the joint when mechanical joining methods are used. This allows the manufacture of large parts for high-temperature applications with a minimal coefficient of thermal expansion mismatch [27,28]. Preceramic polymers can be layered on as adhesives that join other ceramics or composites, with the most crucial properties of the chosen polymer being the ceramic yield, porosity, shrinkage stresses, and joint thickness, all of which determine the adhesion of the generated ceramic to the surface [131]. Fillers added to the preceramic polymer can also be tuned to provide additional reinforcement and bonding ability to further strengthen the material by reacting with the surface or generating new phases that mechanically strengthen the matrix of the composite [27,28,158]. For SiCN adhesives joined in air, the addition of TiB_2 can generate SiO_2-B_2O_3-TiO_2 phases that inhibit diffusion of oxygen and decomposition at high temperatures while healing cracks in the matrix, maintaining an adhesion strength of 8.0 MPa in air at 800°C [159]. Single-source quaternary ceramics from polyborosilazane can further increase the operating temperatures for the joints due to the inherent thermal stability. Wang et al. determined that a SiBCN joint, modified with Al powder could maintain a shear strength of 7.9 MPa at 1600°C, a large improvement on the operating temperature compared with that of ternary ceramics [160]. SiBCN can also show enhanced bonding strength at room temperature of 12.9 MPa and a high ceramic yield for a decreased volume shrinkage of 86 wt% when generated from polysilazane modified with carborane [161]. PDC joints can also provide electrical conductivity for further use in sensors. SiC was used to join conductive SiAlCN ceramics, which are capable of remaining sensitive at 100–550°C and exhibiting similar electrical properties to the SiAlCN with minimal influence, highlighted in Figure 11, a step that could be useful or large sensor designs [162]. Several studies using PDCs as adhesives or joints are compared in Table 1.

Non-silicon-based PDCs have also been used extensively as structural materials in composites and as protective materials. Structurally, AlN can be used in high-temperature crucibles and refractories, as well as components in high temperature composites, and, using its high thermal conductivity as a substrate for integrated circuits and heat exchangers [101,102]. Boron nitride, and other boron-based ceramics manufactured using traditional high-temperature methods have been reported to be used in a large variety of fields, but especially are widely used as components for structural composites in nanoparticle and fibrous forms [168,169]. Notably, fibrous forms of BN manufactured through precursor methods are expected to be applied in composites for air and space crafts, and as components for high temperature applications [96,97,100]. Due to their high melting points and other favourable thermos-mechanical and thermos-chemical properties, UHTCs made through the precursor route such are expected to be useful as protective coatings, refractory insulation, and components in composites, particularly for extreme environments [23,56,120]. UHTCs coatings in particular find applications in the field of nuclear power. In this field, ZrC is shown to be a promising coating for nuclear particle fuels, due to its low neutron absorption and its resistance to radiation damage [116].

2.3.2. Functional materials

Functional materials derived from PDCs span a diverse range of applications, owing to the high tunability of their precursors and resulting ceramics. PDCs have been utilised in biomedical applications, sensors, electromagnetic absorbers, heat exchangers, fuel cells, nuclear systems, and as electrodes in energy storage devices [3,30]. In biomedical applications, certain ceramics have demonstrated the ability to mimic bone structures, coupled with the advantages of 3D-printed polymer precursors. Bernardo et al. combined silicone polymer precursors with calcium carbonate and hydroxyapatite to fabricate wollastonite ($CaSiO_3$) bioceramics as tissue scaffolds [170]. Additionally, coatings of bioactive ceramics and porous SiOC have been explored for their compatibility with the human body, serving as protective coatings and as systems for drug delivery [29]. Further non-silicon based ceramics like AlN has also been evaluated for use in biomedical applications: AlN nanotubes have been investigated as candidates for a drug delivery system for the cancer treatment drug 5-aminosalicylic acid. The surface of the nanotubes could effectively absorb the drug and release it while remaining biologically compatible [171].

As sensors, PDCs are known for their piezoelectric properties and are useful pressure, vibration, and acceleration sensors, even in extreme environments [13,32]. Ternary ceramics SiOC and SiCN are both

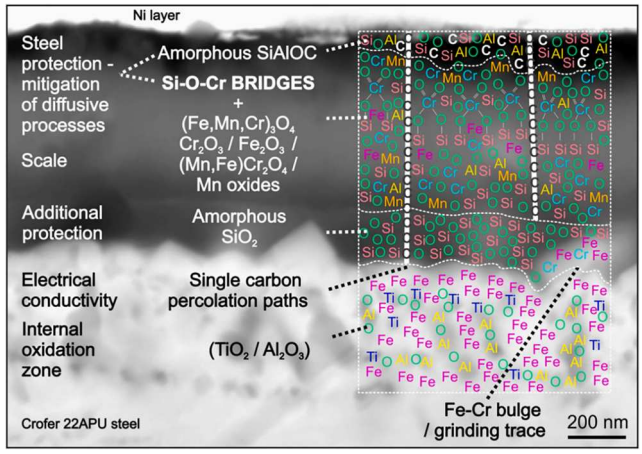

Figure 10. Morphology of SiAlCO EBC. Si-O-Cr bridges increase the layer adhesion and oxidative resistance while carbon within the ceramic offers electrical conductivity and percolation pathways. Reproduced under terms of the CC-BY license [157]. Copyright 2022, Maciej Bik, published by Elsevier.

able to maintain piezoelectric properties up to and above 1000°C and within corrosive or oxidative environments [13,21,22,30]. Quaternary ceramics that have recently been evaluated for their piezoelectric properties are SiOCN, SiAlCO, SiCoOC, and SiBCN. Additionally, AlN ceramics through precursor methods have been evaluated as piezoelectric thin films for biologically compatible thin films [103].

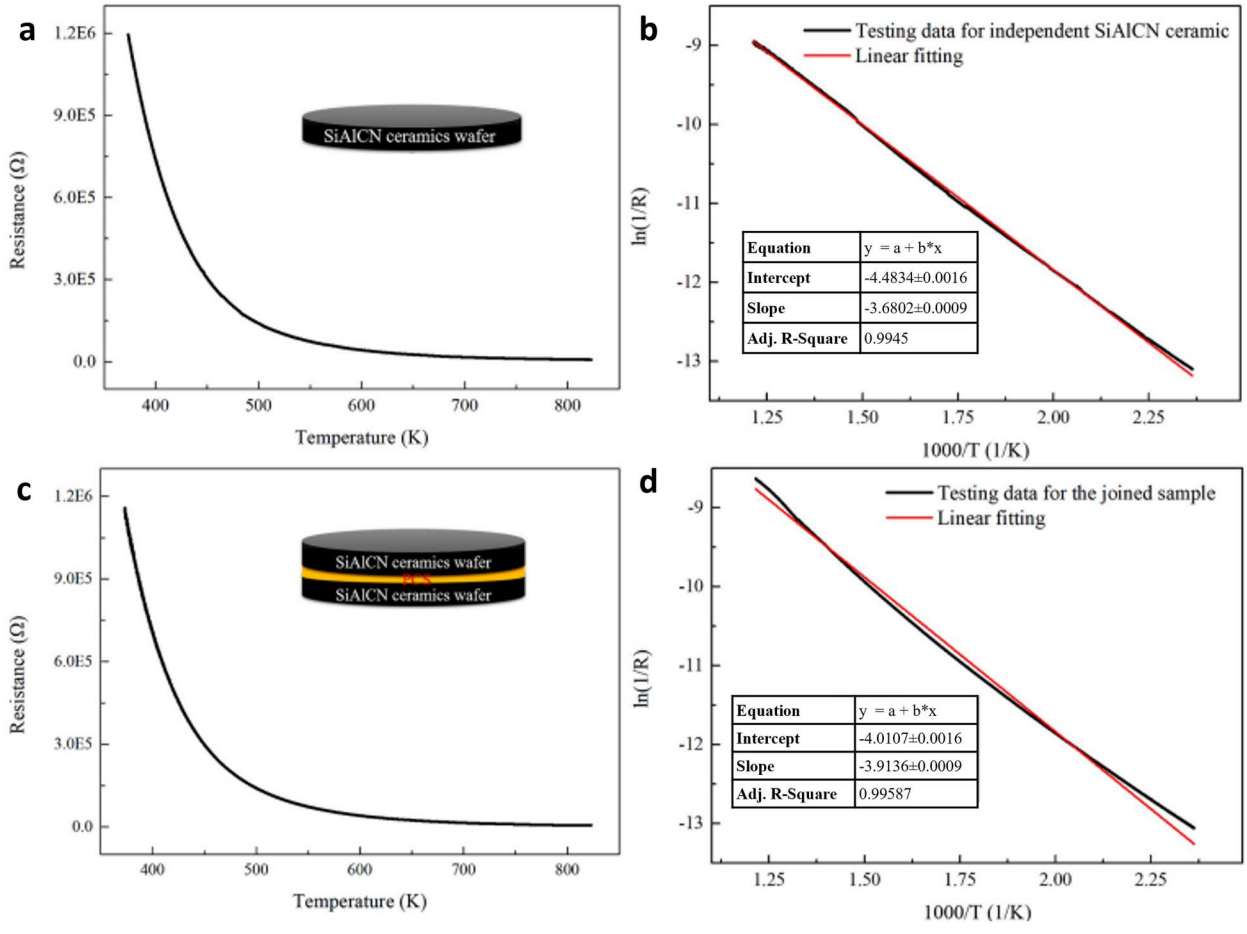

Figure 11. The resistance of (a) SiAlCN ceramic and (c) SiC joints as a function of temperature. A plot of resistance of (b) SiAlCN ceramic and (d) SiC joints as a function of temperature in the form of $\ln(R^{-1})$ vs. $1000T^{-1}$. Reproduced with permission [162]. Copyright 2021, Elsevier.

Table 1. Adhesive or joint applications for PDCs.

Ceramic	Precursor + Additives	Heat Treatment	Reported Properties	References
SiC	Polycarbosilane	850°C	5 µm thickness, 2.12 MPa tensile strength	[162]
SiOC	methyl-hydroxyl-siloxane (SR350)	1200°C in Ar	RT bending strength = 218.7 MPa, Shear strength = 26.6 MPa,	[163]
	V-PMS	1000°C in N_2	Shear Strength = 14.0 MPa, thickness = 28 µm	[131]
	Polymethylsilesquioxane	1100C in Ar	Maximum Strength = 26 MPa	[27]
SiBCN	Polymethylsilazane modified by borazine	1600°C in N_2	Shear Strength = 7.9 MPa	[42]
	Polyborosilazane	1400°C	12.08 MPa RT bond strength RT, 6.65 MPa HT (1000°C) bond strength	[159]
	PSNB + TiB_2	600, 800, 1000, 1200° C in Air	10.07 MPa bond strength at RT, 8.0 MPa at HT (800°C pyrolysis)	[159]
SiBON	Polyborosilazane	200–1650°C in N_2	12.9 MPa bonding strength at RT (800°C pyrolysis)	[164]
	Polyborosilazane + B4C	400–1500°C in N_2	Failure at 1100°C, Cohesion failure	[165]
	PSNB + TiB_2	1000°C	RT Adhesion Strength (AS) = 18.95 ± 1.78 MPa, HT (800°C) AS = 14.6 ± 2.7 MPa, HT (1000°C) AS = 12.3 ± 2.5 MPa	[166]
SiHfBCN	SiHfBCN precursor	1000°C in Air	RT AS = 3.22, 5.47 MPa at 1000°C	[167]
	SiHfBCN precursor + TiB2 + polysiloxane	1000°C in Air	RT AS = 9.49, 6.37 MPA at 1000°C	[167]

Manufactured through PDC methods, these materials have proven capable of sensing with a high degree of accuracy over a large range and have high stability [30]. In addition to their piezoelectric properties, the conductive qualities that PDCs can obtain in unmodified or tuned forms allow for a wider range of sensors. Wu et al. evaluated direct ink written SiBCN film as a ceramic thermistors, observing resistance variations in the film of only 0.09% between 505 and 620°C, and 1.7% between 610 and 720°C, even under aerobic conditions [172].

Owing to the conductive and lightweight nature of PDCs, Si-based ceramics have been evaluated as electromagnetic wave absorbers (EMWA) with the following properties: a strong absorption capability, impedance matching characteristic, a minimum reflection coefficient (Rc) or reflection loss coefficient (Rl), and a wide efficient absorption bandwidth (EAB) [36,37]. The final goal for materials with these properties are applications as radar absorption materials for air and space crafts for stealth and defence [37,38]. PDCs like SiC and Si_3N_4 are easily tailorable to both modify and manufacture with appropriate fillers to improve their capabilities, naturally having the desired low density as compared to metals, and good mechanical properties in a range of potential environments [4,37,157,173–176]. Ternary ceramics of SiOC and SiCN are widely applied in combination with conductive, magnetic fillers like Fe, Ni, and Co, and waste biomass sources of carbon that increase the interfacial polarisation and magnetic loss of the material [76,165,173,177]. Manufacturing a ceramic with several complex and complementary mechanisms, which are illustrated in Figure 12, is one method for obtaining both high absorption quality and mechanical properties that do not otherwise occur in binary or filler-free ceramics. The mechanism involved the addition of Fe and Ni particles to a SiCN precursor, which generated CNTs and mixed Fe- and Ni- microstructures, resulting in an Rl_{min} of −18 dB, an EAB of 2.5 GHz that can be adjusted by altering material thickness, as well as a low density of 2.09 g cm^{-3} and promising mechanical properties [177]. Quaternary ceramics can further improve the range and thermal stability for even more complex thermal environments [38]. Jiang et al. recently developed an SiBCN aerogel with in-situ synthesised SiC_{nw} that is ultra-lightweight (0.142 g cm^{-3}), thermally insulating (TC = 0.052 W m^{-1}*K^{-1}), and maintains good electromagnetic wave (EM) absorption properties, with a minimum reflection loss coefficient (Rl_{min}) of −50.1 dB, a wide EAB of 6.4 GHz and a low thickness of 2 mm [164]. Composites containing non-silicon precursor derived ceramics have recently been noted for their performance as EMWA, specifically in concert with SiC, introducing the exceptionally good high-temperature components that perform well when Rl < −20 dB [178].

The properties and compositions of the PDC EM absorber materials are compared in Table 2.

PDCs, owing to their unique electrical properties, have been extensively evaluated for use as bulk materials or components in electrodes for electrochemical storage systems, including lithium-ion batteries, sodium-ion batteries, and supercapacitors. Materials such as SiOC, SiCN, and SiCNO have been the focus of significant research because of their advantageous thermal and chemical stability, favourable conductivity and resistivity, and the amorphous microstructures they can achieve. Non-silicon-based materials have also been researched for applications in the energy storage and conversion devices; the findings from these studies on both groups of ceramic materials have been thoroughly documented in several comprehensive reviews [29,31,33–35,168,169].

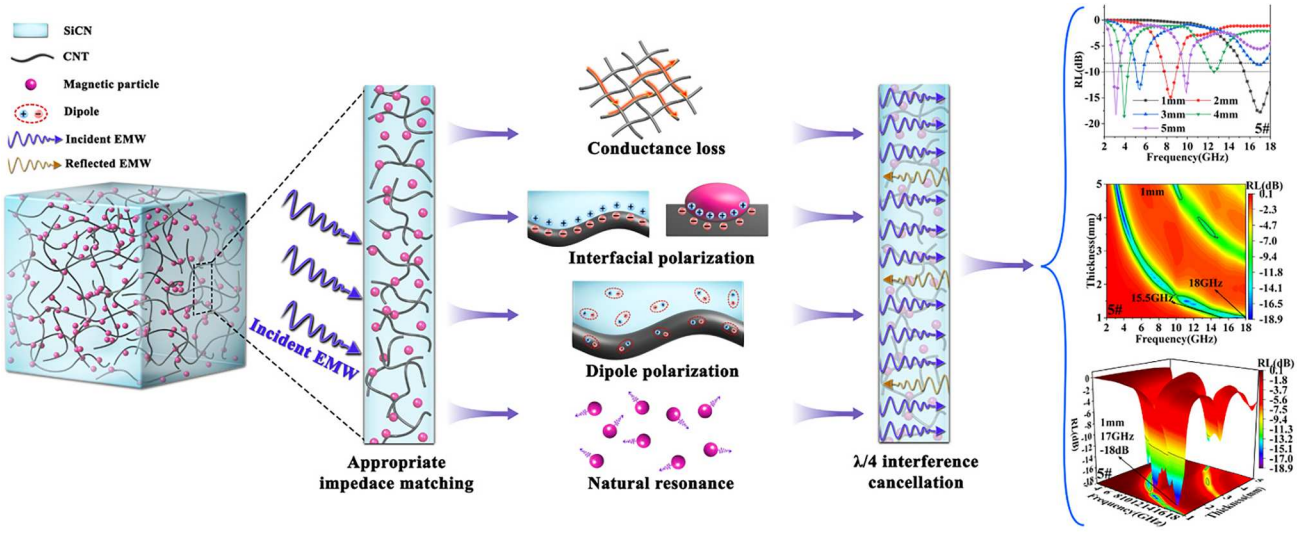

Figure 12. EM absorption mechanisms that can be present and influence the properties. Reproduced with permission [177]. Copyright 2022, Elsevier.

3. Direct ink writing (DIW)

DIW is an material extrusion-based additive manufacturing technique in which a viscoelastic ink is continuously deposited onto a print bed through a nozzle. Also referred to as robocasting, DIW relies on inks with precise rheological properties, including apparent

Table 2. Electromagnetic absorption applications of PDCs.

Ceramic	Precursor + Additives	Heat Treatment	Reported Properties	References
SiC	Methyltrichlorosilane + Carbon fibre	1000°C in Ar	Flex strength = 375 ± 10 MPa, fracture toughness = 21 ± 0.3 MPa*m0.5, EMI SE = 31 ± 1.1 dB, conductivity = 2.7 ± 0.1 S cm^{-1}	[174]
	Polycarbosilane + Paraffin Wax	900°C Pyrolysis, 1600°C Anneal	d = 1.51 mm, RI_{min} = −56.8 dB at 15.2 GHz	[175]
	Polycarbosilane, aerogel	1000, 1200, 1400°C in Ar	d = 2.5 mm, RI_{min} = −26.5 dB at 11.98 GHz, EAB = 5.8 GHz (9.6–15.0 GHz)	[157]
	BN + CNT	1200°C	d = 3.4 mm, RI_{min} = −57.20 dB, EAB = 4.2 GHz (8.2–12.4 GHz)	[179]
SiOC	SiOC (SiC + BYK-430 + tetraethyl orthosilicate + dibutylin dilaurate)	1000°C in N_2	d = 3.5 mm, RI_{min} = −36 dB, EAB = 2 GHz	[165]
	Polymethylsilesquioxane + MWCNT	1400°C in Ar	d = 2.19 mm, RI_{min} = −61.8 dB, EAB = 2.6 GHz (8.2–12.4 GHz)	[42]
	Polysiloxane	1200°C in Ar	d = 2.9 mm, Rc_{min} = −36.33 dB, EAB = 3.76 GHz (X-band)	[176]
	Polycarbosiloxane + ZrB_2	1000°C in Ar	d = 3.00 mm, EAB = 10.85 GHz, up 900°C	[41]
SiCN	SiCN + Co_2Si(Co) (PSZ + filler)	1300°C in N_2	d = 1.31 mm, RI_{min} = −50.04 dB, EAB = 3.48 GHz	[12]
	SiCN + Fe + Ni (5 wt%) (PSZ)	1200°C in N_2	d = 1 mm, RI_{min} = −18 dB, EAB = 2.5 GHz, density = 2.09 g cm^{-1}, CS = 337 MPa	[30]
	SiCN + Ni + BPC (PSZ, HTT1800)	1100°C in N_2	d = 1.33 mm, RI_{min} = −69.44 dB, EAB at 1.49 mm = 4.27 GHz (13.79–18 GHz)	[12]
	SiCN-Fe (7 wt%) (PSZ, Ceraset)	1400°C in N_2	d = 2 mm, RI_{min} = −54 dB, EAB modified by thickness	[175]
	SiCN-CNT (PSZ, HTT1800)	1100°C in N_2	d = 4.4 mm, RI_{min} = −38.4 at 18 GHz, EAB = 1.3 GHz in range of (16.7–18 GHz)	[162]
	Polysilazane + MWCNTs	N/A	d = 1.7 mm, RI_{min} = −21.7 dB, EAB = 4.7 GHz	[30]
	Polysilazane + Ni + Fe + C + HfO_2	N/A	d = 2.27 mm, RI_{min} = −54.07 dB, EAB = 3.95 at RT, d(500°C) = 1.65 mm, RI_{min}(500°C) = −33.72 dB, EAB (500°C) = 1.82 GHz	[169]
	Polysilazane	1000°C in N_2	RI_{min} = −43.37 dB at 7.6 GHz, density = 0.19 g cm^{-3}, SA = 134.48 m^2 g^{-1}	[180]
	Polysilazane + Eu_2O_2 + Fe_2O_3	1100°C in N_2	RI_{min} = −12 dB at 16.6 GHz	[181]
SiZrC	Polyzirconocenesilanes	1000°C	RI_{min} = −34 dB	[182]
SiCNO	SiOCN + CNT + Fe_3Si + Fe (PSZ HTT 1800)	900°C Pyrolysis, 1100–1500°C Sinter	Rc_{min} = −65.3 dB at d = 3.43 mm, EAB = 6 GHz at d = 1.6 mm	[175]
SiBCN	$SiBCN_x$ (Single-source precursor)	1100, 1150, 1200, 1400°C in Ar	Rc = −64.75 dB, EAB = 3.8 GHz in X-band at RT, can still cover 50% of X-band at 600°C	[1]
	SiBCN (polyborosilazane)	1000–1600°C in N_2	Rc_{min} = −56.9 dB, EAB = 3.4 GHz, thickness-d = 2.6 mm, max dielectric constant = 0.44	[38]
	SiBCN + SiCnw (polyborosilane, aerogel)	1400°C in N_2	RI_{min} = −50.0 dB, EAB = 6.4 GHz, d = 2.0 mm, density = 0.142 g cm^{-3}, thermal coeff. = 0.052 W m^{-1}*K^{-1}	[164]
	Polyborosilazane	1000°C in N_2	d = 3.0 mm, RI_{min} = 25.05 dB at 16.07 GHz	[183]

viscosity, yield stress in compression and strain, and loss and elastic moduli, to ensure proper extrusion. A key advantage of DIW is its independence from the chemical composition of the ink, allowing for a highly versatile selection of materials, provided that they exhibit the required rheological characteristics [184]. Compared with many other additive manufacturing techniques, DIW is more cost-effective, making it a preferred choice for numerous applications. Furthermore, DIW is particularly well-suited for printing nano- and microscale materials in small quantities, effectively addressing a challenge commonly encountered in powder bed-based methods [185].

3.1. Comparison of additive manufacturing methods

According to the ISO/ASTM 52900 standards, there are seven processing categories of additive manufacturing technology. These 7 categories are binder jetting (BJT), directed energy deposition (DED), material extrusion (MEX), material jetting (MJT), powder bed fusion (PBF), sheet lamination (SHL), and vat photopolymerization (VPP)[186]. Among these other principles, AM offers various techniques suitable for processing preceramic polymers, as illustrated in Figure 13.

Fused Filament Fabrication (FFF) is another MEX technique, employing a heated extruder to deposit a filament of preceramic polymer onto a substrate layer by layer. This method is valued for its simplicity and cost-effectiveness. However, FFF is limited primarily to thermoplastic materials, constraining the range of properties achievable for advanced ceramics. It also typically delivers lower resolution and surface finish, which can affect the aesthetics and detail of printed parts. Additional challenges include anisotropic properties and weak interlayer adhesion, which may compromise mechanical performance. The process often requires support structures to successfully fabricate complex geometries [191].

Stereolithography (SLA), a VPP process, employs photopolymerization to cure a photosensitive resin layer by layer using a laser. This technique excels in fabricating high-resolution ceramic components with complex geometries. However, SLA faces notable challenges. Its reliance on photocurable resins restricts the range of properties achievable in advanced ceramics. Additionally, the high cost of specialised resins and equipment makes SLA less economically competitive than other methods. The process can also become time-consuming and complex, particularly for intricate designs requiring support structures. Furthermore, SLA-printed parts are susceptible to brittleness, especially under mechanical stress or during thermal cycling, which may limit their practical application [192,193].

Digital Light Processing (DLP) is another VPP technique that cures an entire layer of photosensitive resin simultaneously using a projector. Compared with SLA, DLP enables faster production and is capable of fabricating larger ceramic components. However, it shares similar challenges with SLA, including material limitations and high costs. DLP typically offers lower resolution, which can affect the surface finish and detail of printed parts. Furthermore, incomplete curing of the resin may result in sticky or mechanically weak components, requiring additional post-processing steps to achieve the desired quality and functionality [192,194,195].

Inkjet Printing (IJP) or MJT, uses inkjet nozzles to deposit a slurry of preceramic polymer and additives layer by layer onto a substrate. This technique is highly versatile, enabling the fabrication of ceramic components with varied compositions and properties. However, IJP faces several limitations. It typically offers a smaller build volume, slower printing speeds, and requires specially formulated inks tailored for ceramic applications, which can increase production costs. Additionally, parts produced via IJP often exhibit inherent porosity, necessitating post-processing steps to achieve higher density and improved mechanical strength [196].

Selective Laser Sintering (SLS), a PBF AM technique, uses a laser to sinter layers of preceramic polymer powder sequentially. This process enables the fabrication of ceramic components with high density and excellent mechanical strength. However, SLS is an expensive method due to the high cost of equipment and specialised powders. Additionally, the handling of powders can be messy and potentially hazardous, necessitating specialised equipment and strict safety protocols. Post-processing is typically required to remove excess powder from printed parts, adding complexity and time to the overall manufacturing process [191,197].

Compared to the other methods that have been used for printing PDCs, DIW presents significant advantages for the fabrication of advanced ceramics. It supports a broader range of materials, including ceramic powders, polymers, and composites, offering greater versatility in material selection. DIW achieves high resolution and excellent surface finish, enabling the production of intricate and detailed ceramic components. Unlike many other additive manufacturing techniques, DIW can fabricate complex geometries without requiring support structures, streamlining the process and minimising post-processing requirements. Furthermore, DIW is a

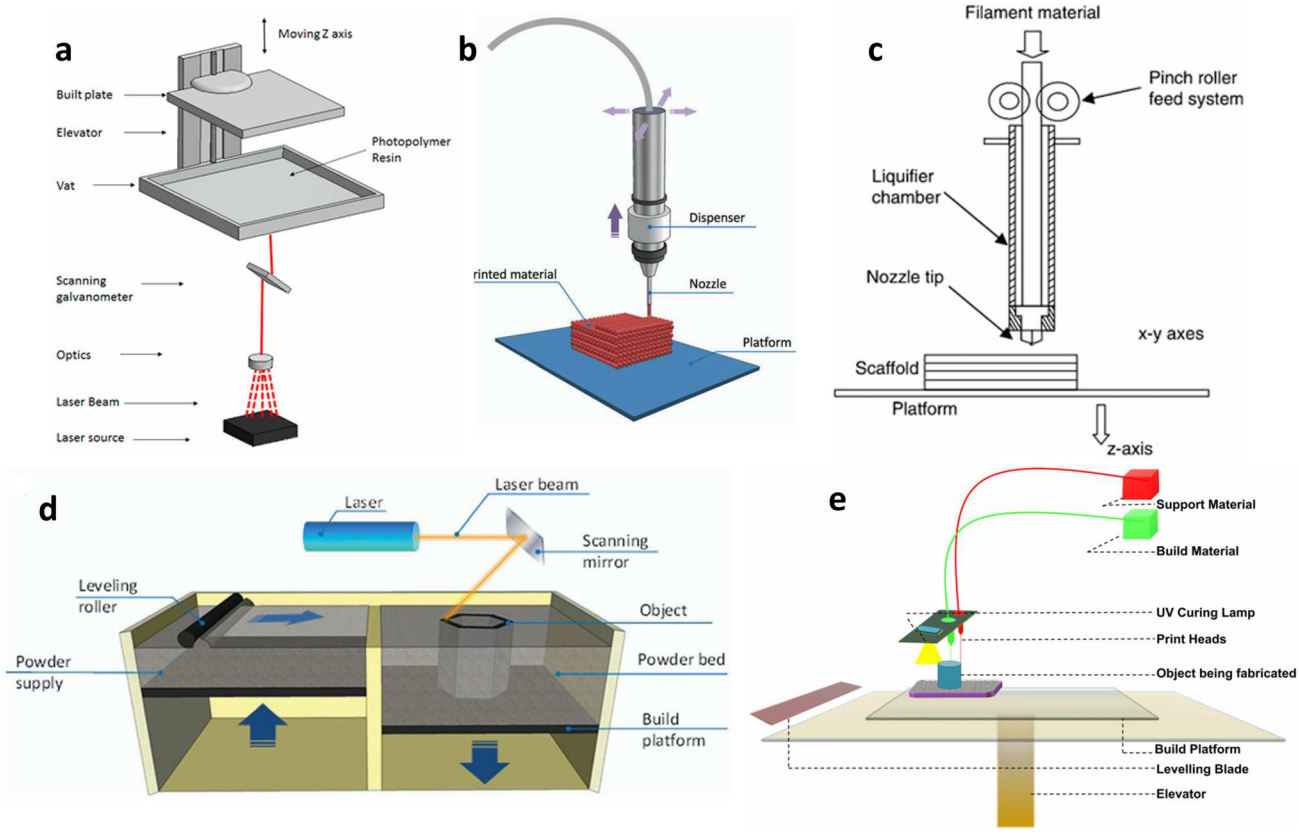

Figure 13. Additive Manufacturing methods that have been used for PDCs. Additive Manufacturing methods that have been used for PDCs. (a) SLA/DLP. Reproduced with permission [187]. Copyright 2018, Elsevier. (b) DIW. Reproduced with permission [188]. Copyright 2016, Royal Society of Chemistry. (c) FFF. Reproduced with permission [189]. Copyright 2019, Elsevier. (d) SLS, and (e) IJP. Reproduced with permission [190]. Copyright 2019, Springer Nature.

cost-effective solution that is particularly well-suited for small-scale production and research applications, addressing several limitations commonly associated with other AM methods [198]. The important properties of these techniques are compared in Table 3.

3.2. Ink rheology requirements

As a liquid or gel feedstock MEX AM technique, the rheological properties of the ink are critical to the printability of materials in DIW. Two primary rheological requirements must be met for an ink to be considered printable. First, the ink must exhibit suitable extrudability, meaning that it should flow smoothly and continuously through the nozzle as a filament to accurately replicate the digital model. This requires consistent flow characteristics, free from discontinuities or clogging, to ensure uninterrupted deposition. Second, the ink must demonstrate strong shape fidelity to maintain the integrity of the structure after deposition, particularly since many PDC inks require subsequent post-printing treatments. Inks with shear-thinning behaviour under variable flow rates have been found to effectively meet these criteria, enabling successful extrusion and structural preservation.

The extrudability of an ink is typically evaluated using two key parameters: the flow stress (T_f) and the flow behaviour index (n). The flow stress indicates the minimum shear stress required to initiate ink flow, whereas the flow behaviour index describes the type of flow behaviour exhibited by the ink. An n-value less than 1 generally indicates shear-thinning behaviour, a characteristic of non-Newtonian fluids. In such fluids, the viscosity decreases as the shear rate increases, meaning that less pressure is required for extrusion at a given speed than inks that behave as Newtonian fluids. This property is particularly advantageous for ensuring smooth, efficient material deposition during the DIW process.

After deposition through the nozzle, the ink's ability to maintain its shape is characterised by parameters such as yield stress (T_y), the storage modulus at rest (G′ eq), and the ratio of the loss modulus (G′′) to the storage modulus (G′). The yield stress (T_y) indicates the maximum load the extruded ink can sustain when forming three-dimensional structures, making it a critical

Table 3. Comparison between AM techniques.

AM technique	Process Type	Build speed	Resolution	Material versatility	Cost	Post-processing	Complex geometries	Strength and density	Limitations	References
Stereolithography (SLA)	Photopolymerization	Moderate	High	Limited to photosensitive resins	High (specialised resins, equipment)	Support removal, brittleness	Yes	Moderate	Material limitations, high cost	[16,192,193]
Digital Light Processing (DLP)	Photopolymerization	High	Moderate	Limited to photosensitive resins	High (similar to SLA)	Incomplete curing, surface finish	Yes	Moderate	Lower resolution, cost	[16,192,194]
Ink Jet Printing (IJP)	Material Extrusion	Slow	Moderate	Versatile (wide range of compositions)	Moderate to High	Porosity, post-processing	Yes	Moderate	Smaller build volume, slower speed	[196]
Fused Filament Fabrication (FFF)	Material Extrusion	Moderate	Low	Restricted to thermoplastics	Low	Anisotropic properties, weak layer adhesion	Yes	Low	Lower resolution, limited materials	[191]
Selective Laser Sintering (SLS)	Powder Fusion	Moderate	High	Limited to specialised powders	High (equipment and materials)	Powder removal, post-processing	Yes	High	High costs, messy and hazardous handling	[197]
Direct Ink Writing (DIW)	Material Extrusion	Moderate	High	Wide material range (ceramic powders, polymers)	Low to Moderate	Minimal	No (no support structures)	High	Versatile, cost-effective	[12,198]

factor for the successful printing of large or complex geometries using DIW. The storage modulus (G′), which arises from the stretching of the internal bonds, reflects the ink's elastic behaviour and indicates the ink's stiffness after extrusion. In contrast, the loss modulus (G″) represents the viscous behaviour of the ink, capturing the internal friction among its components that leads to energy dissipation during flow. The ratio of G″/G′, often referred to as the damping factor, determines whether the ink exhibits more liquid- or solid-like behaviour over time at rest. Ratios below 1 indicate that elastic (solid-like) behaviour dominates, suggesting that the material behaves like a solid at rest. Conversely, ratios greater than 1 signify a dominance of viscous (liquid-like) behaviour at rest [184,199].

The rheology of PDC ink is significantly influenced by the formation of network structures, which depend on the intermolecular forces within the polymer. The functional groups attached to the polymer chain play a critical role in determining these rheological properties. Studies comparing the performance of various carbon-based functional groups have shown that linear groups, such as allyl and vinyl, promote stronger interparticle network formation than cyclic functional groups do. This enhanced network formation improves the shape fidelity of ink formulations utilising polymers with linear functional groups, making them more effective for applications requiring precise structural integrity [200].

Another critical factor influencing the rheology of PDC inks in particular is the effect of filler materials. The interactions between the liquid and solid components in the mixture can significantly impact the viscosity and yield stress of the ink, with both the filler loading and the particulate type playing pivotal roles. In some cases, filler materials disrupt the network structure of the binder, leading to increased viscosity in the ink. Xiao et al. reported such behaviour in a study where the addition of boron nitride to a mixture with PDMS resulted in higher ink viscosity. They identified an optimal filler loading of 40 wt%, which provided the ideal viscosity for extrusion while maintaining effective printability [201]. The addition of solid inclusions is a key factor for developing printable PDC resins, and will be discussed in more detail in later sections.

3.2.1. Rheological characterization

Rheological characterisation of materials is typically conducted using specialised instruments known as rheometers. These devices can apply a broad range of shear stresses, strains, and shear rates to a given sample, enabling precise analysis of its flow and deformation behaviour. Shear parameters are applied by rotating the upper component, either in a continuous direction or in an oscillatory motion with a defined amplitude and frequency, tailored to the specific requirements of the analysis. An overview of the different experiments that will be overviewed here, the parameters of interest, and the types of ink that the experiments are relevant for is given in Figure 14.

3.2.1.1. Flow sweep test.

Shear-thinning materials exhibit a decrease in viscosity with increasing shear rate, a behaviour commonly analyzed using a flow sweep test, also referred to as a rate-dependent viscosity test. In this method, the applied shear rate is gradually increased over time, while continuously measuring the materials viscous response. This test provides valuable insights into the material's flow behaviour under varying shear conditions.

The resulting curve of viscosity vs shear rate can be fitted to Ostwald-de Waele power law models for relating the shear rate ($\dot{\gamma}$) to the apparent viscosity (η) as seen in Equation 1:

$$\eta = k \cdot (\dot{\gamma})^{n-1} \tag{1}$$

where k is the flow consistency parameter and n is the flow index. For shear thinning behaviour, the value of n lies between 0 and 1. The shear stress can similarly be estimated from flow sweep tests by relating it to the applied shear rate as shown in Equation 2:

$$\tau = k \cdot (\dot{\gamma})^{n} \tag{2}$$

This relationship is instrumental in determining the yield stress of the ink by identifying the point on a shear stress versus shear rate plot where flow (shear) initiates [203].

3.2.1.2. Amplitude sweep test.

The storage modulus (G′) and loss modulus (G″) values of a material can vary with applied strain, as the internal network structure may breakdown at higher strain levels. This behaviour is typically analyzed using amplitude sweep tests, where the strain amplitude is incrementally increased over time while maintaining a constant frequency [202]. The results of this test are visualised as a plot of moduli (G′ and G″) versus shear strain. The range of strain values within which the moduli remain constant is referred to as the Linear Viscoelastic Region (LVR), which is material dependent. In this range, G′ represents the elastic modulus of a solid material and is denoted as G'_{eq} for the ink. The strain value at which the network structure begins to break down, known as the yield point, marks the upper limit of the LVR. Beyond this point, G′ decreases, indicating irreversible deformation. These metrics are essential for understanding the viscoelastic properties of the ink.

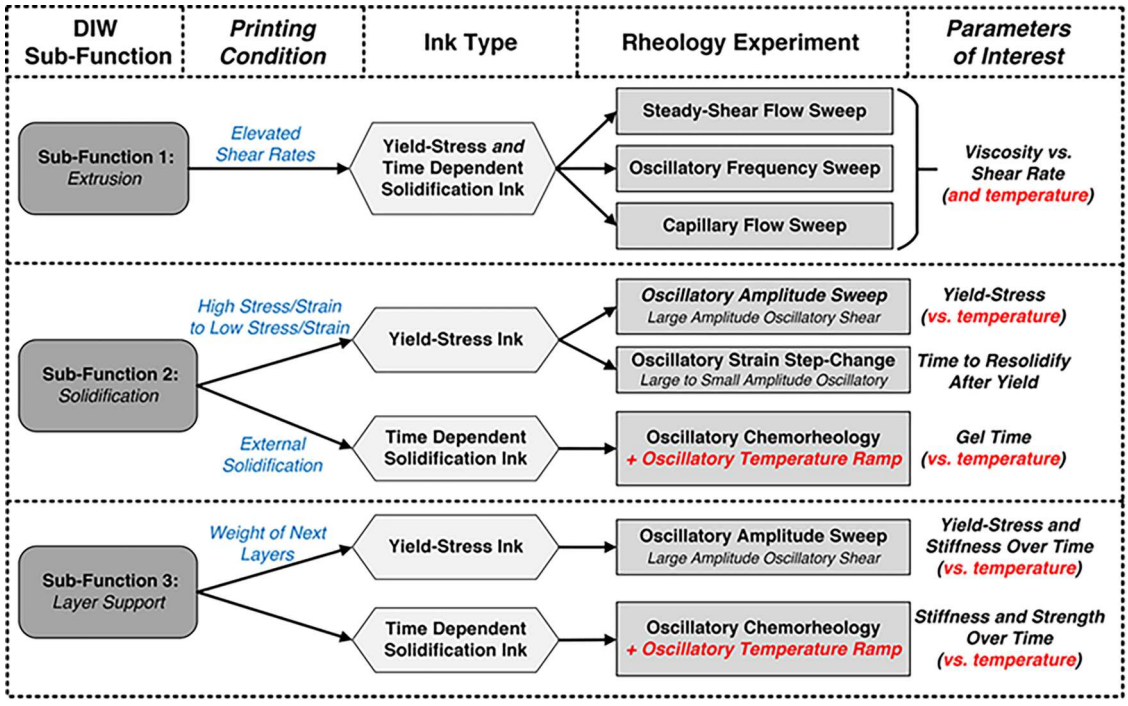

Figure 14. An overview of the rheological techniques that are used to characterise different types of ink used for DIW based on the sub-function that predicts the ink behaviour. Reproduced with permission [202]. Copyright 2023, Elsevier.

Due to the different effects of rheological modifiers on the viscosity and shear thinning behaviour, as well as physics effects such as gravity slumping and capillary forces, it is difficult to provide a definitive numerical range for G′ and G″ values that would make a successful ink for DIW [204]. Instead, there are trends that can indicate when an ink could have printable shear thinning behaviour, which can be refined for the ink depending on the components and the application. Printable inks typically display a crossover, or a flow point from solid-like to liquid-like behaviour within these tests, reflected in the plots of the storage and loss moduli vs. the shear strain in Figure 15. This flow point is identified by the intersection of the G′ and G″ curves, and beyond this point, the material's viscous behaviour dominates [205]. An ink that will not likely be applicable for printing may show curves like that in Figure 15(a), where the filled ink does not exhibit crossover behaviour in its current state. This is in contrast to Figure 15(b), where the filled inks show a flow point and transition to liquid-like behaviour that would allow for flow through a nozzle required DIW [204].

3.2.1.3. Three interval thixotropy test. After extrusion, the ink must quickly regain the viscosity lost under extrusion stresses to preserve its shape fidelity. This behaviour can be evaluated using the Three-Time Interval Thixotropy Test (3ITT), which measures the ink's viscosity or shear strain properties over three distinct time intervals. During the first and third intervals, a low shear rate is applied, simulating the ink at rest in the container and after extrusion from the nozzle, respectively. In the second interval, a high shear rate is applied, mimicking the conditions during extrusion through the nozzle. This test not only assesses the ink's ability to regain its viscosity quickly but also determines whether its viscosity is time dependent [199,205,206]. Time-dependent viscosity could complicate the printing process by affecting the flow consistency, requiring careful adjustment of the printing parameters.

Similar to the trends noted for the G′ and G″ values, providing a definitive numerical value of the storage modulus, viscosity, and relaxation parameters that would make a successful DIW ink is very difficult due to the potential variability and physics factors. However, there are trends that can serve as indicators for when an ink experiences printable thixotropic behaviour. Thixotropic behaviour that could indicate potential for DIW is in the relaxation measured by output viscosity (Figure 16(a)) or storage and loss moduli (Figure 16(b)) vs. time plot from the 3ITT test. During the first and third intervals, the ink should present solid-like behaviour, $G' > G''$, indicative of the unprinted ink not flowing, and the extruded ink holding shape. During the second interval, the ink should present liquid-like behaviour, where $G' < G''$ and the plot shown in Figure

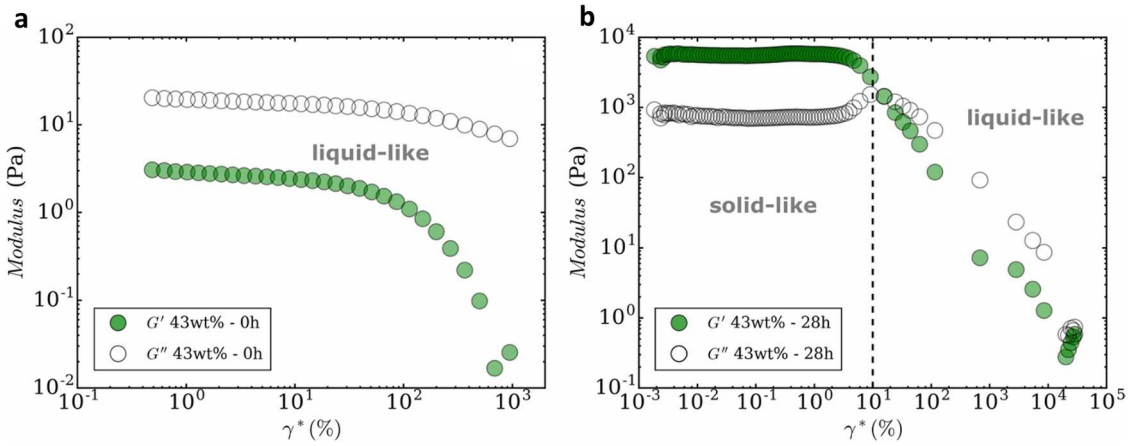

Figure 15. Amplitude sweep test results measured at 1 Hz for a 43 wt% boehmite suspension (A) before and (B) after aging. Reproduced under terms of the CC-BY license [204]. Copyright 2017.

16(b) plateaus, indicative that the ink in the nozzle undergoing shear stress should experience liquid-like viscosity and flow [199]. The most important factors are the transitions between the behaviours during the change from solid-like to liquid-like and back. To best indicate a response favourable for DIW printing, the recovery time between these states should be very fast, in the range of a few seconds to show appropriate recovery after printing [199,207]. Large recovery times, in the order of minutes, typically indicate highly thixotropic inks that would have a limited ability to support subsequent layers [202].

3.3. Effects of print parameters on the quality

In DIW, the printing parameters largely mirror those of other MEX methods. Commonly used FFF parameters – such as layer height, nozzle speed, infill percentage, and the number of perimeter lines – also play key roles in DIW. However, while FFF relies on temperature to control the flow of molten thermoplastic, DIW typically operates at room temperature. In this case, ink formulation and extrusion rate become the critical parameters for managing ink flow and achieving successful prints. More broadly, additive manufacturing research emphasises establishing measurable links between printing parameters and the final product's accuracy. To accomplish this, many studies employ statistical approaches, including Design of Experiments (DOE), to develop predictive models that optimise printing performance and precision.

Tu et al. [208] emphasised that optimising printing parameters requires careful consideration of their interdependencies to improve both reproducibility and efficiency in the optimisation process. They noted that the print speed, V_n, is influenced by the extrusion rate, V_e, which, in turn, is determined by the piston velocity, V_p. Similarly, the layer height, h, is dictated by the nozzle diameter, D_n. To address these dependencies, Tu et al. proposed using two dimensionless ratios as

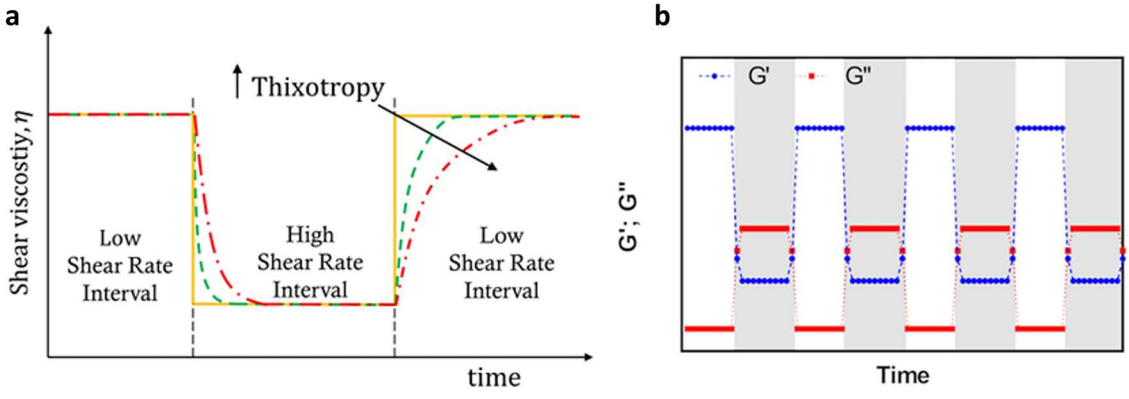

Figure 16. Ideal thixotropic behaviour for printable inks with DIW plotted in terms of the (a) shear viscosity vs. time. Reproduced under terms of the CC-BY license [206]. Copyright 2024. (b) Storage and loss moduli vs. time. Reproduced under terms of the CC-BY license [205]. Copyright 2020.

process parameters: R_c, the ratio of V_p to V_n and H, the ratio of h to D_n. By focusing on optimising these ratios, the complexity of directly managing individual parameter interactions is reduced, streamlining the optimisation process and improving control over printing outcomes.

This approach of accounting for interactions between parameters is well-founded, as similar studies on optimising FFF printing have also highlighted the significance of such interactions. In one study focused on optimising printing for dimensional accuracy and material consumption, the authors reported that the print speed and the density of the outer walls (i.e. the number of lines forming the wall) significantly influenced dimensional accuracy of the final part. Conversely, material consumption is affected primarily by perimeter density and infill percentage, underscoring the importance of parameter interdependencies in achieving optimal printing outcomes [209]. The impact of parameter interactions also depends on how the optimisation objectives are defined during statistical analysis. In a study by Khalid et al., material consumption in FFF was assessed in terms of the weight of the printed part and the scrap generated during the process. This distinction influences the significance of parameter interactions. While perimeter density and infill percentage were significant factors for both weight and scrap, other parameters, such as build orientation and layer height, were also found to have substantial effects. This highlights the importance of carefully defining optimisation metrics to account for the diverse influences of parameter interactions [210].

In DIW processes, interest in the effects of print parameters on the accuracy and porosity of printed products has increased, particularly in the context of structures fabricated using bio-inks for medical applications [49,211,212]. While findings related to print accuracy align closely with those reported in other studies, porosity was found to be predominantly influenced by the rheological properties and chemical composition of the bio-ink.

3.4. Advantages and limitations

DIW is an emerging AM technique with significant potential for producing ceramic components characterised by exceptional density and mechanical strength. Its versatility allows for the fabrication of components using a wide range of materials, including those with complex geometries and intricate microfeatures. These advantages make DIW a promising approach for the additive manufacturing of advanced ceramics, addressing the limitations of other AM methods and enabling the production of high-quality ceramic parts tailored to diverse functionalities and applications.

DIW has several promising applications in the production of structural and functional ceramics. First, DIW excels at crafting intricate shapes and features with high resolution, a feat that is often challenging or impossible with traditional ceramic manufacturing methods [213]. This capability makes DIW ideal for applications such as microfluidic devices, sensors, and actuators. Second, DIW's capacity to produce customised prosthetics and scaffolds with tailored porosity and surface properties holds great potential for medical applications, facilitating tissue ingrowth and cell attachment in the production of biocompatible implants [198,214]. Third, DIW facilitates the development of high-performance ceramic membranes for filtration and separation, offering precise control over the membrane pore size and distribution. This capability leads to efficient substance separation, advancing filtration and separation technologies [215]. Fourth, DIW plays a vital role in manufacturing energy-efficient and lightweight components for the aerospace and automotive industries. It can produce lightweight ceramic components with high strength and thermal resistance, contributing to enhanced fuel efficiency and performance in these sectors [216]. Finally, DIW enables the production of customised ceramic catalysts and supports for chemical reactions by providing precise control over catalyst distribution and morphology [217].

However, DIW also faces limitations and challenges. DIW currently has a narrower range of compatible ceramic materials as compared to some other AM techniques, such as powder bed fusion. Additionally, DIW tends to have slower printing speeds compared to rapid techniques like DLP, particularly for larger components. This limitation arises because the printing speed in DIW is constrained by the viscosity of the slurry and the flow rate of the syringe [218]. Shrinkage and distortion during drying and sintering are also potential issues, requiring careful control and post-processing. Fabricating large ceramic components with DIW can be challenging due to the time-consuming printing process and potential slurry instability over time. Furthermore, specialised inks and printing equipment are required for DIW, increasing costs. Developing and utilising customised ceramic inks and specialised DIW equipment can be expensive, particularly for small-scale production. Moreover, DIW-printed ceramics require post-processing steps like sintering to achieve their final properties, unlike some AM techniques that produce finished parts directly, introducing complexity and extending processing time [195,198,217].

Table 4. Applications, advantages, and limitations of DIW.

Applications	Advantages	Limitations and challenges	References
Microfluidic devices for heat transfer applications	Good at creating intricate shapes and high- resolution features	Smaller range of compatible ceramic materials compared to some other AM techniques.	[213,219,220]
Thin Film Sensors for high temperature applications	Capable of producing dimensionally accurate high temperature resistant ceramic thin films	Potential for shrinkage and cracking during the pyrolysis process	[172,221–224]
Customised prosthetics and biological scaffolds	Capable of producing customised prosthetics and scaffolds with suitable porosity and surface properties for medical applications	Slower printing speeds, especially for larger components	[170,198,214,225,226]
High-performance ceramic membranes	Allow for the development of high-performance ceramic membranes for filtration and separation.	Potential for shrinkage and distortion during drying and sintering processes.	[25,86,215]
Aerospace lightweight components	Energy-efficient and lightweight ceramic components with high strength and thermal resistance.	Challenging for producing large components due to time-consuming printing and slurry instability	[24,216,218]
Automobile lightweight components (brakes, etc)	Energy-efficient and lightweight ceramic components with high strength and thermal resistance.	Challenging for mass production, lower resolution, long-term post-processing	[184,227]
Microwave absorption structures	Allows for tuning the composition and structure for the best performance	Requires specialised ink, increasing costs	[173]
Customised ceramic catalysts and supports	Enables the production of customised ceramic catalysts and supports with precise control over distribution and morphology	Requires specialised inks and printing equipment, increasing costs	[217]

Despite these drawbacks, DIW remains a promising and rapidly evolving technology with significant potential for creating advanced ceramic components for various applications, which are summarised in Table 4. Ongoing research and development efforts are focused on addressing these limitations and expanding the capabilities of DIW, making it an even more valuable tool for engineers and scientists working with structural and functional ceramics.

4. Direct ink writing of polymer-derived ceramics

4.1. Filler materials as a modification method for enabling printable polymer-derived ceramics

The addition of ceramic filler material to inks for DIW applications has been shown to be beneficial due to volume changes and volatile product generation during the heat treatment of polymer-derived ceramics. These fillers often function as rheological modifiers, with their loading and composition significantly influencing the ink's shape fidelity and flow characteristics. Additionally, filler materials enable control over the material properties of the printed product, tailored to its intended application. Based on their behaviour during the heat treatment of the ink, filler materials for polymer-derived ceramics are broadly classified into four categories: inert fillers, active fillers, sacrificial, and meltable fillers.

4.1.1. Inert fillers

Inert or passive filler materials are typically ceramic powders or fibres that remain chemically unreactive with the PDC or the volatile products generated during heat treatment. These materials have included silicon-based ceramic powders such as SiC, silica, Si_3N_4, and fumed alumina [4,43,80,139,173,189,226,228,229]. Pre-synthesised silicon-ceramic fibres or non-silicon ceramics have also been included such as SiC nanofiber or whiskers, boron nitride nanotubes, and boron nitride particulate [33,79,139,228,230]. Alternatively, inert fillers considered as additive manufacturing modifiers have also included carbon materials such as carbon nanotubes, carbon fibres, and graphene [19,140].

The addition of these non-reactive fillers reduces the amount of precursor composing the ink, thereby minimising shrinkage and the generation of gaseous byproducts during heating. This reduction in shrinkage also decreases the stress experienced by the ceramic product, helping to prevent crack formation [19]. Inert fillers can further enhance the mechanical properties of the printed product; for instance, the inclusion of boron nitride has been shown to improve both the bending strength and fracture toughness of SiC/BN composites [231].

4.1.2. Active fillers

In contrast to inert fillers, active fillers react with byproducts generated during heat treatment, enabling the formation of different ceramics such as carbides, nitrides, or silicides to create composites with tailored properties. For example, within carbides, transition metal oxide fillers can mitigate defects in the ceramic crystal structure by reacting with free carbon [232,233]. This reduction in free carbon promotes densely packed crystal structures, enhancing the mechanical properties. In polysilazanes, the incorporation of alumina (Al_2O_3) and silicon nitride (Si_3N_4) further improves the

mechanical properties of the final ceramic. These fillers react with decomposition gases released during pyrolysis, forming secondary ceramic phases. This reaction reduces void formation within the bulk material, improving fracture toughness, whereas the reaction products increase the hardness and elastic modulus [80].

Active fillers can include metallic particulate, or reactive ceramic components. Active metallic fillers have included transition metal powders, chlorides, and alloys. The use of titanium, tungsten, niobium, and molybdenum in particular are effective when added to PDCs for generating transition metal carbide phases within the ceramic [19,139]. Other metallic powders have additional effects. The inclusion of Zr powders have resulted in the generation of ZrO_2 and suppressing the carbothermal reduction of the ceramic [234]. Metallic chlorides have been used for modifying the phases of the ceramic product, although they are rarely used for additive manufacturing, including catalytic metallic compounds $FeCl_2$ [137], $CoCl_2$ [136], $NiCl_2$ [233], and $MoCl_4$ [235]. Alloy powders have also been used as a filler and modifier in DIW of PDCs to generate complex combinations of carbides and silicides. Biasetto et al. utilised Ti_6Al_4V powder to generate multiple phases, as a combination of titanium silicide and vanadium carbide [236].

Active ceramic components are popular as rheological modifiers of PDCs and for the development of biologically compatible ceramics, or generally for the fabrication of specific ceramic phases that are otherwise difficult to produce with traditional ceramic manufacturing methods. Examples of active ceramics used for DIW of PDCs include mullite, Al_2O_3, $CaCO_3$, MgO, ZrO_2, TiO_2, $ZrSiO_2$, Y_2O_3, Eu_2O_3, ZrB_2, Na_2CO_3, Na_2HPO_4, and $Na_4P_2O_6$ [4,19,79,226,230,236]. Of these fillers, oxides in particular react with the decomposition products of the preceramic polymer when pyrolyzed, specifically reacting with the silica and generating new phases with the metallic component [19].

4.1.3. Sacrificial and meltable fillers

A specialised category of active fillers, known as sacrificial fillers, is designed to be removed during heat treatment or through the use of solvents. These fillers are primarily utilised to create controlled porosity in pyrolyzed PDCs [237,238]. The size, shape, and distribution of the resulting pores can be tailored by selecting filler materials with specific particle sizes and geometries. Organic materials are commonly used as sacrificial fillers, as they offer multiple removal pathways without adversely impacting the ceramic structure. A notable example of this approach was demonstrated by Pelanconi et al., where organic polyamides were employed as sacrificial fillers. During the initial heat treatment phase, the fillers were burned out, leaving behind a porous SiOC structure in which the ceramic accounted for only 2% of the total volume of the final product [239]. When involved with additive manufacturing of PDCs, sacrificial fillers have been utilised as framework for the indirect printing of ceramic structures. In this method, the sacrificial poly(lactic) acid structure acted as a framework or preform. Liquid polycarbosilane and polysilazane precursors were then used to infiltrate the porous structure through dip coating, then the impregnated structure was pyrolyzed to burn away the sacrificial framework [240]. Polyurethane has similarly been used as the sacrificial structure for this type of indirect printing of ceramics [241].

Meltable fillers are related to both the active and sacrificial category; they are intended to encourage low shrinkage, densification, and to have stress-relief effects, while densifying the ceramic. During the pyrolysis process, these fillers will soften or melt to seal pores within the structure, and depending on the glass, precursor, and atmosphere combination, can further take on the role of an inert or active filler. Glasses are the most significant type of meltable filler, and their inclusion into a PDC used for coatings resulted in improved oxidation and corrosion resistance, as well as use as a sintering aid [53,242]. To the best of our knowledge, meltable fillers have not been explicitly used for DIW of PDCs and is remarkable as a potential field of study.

The effect of these different types of fillers are illustrated and compared in terms of the generated microstructure in Figure 17.

4.2. Effects of fillers on printed structures

The selection of filler material is a key strategy for developing printable inks for DIW, and for tailoring the properties of the final ceramic product, allowing for enhancements in mechanical, electrical, thermal, and biological performance. The geometry and dispersion of the fillers can influence the mechanical properties of the final product, while the chemical composition and morphology determines many of the mechanical, thermal, electrical, and chemical properties of the final printed parts. This effect of geometry and chemistry is notable for both inert fillers, which serve create composites with unique morphologies, and for active fillers which can fundamentally change the product that is being produced. Examples of printed ceramics are included and summarised in Table 5.

4.2.1. Effect of filler geometry and dispersion

The geometry, including the shape and the size, of filler particles are critical factors in achieving the desired modifications to the properties of ceramic materials.

Fibrous or nanotube structures are most adept at improving the mechanical strength of the ceramic product, although the effect of dispersion and orientation of these filler types must also be carefully considered. A notable example is the incorporation of Multi-Walled Carbon Nanotubes (MWCNTs) into SiCN ceramics. Significant improvements in fracture toughness were observed only when the MWCNTs were uniformly distributed and aligned in a single direction. The aspect ratio (length-to-width) of the nanotubes plays a pivotal role, as demonstrated in Katsuda's research. MWCNTs with small aspect ratios or poorly defined graphene walls were found to provide negligible enhancement to the mechanical and physical properties of the ceramic [251]. While MWCNTs and other fibrous fillers function as inert additions to the polymer precursor, contributing to improved mechanical properties in PDCs, their tendency to agglomerate can lead to inconsistent performance at varying concentrations, unlike active fillers. This underscores the importance of using an effective dispersion mechanism during the preparation of the precursor solution to ensure uniform distribution and optimal performance [80].

In contrast, platelet-shaped filler particles are generally more accommodating for incorporation into inks used for DIW, as their interlocking nature tends to result in more uniform properties. For example, the addition of graphene nanoplatelets to SiC ceramics enhances the strength and hardness of the material. This improvement is attributed to the ability of the platelets to regulate ceramic grain growth during the lower-temperature stages of the heat treatment process, leading to increased density in the final product [252].

Recent research into the flow characteristics of DIW printing processes demonstrates that the shear rates experienced by inks during extrusion can affect the orientation of filler material particles. Leveraging this phenomenon, Xiao et al. utilised varying shear rates to control the alignment of boron nitride (BN) particles within the ink. Since the thermal conductivity of BN platelets is anisotropic, this controlled orientation during deposition allows for precise tuning of the thermal conductivity in the final ceramic prints [201].

4.2.2. Mechanical properties

Filler composition can critically influence the mechanical properties of the ceramic produced using this manufacturing process. Some of the key influences of the fillers, beyond imparting printability of low viscosity precursors, is the reduction of shrinkage, pores, and microcracks in the processed structure, all of which weaken the part. Fillers have also influenced the hardness, flexibility, and strength of these materials.

Inert fillers such as SiC were noted to decrease the shrinkage within the printed structures and increase the strength of the part [253]. Xiong et al. determined that as the mass ratio of SiC nanoparticulate to polymer precursor was increased, the overall weight loss of the printed part and the dimensional shrinkage of the SiOC lattice decreased significantly. The dispersion of the particulate was also made more uniform in the PDC matrix. Additions of fibrous SiC strengthened the part by pull out and crack deflection effects [228]. Similarly, carbon-based inert fillers have also served to reduce shrinkage and act as rheological modifiers. Reduced graphene oxide is notable for its strong effect on the rheological behaviour due to aggregation within the ink and shows the ability to reduce microcracking in the pyrolyzed structure [5]. Carbon fibre has additionally been used as a modifier and filler, with the goal of increasing the strength of the part. Aligned carbon fibres in the ceramic matrix has shown to increase the toughness of printed filaments, and result in less catastrophic failure after maximum stress of the part is reached [43]. Carbon fibre has additionally resulted in increased bending strength and reduced shrinkage of the printed part, increasing the concentration of the fibres while maintaining printability resulted in parts with minimised linear shrinkage following pyrolysis [140].

Reactive and sacrificial fillers utilise different methods to affect the mechanical properties of the part. Reactive fillers in PDC-based ink are typically used to obtain specific phases, which also serve to strength a part that is printed from this ink. Metallic active fillers such as Ti can increase the yield of the ceramic, reduce linear shrinkage, and generating phases such as TiC and TiSi. The presence of these additional phases resulted in increased hardness and density of the pyrolyzed ceramic [139]. Sacrificial fillers uniquely can improve porosity, influencing the mechanical properties through tunable and interconnected pores within the structure. A study by Huang et al. investigated how polymethyl methacrylate beads of varying sizes could be used to generate a printable polymethyl siloxane ink for DIW. Upon removal of the beads, hierarchical pores were formed within the structure with the goal of increasing the compressive strength of the structure for applications as catalyst supports, and for biomedical and energy storage applications [254].

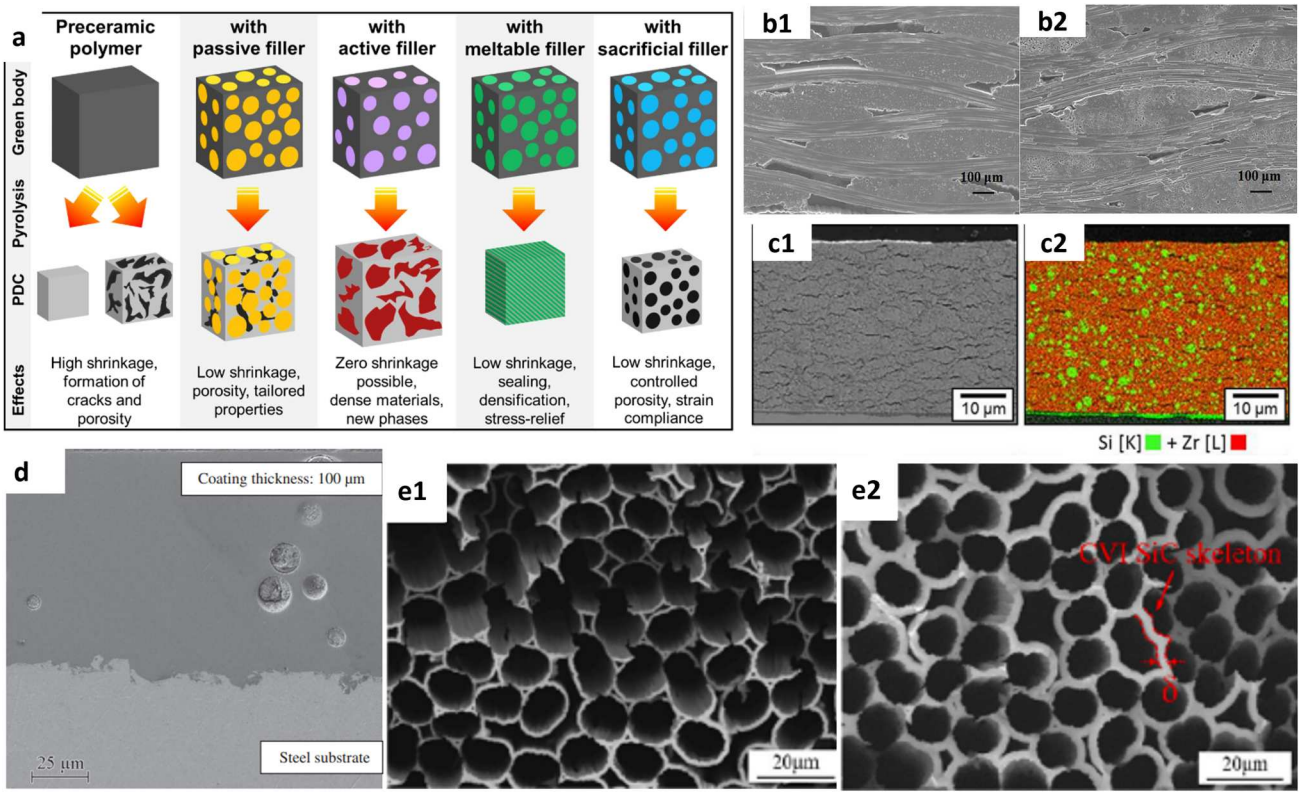

Figure 17. Types of fillers and the structure. (a) Summary of filler types and the resultant structure. Reproduced with permission [53]. Copyright 2019, Royal Society of Chemistry. (b1) Carbon fibre as a passive filler in a SiC matrix, sample 1, (b2) Carbon fibre as a passive filler in a SiC matrix, sample 2. Reproduced with permission [174]. Copyright 2015, Elsevier. (c1) SiCN coating cross section containing active fillers, (c2) EDS mapping of components revealing active filler composition. Reproduced with permission [243]. Copyright 2015, Elsevier. (d) Cross section of PDC coating containing glass or meltable fillers after pyrolysis. Reproduced with permission [244]. Copyright 2012, Elsevier. (e1) Skeleton of porous PDC generated with sacrificial fillers, (e2) SiC ceramic skeleton generated by sacrificial fillers indicated in red. Reproduced with permission [245]. Copyright 2023, Elsevier.

4.2.3. Thermal and electrical properties

The thermal and electrical properties are of particular importance to several applications of ceramics. These properties can be modified in the treatment methods of the polymer, as well as by the fillers that are used during the printing process. Thermal properties that have been modified include the coefficient of thermal expansion, the thermal stability, and the thermal conductivity. Common electrical properties that are modified include the electrical conductivity and resistivity.

The heating of PDCs often induces volumetric changes due to thermal expansion, which is quantified by the Coefficient of Thermal Expansion (CTE). Most PDCs exhibit a positive CTE, which can pose challenges in applications where volumetric stability is critical. To address this issue, lithium aluminum silicates, a class of materials known for their low or negative CTE, have been investigated as filler materials. In a recent study, spodumene, an inexpensive and naturally abundant lithium aluminum silicate, was utilised as an active filler in SiOC-based composites [255]. The incorporation of spodumene enabled precise tuning of the CTE in the final ceramic product, offering a solution to mitigate thermal expansion effects in sensitive applications. Active fillers, TiB_2 and B mitigated the volume shrinkage of a printed SiCN ceramic, also reducing the delamination of layers due to the effect of thermal mismatch [221].

The thermal stability of SiOC ceramics can be improved by incorporating metallic fillers such as zirconium (Zr). This improvement is achieved through the formation of ZrO_2 nanocrystals, which suppress the carbothermal reduction of carbon products during processing. The reduction in free carbon content results in a greater ceramic yield and improved mechanical properties, particularly after exposure to high-temperature conditions [234]. The thermal conductivity is a yet another important thermal property that can be tuned by the presence of fillers in printed ceramics, either increasing this property, or decreasing it further for use as insulators. Thermal conductivity has improved in

Table 5. PDCs printed with the DIW technique.

Ceramic	Precursor	Modifiers	Printed Structure	Heat Treatment	Reported Properties	References
SiC	Polycarbosilane	N-hexane	3D Scaffold	1400°C in Ar	N/A	[246]
	Polymethylsilesquioxane	SiC powder, BYK-180, Carbon fibre, Fumed Silica	410 and 580 µm Filaments	1000°C in N_2	30 MPa Flexural Strength	[43]
	Polymethylsilesquioxane	Dabco $T_{12}N$, Graphene Oxide	Scaffold/Lattice	1000°C in Ar	2.5 ± 0.97 MPa compressive strength	[5]
	Polycarbosilane (SMP-877)	Si_3N_4 powder, Al_2O_3 powder, Y_2O3 powder, crosslinker, photoinitiator	Hexagonal Array, Lattice, Twisted Vase	1200°C in Ar	85–88% Ceramic Yield	[247]
	Polymethylsilesquioxane	3-(trimethoxysilyl)propyl methacrylate, Trimethylolpropane triacrylate, photoinitiator	Lattice	800–1600°C	25%-line shrinkage, 70% Ceramic Yield	[133]
	Polycarbosilane (SMP-10)	ZrB_2 powder, SiC fibre	Lattice, Honeycomb	1200°C in Ar	Pore Area% = 11.16 ± 5.34% to 24.63 ± 5.58%, Avg. Pore Size = 588.1 ± 5.37 µm, 667.2 ± 108.5 µm (major axis)	[80]
	Polymethylsilesquioxane	Zirconium acetylacetonate, TinOc	Kagome Lattice	1000–1200°C in N2	22–32% shrinkage	[225]
	Polycarbosilane	SiC whiskers, SiC powder	Lattice	1000–1400°C	21.3 MPa Tensile strength	[228]
	Polycarbosilane	Chopped Carbon Fibres	Scaffold/Lattice	1200°C	Bending strength maximum at 30 wt% Cf	[195]
	Polycarbosilane	SiC particles, Ti particles	Scaffold/Lattice	1200°C in Ar	19.7 ± 1 MPa tensile strength (without Ti)	[140]
	Polycarbosilane (SMP-10)	ZrB_2 powder, Fumed Alumina	Lattice, Filament	1200°C in Ar	117–458 MPa Flexural strength	[229]
	Polycarbosilane	n-hexane, toluene	Scaffold/Lattice	1100°C in Ar	50–80% porosity, 64.81 ml min^{-1} max H2 production	[150]
SiC + SiOC	Polysiloxane (Nuva-Sil 5039)	SiC powder, Al_2O_3 powder, Y_2O_3 powder, Carbon Black	Turbine, Lattice, Microwave Feedhorn	1250°C Pyrolysis, 1800°C Sinter	microwave transmission band in 8–9 GHz	[175]
SiOC	Silicone Elastomer	Ti-6Al-4V powder, $CaCO_3$ powder	Lattice	1000°C in N_2	Reduced shrinkage with filler	[236]
	Hydroxyl Silicone Oil	SiC powder, nano fused silica	Lattice	1000°C in N_2	Rlmin = −36 dB, thickness = 3.5 mm, EAB = 2 GHz	[166]
SiOC + SiC	Polycarbosilane (SMP-10)	poly(methyl methacrylate), poly(n-butyl acrylate)	Lattice	800°C in Ar	1.946 ± 0.002 g cm^{-3} density,	[13]
SiCN	Polysilazane (Durazane 1800)	H-BN	Flexural Bars, Honeycomb	1000°C in N_2	56.4 ± 0.76 MPa flexural strength, 28.9 ± 1.3 GPa flexural modulus, 111.9 ± 7.11 Vickers microhardness,	[80]
	Polysilazane	TiB_2 powder	Thin-Film Resistor Grid	800°C in Air	0.005–3.4 S cm^{-1} electrical conductivity, stable and low variance up to 800°C	[166]
	Polysilazane	ITO powder B, TiB_2	Thin-Film	Rapid Laser Fabrication	4.7% drift rate at 1000°C for 25 hr, resistance to temperatures up to 1250°C	[222]
	Polysilazane	ITO B, TiB_2	Thin Film	Ultrafast High Temperature Sintering	0.54%h^{-1} drift rate at 900°C	[221]
SiBCN	Polyborosilazane	TiB_2 powder	Filament (Conductive)	1200°C in N_2	Stable and low variance at and under 700C	[166]
$CasSiO_3$ + SiO_2	Polymethylsilesquioxane	Fumed Silica, $CaCO_3$ powder	Scaffold/Lattice	600°C	56–64% interconnected porosity, 2.9–5.5 MPa compressive strength	[248]
Hardystonite	Polymethylsilesquioxane	ZnO, $CaCO_3$, $SrCO_3$, $Mg(OH)_2$, fine glass powders	Scaffold/Lattice	1100°C	0.6–11.6 MPa compressive strength, 48–77% porosity	[249]
Sphene ($CaTiSiO_5$)	Polymethylsilesquioxane	$CaCO_3$, TiO_2	Scaffold/Lattice	1300°C	Low density, high compressive strength, good permeability	[169]
$CaSiO_3$	Polymethylsilesquioxane	$CaCO_3$ powder, methyltriethylsilane, oleic acid	Scaffold/Lattice	900°C	Cold Extrusion: 63% porosity, 2.7 ± 0.62 MPa crushing strength. Hot extrusion: 84% porosity, 0.34 ± 0.02 MPa crushing strength	[29]
Biosilicate Glass	Polymethyl siloxane	$CaCO_3$, Na_2CO_3, Na_2PO_4, Biosilicate™ glass powder	Scaffold	1000°C	Glass-Ceramic foams, 6.7 MPa compressive strength	[250]

DIW ceramics by inclusion of fillers with naturally high thermal conductivity such as inert SiC, and reactive products TiC and ZrC [23,256,257]. The thermal conductivity has also been improved by the orientation of fibrous fillers that have been observed during the printing process due to the shear strain of extrusion. Xiao, et al. noted that the thermal conductivity of the polymer precursor was enhanced as the orientation of the fibres was refined through printing [201].

Electrical properties are of particular interest for applications in the field of energy storage and electrocatalysis, where conductive ceramics would be highly effective [253]. Fibrous SiC, graphene and other carbon-based inert fillers are very commonly added to increase the electrical conductivity of the ceramic, while also modifying the printability of the ink. Graphene is most notable for its ability to improve the electrical conductivity of the composite [81,258,259]. Even in small doping quantities, reduced graphene oxide incorporated into the DIW ink can result in an order of magnitude higher electrical conductivity as when it is present as the only additive [5]. Further improvements in the printability and the electrical conductivity can be made when compatible fillers are paired. Utilising polycarbosilane (PCS) as a SiC source, along with β-SiC particulate and porous graphene as modifiers, a highly conductive, yet lightweight composite structure was printed, achieving a conductivity of 670 Sm^{-1}, attributed to the low resistivity of β-SiC, and the pyrocarbons from the pyrolysis of the PCS forming a network of conductive channels with the porous graphene additive [253].

Alternatively, oxide fillers have proven effective for modifying the electrical properties to obtain high temperature resistance, thin-film sensors. Indium tin oxide (ITO) has acted as the rheological modifier, and electrical property modifying component for printing both conductive SiOC and SiCN ceramics [221,222]. Upon activation the ITO/PDC exhibited monotonic resistance-temperature characteristics, making them feasible for new high-temperature thermistor materials. The printed SiOC/ITO structure achieved extreme temperature resistance of up to 1250°C, with reduced drift at temperatures at or near 1000°C [222]. The printed SiCN/ITO resistance grid obtained very promising electrical conductivity results (706.89 S m^{-1}) while keeping the resistance drift at 900°C very low, showing that ITO as filler and modifier was very effective for obtaining the desired electrical properties [221].

4.2.4. Biological properties

Filler chemistry, particularly the use of active fillers, can influence the generation of materials that are considered biologically compatible, such as the case for bone implants. The inclusion of such active fillers can also have marked effects on the porosity and strength of the part. Studies have used active fillers such as $CaCO_3$ and ZnO to generate hardystonite bioceramic scaffolds, however, volatile byproducts and the porosity generated during the pyrolysis reactions associated with these fillers have shown to compromise the strength of biocompatible materials. To alleviate this problem, researchers have also investigated the usage of pre-synthesised hardystonite to minimise microfractures such as illustrated in Figure 18, combining effects of inert and active fillers, and enhancing the strength of the prints after heat treatment [225]. Additionally, while $CaCO_3$ is commonly used as an active filler, its biocompatibility for bone grafts has led to investigations into its role as an inert filler. Below 600°C, $CaCO_3$ does not decompose and behaves as an inert filler. Fiocco et al. demonstrated that using $CaCO_3$ in combination with polysiloxane and fumed silica for printing bone replacement implants produced scaffolds with mechanical strength comparable to that of natural bone. This outcome was attributed to the complete transformation of the polymer into a ceramic without $CaCO_3$ decomposition. Additionally, the resulting porosity of the printed scaffolds made them suitable for cell adhesion, further supporting their viability for biomedical applications [248].

4.3. Future of additive manufacturing of PDCs

Additive manufacturing is an increasingly well-researched field for the manufacturing of PDCs. There are still many places that this field can be improved, and directions that research can be expanded into.

4.3.1. Hybrid and alternative printing methods for PDCs

UV-Assisted DIW (UV-DIW) is a hybrid method that shows promise for relaxing the rheological constraints that are required for the standard DIW process. This hybrid printing method utilises UV light to cure the printed ink in-situ. This effect is notable for improving the self-supporting nature of the ink and broadening the range of materials that can be printed, even with imperfect rheological properties for DIW under ambient conditions, and imperfect optical conditions for vat polymerisation methods of printing [247,260]. Utilising UV curing in this process can further improve the shape fidelity as well as the strength of the polymer through more extensive crosslinking, further reducing the crack formation during pyrolysis and increasing yield [127,261]. However, this method introduces the need for photocurable inks, which could

potentially be more favourable for printing through alternative printing methods such as vat polymerisation, provided the resin has favourable optical properties.

Beyond DIW, alternative additive manufacturing methods that have been utilised for processing PDCs have included vat polymerisation methods, requiring a photocurable precursor resin, similar to the requirement for UV-DIW. Preceramic precursors are considered very promising for this category of additive manufacturing due to the transparency of the precursor preventing scattering, their stability, and low viscosity. Precursors have been made photocurable through three different methods: functionalization of acrylic or vinyl groups into the precursor, mixing the precursor with a compatible photocurable polymer, or copolymerisation [58]. Of these methods, mixing the precursor with a photocurable polymer is among the most commonly researched; several studies have been dedicated to understanding this type of manufacturing, and have noted a common issue of low yield due to the presence of the photocurable component influencing the crosslinking of the precursor [262–269]. This additive manufacturing method is considered most promising for PDCs due to the dimensional accuracy and the high resolution that vat polymerisation printers are currently capable of, and will become more effective as the high shrinkage and low yield is addressed.

A final glaring knowledge gap is the absence of non-silicon-based PDCs manufactured through the DIW process. UHTCs have several extraordinary properties, but precursors and their synthesis pathways are limited, particularly in the formation of UV-curable precursors [23,270]. Limited synthesis pathways and low yield have limited the application of UHTC and non-silicon-based precursors from additive manufacturing methods outside of pre-synthesised ceramic particulate, which has been manufactured in select studies using DIW [271]. Improvements in the synthesis of UHTC precursors could be highly useful for manufacturing complex parts utilising additive manufacturing methods without the current drawbacks that are seen with particulate methods.

4.3.2. Artificial intelligence as a tool

Artificial intelligence (AI) and machine learning (ML) are novel tools that can potentially be utilised to improve the field of additive manufacturing. In the case of DIW and materials development, ML is beginning to be utilised for developing ink formations, and for the evaluation and refinement of the printing parameters. Chen et al. has evaluated ML as a tool to predict the printability of biomaterial formulations, training the algorithm with 210 different formulations made from 16 different biomaterials, and achieving an accuracy of greater than 80% for the ML methods of decision tree, random forest, and deep learning [272]. ML classifications have evaluated printing parameters, trained on a singular type of ink, based on a polydimethylsiloxane precursor. Four printing parameters were measured, the nozzle diameter, layer height in ratio to the nozzle diameter, the extrusion pressure, and the printing speed, and the results were analyzed with ML models in order to predict the properties that would be best for printing representative structures [273]. Recently ML has been used to also fabricate DIW-printed structures with specific properties. This was done through training a ML model to customise the fabrication of a DIW printed film to achieve the optimum performance with high accuracy [274]. These methods of using ML to improve the printing process could be potentially adapted to DIW and PDCs, to effectively design precursors and inks, as well as optimising the printing parameters for the desired performance.

5. Conclusions and future work

Despite significant advancements in PDCs and their DIW applications, several challenges and areas for further development remain. Polymer-derived ceramics (PDCs) are inherently brittle – a limitation shared with most ceramics. Efforts to address this brittleness and enhance their mechanical and thermal properties have focused on incorporating fillers to create ceramic matrix composites. However, the effects of these inclusions and precursors are only beginning to be studied despite the presented progress on PDCs and their DIW applications. Several areas of work still exist for these materials and methods: Polymer derived ceramics suffer from limitations in their mechanical properties that are common for all ceramics, such as their brittleness. Methods of alleviating the brittleness and improving the mechanical and thermal properties include the inclusion of fillers to create ceramic matrix composites, but the effects of these inclusions and precursors is only now beginning to be covered in depth [38,275,276]. The fabrication of dense bulk structures remains a challenge due to extensive cracking and other defects that can occur during pyrolysis, particularly when the polymer exceeds a critical thickness [229]. Polymer Infiltration and Pyrolysis (PIP) has been explored as a method to produce dense bulk structures, including from 3D-printed scaffolds, but it is a time-intensive process and is limited to low-viscosity precursors [239,240,277,278]. Additionally, the development of high-ceramic-yield precursors for non-silicon-based ceramics is still in its early stages. Current research is limited to specific synthesis reactions that

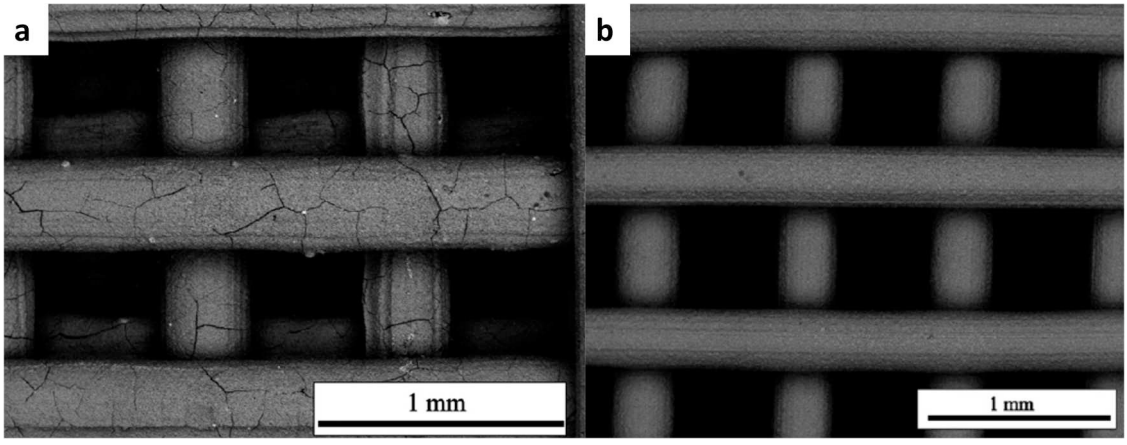

Figure 18. Formation of microcracks in the printed bioceramic scaffold can be seen in (a) after heat treatment at 1200°C. The addition of inert filler in (b) reduces the crack formation. Reproduced with permission [225]. Copyright 2016, Wiley.

often result in decreased or impure ceramics, highlighting a critical need for further innovation and refinement in precursor design [23,105].

Achieving the appropriate rheological properties for DIW inks containing fillers remains a critical challenge. Currently, most fillers are assessed through a trial-and-error approach, which is inefficient for developing a broad range of printable inks. The impact of fillers on the rheological properties of preceramic polymers, as well as their influence on the final ceramic composition, requires more detailed investigation. Additionally, ensuring high shape fidelity during printing is an ongoing challenge. Since print parameters vary depending on ink composition and printer design, developing standardised parameters and designs would greatly facilitate the comparison of inks, print settings, and resulting ceramic compositions.

Future advancements in DIW and for manufacturing PDCs may extend to alternative printing methods, the incorporation of ML, and even beyond Earth. Additive manufacturing, including DIW, has been explored for constructing habitats on the Moon and Mars using local regolith. Current research has focused on leveraging geopolymer reactions or polymers as binders for regolith-based construction materials [279–284]. However, to our knowledge, the use of PDC precursors as binders for such applications has not yet been explored. PDC precursors could potentially serve as effective binders for creating robust composites suited to the extreme conditions of lunar and Martian environments, representing a promising avenue for future research.

The increasing demand for complex high-temperature ceramics and their composites has driven significant research into polymer-derived ceramics (PDCs) and additive manufacturing techniques for ceramics. A diverse range of ceramics can be produced from preceramic polymers, offering properties that are well-suited for high-temperature environments. Precursors have been developed to yield binary, ternary, quaternary, and even non-silicon-based ceramics, each characterised by unique microstructures and properties influenced by curing and pyrolysis conditions. These properties can be further tailored through the incorporation of various fillers. Importantly, PDCs can be processed using methods specific to polymers, including additive manufacturing, enabling the production of intricate and customised ceramic components. The applications of PDCs span structural roles such as components, adhesives, and composite reinforcements, as well as functional uses including electromagnetic wave absorbers, sensors, and electrical components. However, challenges such as brittleness, limited critical thickness, and shrinkage have constrained their broader adoption. Despite these limitations, PDCs present an innovative and versatile alternative to traditional ceramic manufacturing methods, offering exciting opportunities for advancements in high-performance materials.

Direct Ink Writing (DIW) has garnered significant attention in recent years because of its versatility and cost-effectiveness in printing a wide range of materials. With minimal modifications required to produce extrudable inks, DIW offers a straightforward and adaptable approach to additive manufacturing. The most critical property influencing ink extrudability in DIW is rheology, which governs two essential characteristics: flow behaviour and shape fidelity. These requirements are most effectively met by shear-thinning inks. The rheological properties of DIW inks can be assessed through various tests to confirm shear-thinning behaviour, which directly impacts the selection of print parameters. This straightforward printing process enables the

fabrication of complex geometries on both small and large scales. However, when applied to PDCs and ceramics, DIW faces certain limitations, including slower printing speeds and a strong dependency on the viscosity of the slurry ink. Despite these challenges, DIW remains one of the most extensively studied additive manufacturing techniques. Continued advancements are expected to improve both print quality and speed, enhancing its potential for diverse applications.

Disclosure statement

No potential conflict of interest was reported by the author(s).

Data availability statement

Data sharing not applicable – no new data generated.

References

[1] He J, Song M, Chen K, et al. Polymer-derived ceramics technology: characteristics, procedure, product structures, and properties, and development of the technology in high-entropy ceramics. Crystals (Basel). 2022;12:1292. doi:10.3390/cryst12091292

[2] Mera G, Gallei M, Bernard S, et al. Ceramic nanocomposites from tailor-made preceramic polymers. Nanomaterials. 2015;5:468–540. doi:10.3390/nano5020468

[3] Fu S, Zhu M, Zhu Y. Organosilicon polymer-derived ceramics: an overview. J Adv Ceram. 2019;8(4):457–478. doi:10.1007/s40145-019-0335-3

[4] Larson CM, Choi JJ, Gallardo PA, et al. Direct ink writing of silicon carbide for microwave optics. Adv Eng Mater. 2016;18(1):39–45. doi:10.1002/adem.201500298

[5] Pierin G, Grotta C, Colombo P, et al. Direct ink writing of micrometric SiOC ceramic structures using a preceramic polymer. J Eur Ceram Soc. 2016;36(7):1589–1594. doi:10.1016/j.jeurceramsoc.2016.01.047

[6] Marciniec B. Organosilicon – organic hybrid polymers and materials. In: B Marciniec, editor. *Hydrosilylation: a comprehensive review on recent advances*. Dordrecht: Springer Netherlands; 2009. p. 241–286.

[7] Marciniec B. Functionalisation and cross-linking of organosilicon polymers. In: B Marciniec, editor. *Hydrosilylation: a comprehensive review on recent advances* Dordrecht: Springer Netherlands; 2009. p. 159–189.

[8] Colombo P, Mera G, Riedel R, et al. Polymer-derived ceramics: 40 years of research and innovation in advanced ceramics. J Am Ceram Soc. 2010;93(7):1805–1837. doi:10.1111/j.1551-2916.2010.03876.x

[9] Yajima S, Hayashi J, Omori M. Continuous silicon carbide fiber of high tensile strength. Chem Lett. 1975;4(9):931–934. doi:10.1246/cl.1975.931

[10] Ichikawa H. Polymer-derived ceramic fibers. Annu Rev Mater Res. 2016;46(1):335–356. doi:10.1146/annurev-matsci-070115-032127

[11] Chaudhary P, Idrees C, Rasaki M, et al. Additive manufacturing of polymer-derived ceramics: materials, technologies, properties and potential applications. Prog Mater Sci. 2022;128:100969. doi:10.1016/j.pmatsci.2022.100969

[12] Han J, Bradford-Vialva LC, Klosterman RL, et al. Additive manufacturing of advanced ceramics using preceramic polymers. Materials (Basel). 2023;16:4636. doi:10.3390/ma16134636

[13] Bowen JJ, Mooraj S, Goodman JA, et al. Hierarchically porous ceramics via direct writing of preceramic polymer-triblock copolymer inks. Mater Today. 2022;58:71–79. doi:10.1016/j.mattod.2022.07.002

[14] Mamatha S, Biswas P, Johnson R. Digital light processing of ceramics: an overview on process, materials and challenges. Progress in Addit Manuf. 2023;8(5):1083–1102. doi:10.1007/s40964-022-00379-3

[15] Zakeri S, Vippola M, Levänen E. A comprehensive review of the photopolymerization of ceramic resins used in stereolithography. Addit Manuf. 2020;35:101177. doi:10.1016/j.addma.2020.101177

[16] Brinckmann SA, Patra N, Yao J, et al. Stereolithography of SiOC polymer-derived ceramics filled with SiC micronwhiskers. Adv Eng Mater. 2018;20(11):1800593. doi:10.1002/adem.201800593

[17] Reschke V, Bordia RK, Scheffler F, et al. Rheology and crosslinking of a low-viscosity SiOC preceramic polymer. Ceram Int. 2016;42(6):7620–7625. doi:10.1016/j.ceramint.2016.01.171

[18] Greil P. Polymer derived engineering ceramics. Adv Eng Mater. 2000;2(6):339–348. doi:10.1002/1527-2648(200006)2:6<339::AID-ADEM339>3.0.CO;2-K

[19] Colombo P, Bernardo E, Parcianello G. Multifunctional advanced ceramics from preceramic polymers and nano-sized active fillers. J Eur Ceram Soc. 2013;33(3):453–469. doi:10.1016/j.jeurceramsoc.2012.10.006

[20] Zhang Z, Bordia RK, Peng F. Critical thickness of polymer-derived ceramic coatings with particulate fillers. Int J Appl Ceram Technol. 2023;20(1):84–93. doi:10.1111/ijac.14269

[21] Matsoso B, Hao W, Li Y, et al. Synthesis of hexagonal boron nitride 2D layers using polymer derived ceramics route and derivatives. J Phys Mater. 2020;3(3):034002. doi:10.1088/2515-7639/ab854a

[22] Wen Q, Yu Z, Riedel R. The fate and role of in situ formed carbon in polymer-derived ceramics. Prog Mater Sci. 2020;109:100623. doi:10.1016/j.pmatsci.2019.100623

[23] Ackley BJ, Martin KL, Key TS, et al. Advances in the synthesis of preceramic polymers for the formation of silicon-based and ultrahigh-temperature non-oxide ceramics. Chem Rev. 2023;123(8):4188–4236. doi:10.1021/acs.chemrev.2c00381

[24] Wang X, Gao X, Zhang Z, et al. Advances in modifications and high-temperature applications of silicon carbide ceramic matrix composites in aerospace: a focused review. J Eur Ceram Soc. 2021;41(9):4671–4688. doi:10.1016/j.jeurceramsoc.2021.03.051

[25] Ren Z, Mujib SB, Singh G. High-temperature properties and applications of Si-based polymer-derived ceramics: a review. Materials (Basel). 2021;14:614. doi:10.3390/ma14030614

[26] Nyczyk-Malinowska A, Niemiec W, Smoła G, et al. Preparation and characterization of oxidation-resistant

black glass (SiCO) coatings obtained by hydrosilylation of polysiloxanes. Surf Coat Technol. 2021;407:126760. doi:10.1016/j.surfcoat.2020.126760

[27] Wang M, Dong X, Tao X, et al. Joining of various engineering ceramics and composites by a modified preceramic polymer for high-temperature application. J Eur Ceram Soc. 2015;35(15):4083–4097. doi:10.1016/j.jeurceramsoc.2015.07.036

[28] Luan XG, Chang S, Riedel R, et al. An air stable high temperature adhesive from modified SiBCN precursor synthesized via polymer-derived-ceramic route. Ceram Int. 2018;44(7):8476–8483. doi:10.1016/j.ceramint.2018.02.045

[29] Francis A. Progress in polymer-derived functional silicon-based ceramic composites for biomedical and engineering applications. Mater Res Express. 2018;5(6):062003. doi:10.1088/2053-1591/aacd28

[30] Cramer CL, Ionescu E, Graczyk-Zajac M, et al. Additive manufacturing of ceramic materials for energy applications: road map and opportunities. J Eur Ceram Soc. 2022;42(7):3049–3088. doi:10.1016/j.jeurceramsoc.2022.01.058

[31] Zhang Z, Calderon JE, Fahad S, et al. Polymer-derived ceramic nanoparticle/edge-functionalized graphene oxide composites for lithium-ion storage. ACS Appl Mater Interfaces. 2021;13(8):9794–9803. doi:10.1021/acsami.0c19681

[32] Wen Q, Qu F, Yu Z, et al. Si-based polymer-derived ceramics for energy conversion and storage. J Adv Ceram. 2022;11(2):197–246. doi:10.1007/s40145-021-0562-2

[33] Abass MA, Syed AA, Gervais C, et al. Synthesis and electrochemical performance of a polymer-derived silicon oxycarbide/boron nitride nanotube composite. RSC Adv. 2017;7(35):21576–21584. doi:10.1039/C7RA01545C

[34] Mukherjee S, Ren Z, Singh G. Molecular polymer-derived ceramics for applications in electrochemical energy storage devices. J Phys D: Appl Phys. 2018;51(46):463001. doi:10.1088/1361-6463/aadb18

[35] Loughney PA, Mujib SB, Pruyn TL, et al. Enhancing organosilicon polymer-derived ceramic properties. J Appl Phys. 2022;132(7):070901. doi:10.1063/5.0085844

[36] Xia A, Yin J, Chen X, et al. Polymer-Derived Si-based ceramics: recent developments and perspectives. Crystals (Basel). 2020;10:824. doi:10.3390/cryst10090824

[37] Duan W, Yin X, Li Q, et al. A review of absorption properties in silicon-based polymer derived ceramics. J Eur Ceram Soc. 2016;36(15):3681–3689. doi:10.1016/j.jeurceramsoc.2016.02.002

[38] Chen Q, Li D, Liao X, et al. Polymer-derived lightweight SiBCN ceramic nanofibers with high microwave absorption performance. ACS Appl Mater Interfaces. 2021;13(29):34889–34898. doi:10.1021/acsami.1c07912

[39] Farahani RD, Dubé M, Therriault D. Three-dimensional printing of multifunctional nanocomposites: manufacturing techniques and applications. Adv Mater. 2016;28(28):5794–5821. doi:10.1002/adma.201506215

[40] Wohlers T, et al. Wohlers report 2020 3D printing and additive manufacturing state of the industry. Fort Collins: Wohlers Associates; 2020.

[41] Brinckmann SA, Yao J, Young JC, et al. Additive manufacturing of SiCNO polymer-derived ceramics via step-growth polymerization. Open Ceram. 2023;15:100414. doi:10.1016/j.oceram.2023.100414

[42] Chen L, Zhao J, Wang L, et al. In-situ pyrolyzed polymethylsilsesquioxane multi-walled carbon nanotubes derived ceramic nanocomposites for electromagnetic wave absorption. Ceram Int. 2019;45(9):11756–11764. doi:10.1016/j.ceramint.2019.03.052

[43] Franchin G, Wahl L, Colombo P. Direct ink writing of ceramic matrix composite structures. J Am Ceram Soc. 2017;100(10):4397–4401. doi:10.1111/jace.15045

[44] Kocyło E, Franchin G, Colombo P, et al. Hydroxyapatite-coated ZrO2 scaffolds with a fluorapatite intermediate layer produced by direct ink writing. J Eur Ceram Soc. 2021;41(1):920–928. doi:10.1016/j.jeurceramsoc.2020.08.021

[45] Elsayed H, Chmielarz A, Potoczek M, et al. Direct ink writing of three dimensional Ti_2AlC porous structures. Addit Manuf. 2019;28:365–372. doi:10.1016/j.addma.2019.05.018

[46] Lamnini S, Elsayed H, Lakhdar Y, et al. Robocasting of advanced ceramics: ink optimization and protocol to predict the printing parameters-A review. Heliyon. 2022;8(9):e10651.

[47] Kaindl A, Lehner W, Greil P, et al. Polymer-filler derived Mo_2C ceramics. Mater Sci Eng A. 1999;260(1-2):101–107. doi:10.1016/S0921-5093(98)00987-3

[48] Dernovsek O, Bressiani JC, Bressiani AHA, et al. Reaction bonded niobium carbide ceramics from polymer-filler mixtures. J Mater Sci. 2000;35:2201–2207. doi:10.1023/A:1004766607619

[49] Jiang Z, Erol O, Chatterjee D, et al. Direct ink writing of poly (tetrafluoroethylene)(PTFE) with tunable mechanical properties. ACS Appl Mater Interfaces. 2019;11(31):28289–28295. doi:10.1021/acsami.9b07279

[50] Shibuya M, Sakurai M, Takahashi T. Preparation and characteristics of a vapor-grown carbon fiber/ceramic composite using a methylsilicone precursor. Compos Sci Technol. 2007;67(15–16):3338–3344. doi:10.1016/j.compscitech.2007.03.023

[51] Ionescu E, Kleebe H-J, Riedel R. Silicon-containing polymer-derived ceramic nanocomposites (PDC-NCs): preparative approaches and properties. Chem Soc Rev. 2012;41(15):5032–5052. doi:10.1039/c2cs15319j

[52] Bernardo E, Fiocco L, Parcianello G, et al. Advanced ceramics from preceramic polymers modified at the nanoscale: a review. Materials (Basel). 2014;7(3):1927–1956. doi:10.3390/ma7031927

[53] Barroso G, Li Q, Bordia RK, et al. Polymeric and ceramic silicon-based coatings–a review. J Mater Chem A. 2019;7(5):1936–1963. doi:10.1039/C8TA09054H

[54] Eckel ZC, Zhou C, Martin JH, et al. Additive manufacturing of polymer-derived ceramics. Science. 2016;351(6268):58–62. doi:10.1126/science.aad2688

[55] Packirisamy S, Sreejith KJ, Devapal D, et al. Polymer-derived ceramics and their space applications. In: Y Mahajan, J Roy, editors. *Handbook of advanced ceramics and composites: defense, security, aerospace and energy applications*. Cham: Springer International Publishing; 2020. p. 1–107.

[56] Ionescu E, Bernard S, Lucas R, et al. Polymer-derived ultra-high temperature ceramics (UHTCs) and related

materials. Adv Eng Mater. 2019;21(8):1900269. doi:10.1002/adem.201900269
[57] Zunjarrao SC, Rahman A, Singh RP. Characterization of the evolution and properties of silicon carbide derived from a preceramic polymer precursor. J Am Ceram Soc. 2013;96(6):1869–1876. doi:10.1111/jace.12273
[58] Lacelle T, Sampson KL, Yazdani Sarvestani H, et al. Additive manufacturing of polymer derived ceramics: materials, methods, and applications. APL Mater. 2023;11(7):070602. doi:10.1063/5.0151661
[59] Hilbig A, Müller E, Wenzel R, et al. The microstructure of polymer-derived amorphous silicon carbide layers. J Eur Ceram Soc. 2005;25(2):151–156. doi:10.1016/j.jeurceramsoc.2004.07.011
[60] Chaim R, Heuer AH, Chen RT. Microstructural and microchemical characterization of silicon carbide and silicon carbonitride ceramic fibers produced from polymer precursors. J Am Ceram Soc. 1988;71(11):960–969. doi:10.1111/j.1151-2916.1988.tb07566.x
[61] Higginbotham AL, Moloney PG, Waid MC, et al. Carbon nanotube composite curing through absorption of microwave radiation. Compos Sci Technol. 2008;68(15):3087–3092. doi:10.1016/j.compscitech.2008.07.004
[62] Okoroanyanwu U, Bhardwaj A, Einck V, et al. Rapid preparation and electrochemical energy storage applications of silicon carbide and silicon oxycarbide ceramic/carbon nanocomposites derived via flash photothermal pyrolysis of organosilicon preceramic polymers. Chem Mater. 2021;33(2):678–694. doi:10.1021/acs.chemmater.0c04048
[63] Wang Z, Ge M, Yu S, et al. Microstructural evolution of polymer-derived hexagonal boron nitride fibres under high-temperature stretching. J Adv Ceram. 2023;12(10):1973–1988. doi:10.26599/JAC.2023.9220801
[64] Riedel R, Seher M, Mayer J, et al. Polymer-derived Si-based bulk ceramics, Part I: preparation, processing and properties. J Eur Ceram Soc. 1995;15(8):703–715. doi:10.1016/0955-2219(95)00041-R
[65] Kizhakke Veettil S, Kollarigowda RH, Thakur P. Approaches to preceramic polymer fiber fabrication and on-demand applications. Materials (Basel). 2022;15:4546. doi:10.3390/ma15134546
[66] Bao X, Edirisinghe MJ. Polycyclodisilazane: a new polymeric precursor for silicon nitride-based ceramics. J Mater Chem. 2000;10(2):395–401. doi:10.1039/a907898c
[67] Mera G, Navrotsky A, Sen S, et al. Polymer-derived SiCN and SiOC ceramics – structure and energetics at the nanoscale. J Mater Chem A. 2013;1(12):3826–3836. doi:10.1039/c2ta00727d
[68] Barrios E, Zhai L. A review of the evolution of the nanostructure of SiCN and SiOC polymer derived ceramics and the impact on mechanical properties. Mol Syst Des Eng. 2020;5(10):1606–1641. doi:10.1039/D0ME00123F
[69] Bik M, Jeleń P, Długoń E, et al. SiAlOC glasses derived from sol-gel synthesized ladder-like silsesquioxanes. Ceram Int. 2019;45(2, Part A):1683–1690. doi:10.1016/j.ceramint.2018.10.047
[70] Sugie C, Navrotsky A, Lauterbach S, et al. Structure and thermodynamics of silicon oxycarbide polymer-derived ceramics with and without mixed-bonding. Materials (Basel). 2021;14:4075. doi:10.3390/ma14154075
[71] Costa BH, de Silva M, Tarley CR, et al. Influence of polymer synthesis route and organic fraction content on structure and porosity of silicon oxycarbide ceramics. Process Appl Ceram. 2023;17(2):118–132. doi:10.2298/PAC2302118C
[72] Kim KJ, Eom J-H, Koh TY, et al. Effects of carbon addition on the electrical properties of bulk silicon-oxycarbide ceramics. J Eur Ceram Soc. 2016;36(11):2705–2711. doi:10.1016/j.jeurceramsoc.2016.04.034
[73] Sorarù GD, Kundanati L, Santhosh B, et al. Influence of free carbon on the Young's modulus and hardness of polymer-derived silicon oxycarbide glasses. J Am Ceram Soc. 2019;102(3):907–913. doi:10.1111/jace.16131
[74] Drechsel C, Peterlik H, Gierl-Mayer C, et al. Influence of DVB as linker molecule on the micropore formation in polymer-derived SiCN ceramics. J Eur Ceram Soc. 2021;41(6):3292–3302. doi:10.1016/j.jeurceramsoc.2021.01.051
[75] Leonel GJ, Guo X, Singh G, et al. Energetics and structure of SiC(N)(O) polymer-derived ceramics. J Am Ceram Soc. 2023;106(8):5086–5101. doi:10.1111/jace.19153
[76] Liu M, Wang G, Miao Y, et al. Polymer-derived $Co_2Si(Co)$/SiCN composite ceramics with tunable microwave absorption properties. Int J Appl Ceram Technol. 2023;20(5):2930–2941. doi:10.1111/ijac.14395
[77] Golczewski JA, Aldinger F. Phase separation in Si–(B)–C–N polymer-derived ceramics. Int J Mater Res. 2006;97(2):114–118.
[78] Adigun OD, Ricohermoso E, Daniyan AA, et al. Structure and electrical properties of carbon-rich polymer derived silicon carbonitride (SiCN). Ceramics. 2022;5:690–705. doi:10.3390/ceramics5040050
[79] Kemp JW. Processing of preceramic polymers for direct-ink writing. Knoxville: University of Tennessee; 2021. p. 151.
[80] Mirkhalaf M, Yazdani Sarvestani H, Yang Q, et al. A comparative study of nano-fillers to improve toughness and modulus of polymer-derived ceramics. Sci Rep. 2021;11(1):6951. doi:10.1038/s41598-021-82365-3
[81] Román-Manso B, Moyano JJ, Pérez-Coll D, et al. Polymer-derived ceramic/graphene oxide architected composite with high electrical conductivity and enhanced thermal resistance. J Eur Ceram Soc. 2018;38(5):2265–2271. doi:10.1016/j.jeurceramsoc.2017.12.060
[82] Chen Y, Yang X, Cao Y, et al. Quantitative study on structural evolutions and associated energetics in polysilazane-derived amorphous silicon carbonitride ceramics. Acta Mater. 2014;72:22–31. doi:10.1016/j.actamat.2014.03.049
[83] Mocaer D, Pailler R, Naslain R, et al. Si-C-N ceramics with a high microstructural stability elaborated from the pyrolysis of new polycarbosilazane precursors. J Mater Sci. 1993;28(10):2639–2653. doi:10.1007/BF00356198
[84] Ryu H-Y, Wang Q, Raj R. Ultrahigh-Temperature semiconductors made from polymer-derived ceramics. J Am Ceram Soc. 2010;93(6):1668–1676. doi:10.1111/j.1551-2916.2010.03623.x
[85] Yang W, Wang W, Xie C. Amorphous SiCNO hollow nanofibers with mesoporous walls. J Am Ceram Soc. 2019;102(4):1553–1559. doi:10.1111/jace.16222

[86] Hauser R, Nahar-Borchard S, Riedel R, et al. Polymer-Derived SiBCN ceramic and their potential application for high temperature membranes. J Ceram Soc Jpn. 2006;114(1330):524–528.
[87] Wang B, Song Y, Zhang X, et al. Polymer derived SiBCN(O) ceramics with tunable element content. Ceram Int. 2022;48(7):10280–10287. doi:10.1016/j.ceramint.2021.12.246
[88] Viard A, Fonblanc D, Lopez-Ferber D, et al. Polymer derived Si–B–C–N ceramics: 30 years of research. Adv Eng Mater. 2018;20(10):1800360. doi:10.1002/adem.201800360
[89] Ambadas G, Packirisamy S, Ninan KN. Synthesis, characterization and thermal properties of boron and silicon containing preceramic oligomers. J Mater Sci Lett. 2002;21(13):1003–1005. doi:10.1023/A:1016004522824
[90] Sarkar S, Gan Z, An L, et al. Structural evolution of polymer-derived amorphous SiBCN ceramics at high temperature. J Phys Chem C. 2011;115(50):24993–25000. doi:10.1021/jp203287h
[91] Yu Y, Li J, Niu J, et al. Preparation and temperature-resistance characteristics of novel dense SiAlCN ceramics. Ceram Int. 2018;44(18):22473–22480. doi:10.1016/j.ceramint.2018.09.016
[92] Wang Y, Fan Y, Zhang L, et al. Polymer-derived SiAlCN ceramics resist oxidation at 1400°C. Scr Mater. 2006;55(4):295–297. doi:10.1016/j.scriptamat.2006.05.004
[93] Yu Y, Li J, Niu J, et al. The stability and repeatability of high temperature electrical properties of SiAlCN ceramic sensor heads. Ceram Int. 2019;45(6):7588–7593. doi:10.1016/j.ceramint.2019.01.053
[94] Liu K, Ma C, Han D, et al. Temperature-dependent electrical and dielectric behavior of polymer-derived SiAlCN ceramics. Ceram Int. 2024;50(4):6146–6153. doi:10.1016/j.ceramint.2023.11.324
[95] Dhamne A, Xu W, Fookes BG, et al. Polymer–ceramic conversion of liquid polyaluminasilazanes for SiAlCN ceramics. J Am Ceram Soc. 2005;88(9):2415–2419. doi:10.1111/j.1551-2916.2005.00481.x
[96] Bernard S, Miele P. Polymer-derived boron nitride: a review on the chemistry, shaping and ceramic conversion of borazine derivatives. Materials (Basel). 2014;7:7436–7459. doi:10.3390/ma7117436
[97] Lei Y-p, Wang Y-d, Song Y-c, et al. Novel processable precursor for BN by the polymer-derived ceramics route. Ceram Int. 2011;37(8):3005–3009. doi:10.1016/j.ceramint.2011.04.021
[98] Fazen PJ, Remsen EE, Beck JS, et al. Synthesis, properties, and ceramic conversion reactions of polyborazylene. A high-yield polymeric precursor to boron nitride. Chem Mater. 1995;7(10):1942–1956. doi:10.1021/cm00058a028
[99] Eichler J, Lesniak C. Boron nitride (BN) and BN composites for high-temperature applications. J Eur Ceram Soc. 2008;28(5):1105–1109. doi:10.1016/j.jeurceramsoc.2007.09.005
[100] Cornu D, Bernard S, Duperrier S, et al. Alkylaminoborazine-based precursors for the preparation of boron nitride fibers by the polymer-derived ceramics (PDCs) route. J Eur Ceram Soc. 2005;25(2):111–121. doi:10.1016/j.jeurceramsoc.2004.07.016
[101] Interrante LV, Carpenter LE, Whitmarsh C, et al. Studies of organometallic precursors to aluminum nitride. MRS Online Proc Lib. 1986;73(1):359–366. doi:10.1557/PROC-73-359
[102] Baik Y, Drew RAL. Aluminum nitride: processing and applications. Key Eng Mater. 1996;122-124:553. doi:10.4028/www.scientific.net/KEM.122-124.553
[103] Haider ST, Shah MA, Lee D-G, et al. A review of the recent applications of aluminum nitride-based piezoelectric devices. IEEE Access. 2023;11:58779–58795. doi:10.1109/ACCESS.2023.3276716
[104] Termoss H, Bechelany M, Toury B, et al. Shaping potentialities of aluminum nitride polymeric precursors: preparation of thin coatings and 1D nanostructures in liquid phase. J Eur Ceram Soc. 2009;29(5):857–861. doi:10.1016/j.jeurceramsoc.2008.07.006
[105] Shimokawa Y, Fujiwara A, Ionescu E, et al. Formation of aluminum nitride from metal-organic precursors synthesized by reacting aluminum tri-chloride with bis(trimethylsilyl)carbodiimide. J Ceram Soc Jpn. 2015;123(1435):106–113.
[106] Zhang X, Yu M, Indris S, et al. Reactions of metal chlorides with hexamethyldisilazane: novel precursors to aluminum nitride and beyond. J Am Ceram Soc. 2022;105(4):2474–2488. doi:10.1111/jace.18271
[107] Keller TM, Laskoski M, Saab AP, et al. In situ formation of nanoparticle titanium carbide/nitride shaped ceramics from meltable precursor composition. J Phys Chem C. 2014;118(51):30153–30161. doi:10.1021/jp5082388
[108] Liu S, Li B, Wu Y, et al. Mechanochemically assisted synthesis of titanium carbonitride from metal and organic precursor. J Am Ceram Soc. 2020;103(11):6112–6119. doi:10.1111/jace.17329
[109] Su K, Sneddon LG. Polymer-precursor routes to metal borides: synthesis of titanium boride (TiB_2) and zirconium boride (ZrB_2). Chem Mater. 1991;3(1):10–12. doi:10.1021/cm00013a005
[110] Kim B-S, Kim DJ. Ti-based ceramic composites derived from polymer pyrolysis. J Eur Ceram Soc. 2007;27(2):837–841. doi:10.1016/j.jeurceramsoc.2006.04.035
[111] Kim BS, Hong SJ, Kim DJ. Formation of high-density TiN/Ti_5Si_3 ceramic composites using preceramic polymer. Met Mater Int. 2010;16(4):565–568. doi:10.1007/s12540-010-0807-z
[112] Seyferth D, Mignani G. Preparation of titanium nitride and titanium carbonitride by the preceramic polymer route. J Mater Sci Lett. 1988;7(5):487–488. doi:10.1007/BF01730700
[113] Bechelany MC, Proust V, Lale A, et al. Nanocomposites through the chemistry of single-source precursors: understanding the role of chemistry behind the design of monolith-type nanostructured titanium nitride/silicon nitride. Chem – A Eur J. 2017;23(4):832–845. doi:10.1002/chem.201603661
[114] Gong W, Ye L, Song R, et al. Polymer-derived W-doping (Zr, Hf, Nb, Ta)C high entropy ceramics: preparation, properties and DFT calculation. Ceram Int. 2024;50(5):8284–8293. doi:10.1016/j.ceramint.2023.12.162
[115] Zhou Y, Lu K. Polymer-Derived high-temperature nonoxide materials: a review. Adv Eng Mater. 2023;25(9):2200967. doi:10.1002/adem.202200967

[116] Dong Z, Zhang X, Huang Q, et al. Synthesis and pyrolysis behavior of a soluble polymer precursor for ultra-fine zirconium carbide powders. Ceram Int. 2015;41(6):7359–7365. doi:10.1016/j.ceramint.2015.02.039
[117] Fu Y, Zhang Y, Yan H, et al. Microstructure and evolution of hafnium carbide whiskers via polymer-derived ceramics: A novel formation mechanism. J Adv Ceram. 2023;12(3):578–586. doi:10.26599/JAC.2023.9220706
[118] Du B, Liu H, Chu Y. Fabrication and characterization of polymer-derived high-entropy carbide ceramic powders. J Am Ceram Soc. 2020;103(8):4063–4068. doi:10.1111/jace.17134
[119] Wang K, Zhao K, Meng Q, et al. Preparation of zirconium carbide nanofibers by electrospinning of pure zirconium-containing polymer. Ceram Int. 2022;48(17):25474–25483. doi:10.1016/j.ceramint.2022.05.226
[120] Liu H, Du B, Chu Y. Synthesis of the ternary metal carbide solid-solution ceramics by polymer-derived-ceramic route. J Am Ceram Soc. 2020;103(5):2970–2974. doi:10.1111/jace.16993
[121] Key TS, Patel DK, Wilks GB, et al. Modeling the pyrolysis of preceramic polymers: A kinetic study of the polycarbosilane SMP-10. J Eur Ceram Soc. 2021;41(13):6356–6365. doi:10.1016/j.jeurceramsoc.2021.06.011
[122] Traßl S, Suttor D, Motz G, et al. Structural characterisation of silicon carbonitride ceramics derived from polymeric precursors. J Eur Ceram Soc. 2000;20(2):215–225. doi:10.1016/S0955-2219(99)00142-9
[123] Deriabin KV, Lobanovskaia EK, Novikov AS, et al. Platinum-catalyzed reactions between Si–H groups as a new method for cross-linking of silicones. Org Biomol Chem. 2019;17(22):5545–5549. doi:10.1039/C9OB00791A
[124] Deriabin KV, Dobrynin MV, Islamova RM. A metal-free radical technique for cross-linking of polymethylhydrosiloxane or polymethylvinylsiloxane using AIBN. Dalton Trans. 2020;49(26):8855–8858. doi:10.1039/D0DT01061H
[125] Qazzazie-Hauser A, Honnef K, Hanemann T. Crosslinking behavior of UV-cured polyorganosilazane as polymer-derived ceramic precursor in ambient and nitrogen atmosphere. Polymers (Basel). 2021;13:2424. doi:10.3390/polym13152424
[126] Decker C. Photoinitiated crosslinking polymerisation. Prog Polym Sci. 1996;21(4):593–650. doi:10.1016/0079-6700(95)00027-5
[127] Wei L, Li J, Zhang S, et al. Fabrication of SiOC ceramic with cellular structure via UV-assisted direct ink writing. Ceram Int. 2020;46(3):3637–3643. doi:10.1016/j.ceramint.2019.10.083
[128] Al-Ajrash SMN, Al-Ajrash SMN, Browning C, et al. Innovative procedure for 3D printing of hybrid silicon carbide/carbon fiber nanocomposites. Nano Select. 2021;2(11):2201–2208. doi:10.1002/nano.202100011
[129] Poerschke DL, Braithwaite A, Park D, et al. Crystallization behavior of polymer-derived Si-O-C for ceramic matrix composite processing. Acta Mater. 2018;147:329–341. doi:10.1016/j.actamat.2018.01.052
[130] Chauhan PK, Sujith R, Parameshwaran R, et al. Role of polysiloxanes in the synthesis of aligned porous silicon oxycarbide ceramics. Ceram Int. 2019;45(7, Part A):8150–8156. doi:10.1016/j.ceramint.2019.01.116
[131] Wang X, Wang J, Wang H. Joining of Al_2O_3 ceramics via preceramic polymer and inorganic additives. Mater Sci Eng A. 2013;576:1–5. doi:10.1016/j.msea.2013.03.060
[132] Apostolov ZD, Heckman EP, Key TS, et al. Effects of low-temperature treatment on the properties of commercial preceramic polymers. J Eur Ceram Soc. 2020;40(8):2887–2895. doi:10.1016/j.jeurceramsoc.2020.02.030
[133] Torrey JD, Bordia RK, Henager CH, et al. Composite polymer derived ceramic system for oxidizing environments. J Mater Sci. 2006;41(14):4617–4622. doi:10.1007/s10853-006-0242-1
[134] Nedunchezhian S, Sujith R, Kumar R. Processing and characterization of polymer precursor derived silicon oxycarbide ceramic foams and compacts. J Adv Ceram. 2013;2(4):318–324. doi:10.1007/s40145-013-0078-5
[135] Sujith R, Jothi S, Zimmermann A, et al. Mechanical behaviour of polymer derived ceramics – a review. Int Mater Rev. 2021;66(6):426–449. doi:10.1080/09506608.2020.1784616
[136] Vakifahmetoglu C, Colombo P, Carturan SM, et al. Growth of one-dimensional nanostructures in porous polymer-derived ceramics by catalyst-assisted pyrolysis. Part II: cobalt catalyst. J Am Ceram Soc. 2010;93(11):3709–3719. doi:10.1111/j.1551-2916.2010.03974.x
[137] Vakifahmetoglu C, Pippel E, Woltersdorf J, et al. Growth of one-dimensional nanostructures in porous polymer-derived ceramics by catalyst-assisted pyrolysis. Part I: iron catalyst. J Am Ceram Soc. 2010;93(4):959–968. doi:10.1111/j.1551-2916.2009.03448.x
[138] Yan Y, Fei X, Huang L, et al. Effect of BN content on the structural, mechanical, and dielectric properties of PDCs-SiCN(BN) composite ceramics. J Am Ceram Soc. 2023;106(11):6951–6961. doi:10.1111/jace.19300
[139] Xiong H, Zhao L, Chen H, et al. Building SiC-based composites from polycarbosilane-derived 3D-SiC scaffolds via polymer impregnation and pyrolysis (PIP). J Eur Ceram Soc. 2021;41(2):1121–1131. doi:10.1016/j.jeurceramsoc.2020.09.059
[140] Liu H, Mei D, Yu S, et al. Direct ink writing of chopped carbon fibers reinforced polymer-derived SiC composites with low shrinkage and high strength. J Eur Ceram Soc. 2023;43(2):235–244. doi:10.1016/j.jeurceramsoc.2022.10.012
[141] Liu X, Li Y-L, Hou F. Fabrication of SiOC ceramic microparts and patterned structures from polysiloxanes via liquid cast and pyrolysis. J Am Ceram Soc. 2009;92(1):49–53. doi:10.1111/j.1551-2916.2008.02849.x
[142] Narisawa M, Funabiki F, Iwase A, et al. Effects of atmospheric composition on the molecular structure of synthesized silicon oxycarbides. J Am Ceram Soc. 2015;98(10):3373–3380. doi:10.1111/jace.13756
[143] Liang T, Li Y-L, Su D, et al. Silicon oxycarbide ceramics with reduced carbon by pyrolysis of polysiloxanes in water vapor. J Eur Ceram Soc. 2010;30(12):2677–2682. doi:10.1016/j.jeurceramsoc.2010.04.005
[144] Bawane K, Erb D, Lu K. Carbon content and pyrolysis atmosphere effects on phase development in SiOC systems. J Eur Ceram Soc. 2019;39(9):2846–2854. doi:10.1016/j.jeurceramsoc.2019.03.032

[145] Erb D, Lu K. Additive and pyrolysis atmosphere effects on polysiloxane-derived porous SiOC ceramics. J Eur Ceram Soc. 2017;37(15):4547–4557. doi:10.1016/j.jeurceramsoc.2017.06.036
[146] Takeda M, Saeki A, Sakamoto J, et al. Effect of hydrogen atmosphere on pyrolysis of cured polycarbosilane fibers. J Am Ceram Soc. 2000;83(5):1063–1069. doi:10.1111/j.1151-2916.2000.tb01331.x
[147] Mutin PH. Control of the composition and structure of silicon oxycarbide and oxynitride glasses derived from polysiloxane precursors. J Sol-Gel Sci Technol. 1999;14(1):27–38. doi:10.1023/A:1008769913083
[148] Jiang Z, Rhine WE. Preparation of titanium nitride (TiN) and titanium carbide (TiC) from a polymeric precursor. Chem Mater. 1991;3(6):1132–1137. doi:10.1021/cm00018a033
[149] Yu SH, Riman RE, Danforth SC, et al. Pyrolysis of titanium-metal-filled poly(siloxane) preceramic polymers: effect of atmosphere on pyrolysis product chemistry. J Am Ceram Soc. 1995;78(7):1818–1824. doi:10.1111/j.1151-2916.1995.tb08894.x
[150] Cheng T, Wang X, Zhang R, et al. Tensile properties of two-dimensional carbon fiber reinforced silicon carbide composites at temperatures up to 2300 °C. J Eur Ceram Soc. 2020;40(3):630–635. doi:10.1016/j.jeurceramsoc.2019.10.030
[151] Guria JF, Bansal A, Kumar V. Effect of additives on the thermal conductivity of zirconium diboride based composites – a review. J Eur Ceram Soc. 2021;41(1):1–23. doi:10.1016/j.jeurceramsoc.2020.08.051
[152] Wang K, Unger J, Torrey JD, et al. Corrosion resistant polymer derived ceramic composite environmental barrier coatings. J Eur Ceram Soc. 2014;34(15):3597–3606. doi:10.1016/j.jeurceramsoc.2014.05.036
[153] Torrey JD, Bordia RK. Processing of polymer-derived ceramic composite coatings on steel. J Am Ceram Soc. 2008;91(1):41–45. doi:10.1111/j.1551-2916.2007.02019.x
[154] Torrey JD, Bordia RK. Mechanical properties of polymer-derived ceramic composite coatings on steel. J Eur Ceram Soc. 2008;28(1):253–257. doi:10.1016/j.jeurceramsoc.2007.05.013
[155] Alvi SA, Akhtar F. High temperature tribology of polymer derived ceramic composite coatings. Sci Rep. 2018;8(1):15105. doi:10.1038/s41598-018-33441-8
[156] Wendel J-F, Lenz Leite M, Furtat P, et al. New coatings systems with improved mechanical properties by combining polymer derived ceramic and physical vapor deposition coating methods. Adv Mater Interfaces. 2022;9(34):2201654. doi:10.1002/admi.202201654
[157] Bik M, Galetz M, Dąbrowa J, et al. Polymer derived ceramics based on SiAlOC glasses as novel protective coatings for ferritic steel. Appl Surf Sci. 2022;576:151826. doi:10.1016/j.apsusc.2021.151826
[158] Xue J, Hou Y, Chu W, et al. Advanced pressurelessly prepared adhesive composites based on modified preceramic polymer for the joining of amorphous SiBON ceramics. Ceram Int. 2023;49(16):26847–26859. doi:10.1016/j.ceramint.2023.05.221
[159] Luan X, Chang S, Riedel R, et al. The improvement in thermal and mechanical properties of TiB_2 modified adhesive through the polymer-derived-ceramic route. Ceram Int. 2018;44(16):19505–19511. doi:10.1016/j.ceramint.2018.07.190
[160] Wang X, Shi J, Wang H. Preparation, properties, and structural evolution of a novel polyborosilazane adhesive, temperature-resistant to 1600°C for joining SiC ceramics. J Alloys Compd. 2019;772:912–919. doi:10.1016/j.jallcom.2018.09.110
[161] Xue J, Hou Y, Zhang L, et al. Synthesis of novel vinyl preceramic polymer (PBSZ) adhesives and their performances in ceramic joints. Ceram Int. 2024;50(1, Part A):1038–1049. doi:10.1016/j.ceramint.2023.10.197
[162] Chen Y, Cao Y, Wang Y. Electrical property of joints made of polymer-derived SiAlCN ceramic via adhesive joining. Ceram Int. 2021;47(3):3649–3656. doi:10.1016/j.ceramint.2020.09.216
[163] Colombo P, Sglavo V, Pippel E. Joining of reaction-bonded silicon carbide using a preceramic polymer. J Mater Sci. 1998;33(9):2405–2412. doi:10.1023/A:1004312109836
[164] Jiang J, Yan L, Xue Y, et al. Lightweight and thermally insulating polymer-derived SiBCN/SiCnw ceramic aerogel with enhanced electromagnetic wave absorbing performance. Chem Eng J. 2024;482:148878. doi:10.1016/j.cej.2024.148878
[165] Liu J, Wang G, Tong Y, et al. Novel lightweight and efficient electromagnetic waves absorbing performance of biomass porous carbon/polymer-derived composite ceramics. Ceram Int. 2023;49(9, Part A):13742–13751. doi:10.1016/j.ceramint.2022.12.252
[166] Luan X, Chang S, Yu R, et al. Effect of PSO and TiB_2 content on the high temperature adhesion strength of SiBCNO ceramic. Ceram Int. 2019;45(7, Part B):9515–9521. doi:10.1016/j.ceramint.2018.09.229
[167] Luan X, Dong X, Li M, et al. Properties of TiB_2–PSO modified SiHfBCN-based adhesive through polymer-derived-ceramic route. Ceram Int. 2022;48(21):31627–31635. doi:10.1016/j.ceramint.2022.07.084
[168] Hayat A, Sohail M, Hamdy MS, et al. Fabrication, characteristics, and applications of boron nitride and their composite nanomaterials. Surf Interf. 2022;29:101725. doi:10.1016/j.surfin.2022.101725
[169] Roy S, Zhang X, Puthirath AB, et al. Structure, properties and applications of two-dimensional hexagonal boron nitride. Adv Mater. 2021;33(44):2101589. doi:10.1002/adma.202101589
[170] Bernardo E, Colombo P, Dainese E, et al. Novel 3D wollastonite-based scaffolds from preceramic polymers containing micro- and nano-sized reactive particles. Adv Eng Mater. 2012;14(4):269–274. doi:10.1002/adem.201100241
[171] Obaid Saleh R, Olegovich Bokov D, Fenjan MN, et al. Application of aluminum nitride nanotubes as a promising nanocarriers for anticancer drug 5-aminosalicylic acid in drug delivery system. J Mol Liq. 2022;352:118676. doi:10.1016/j.molliq.2022.118676
[172] Wu C, Pan X, Lin F, et al. High-temperature electrical properties of polymer-derived ceramic SiBCN thin films fabricated by direct writing. Ceram Int. 2022;48(11):15293–15302. doi:10.1016/j.ceramint.2022.02.063
[173] Miao Y, Wang G, Gong H, et al. Direct ink writing of SiOC ceramics with microwave absorption properties. Ceram Int. 2023;49(8):12710–12724. doi:10.1016/j.ceramint.2022.12.136

[174] Chen L, Yin X, Fan X, et al. Mechanical and electromagnetic shielding properties of carbon fiber reinforced silicon carbide matrix composites. Carbon N Y. 2015;95:10–19. doi:10.1016/j.carbon.2015.08.011
[175] Guo X, Feng Y, Sun H, et al. Novel electromagnetic metamaterial: polymer-derived SiCN(Fe) ceramics. Ceram Int. 2020;46(17):27634–27640. doi:10.1016/j.ceramint.2020.07.258
[176] Liu D, Zhou Z, Wang Y, et al. Preparation and characterization of polymer-derived SiC ceramic aerogels toward excellent electromagnetic wave absorption properties. J Mater Res Technol. 2022;19:507–519. doi:10.1016/j.jmrt.2022.05.062
[177] Wang S, Ashfaq MZ, Qi D, et al. Electromagnetic wave absorption properties of polymer-derived magnetic carbon-rich SiCN-based composite ceramics. Ceram Int. 2022;48(4):4986–4998. doi:10.1016/j.ceramint.2021.11.036
[178] Liu S, Dai M, Jia Y, et al. Electromagnetic wave-absorbing of polymer derived rod-like ZrB2 ultrahigh-temperature ceramic composites. J Eur Ceram Soc. 2024;44(13):7668–7679. doi:10.1016/j.jeurceramsoc.2024.05.040
[179] Elsayed H, Grigolato L, Savio G, et al. Direct ink writing of silicone/filler mixtures for sphene scaffolds with advanced topologies. Int J Appl Ceram Technol. 2023;20(1):131–140. doi:10.1111/ijac.14168
[180] Zhao W, Shao G, Jiang M, et al. Ultralight polymer-derived ceramic aerogels with wide bandwidth and effective electromagnetic absorption properties. J Eur Ceram Soc. 2017;37(13):3973–3980. doi:10.1016/j.jeurceramsoc.2017.04.068
[181] Liu Y, Feng Y, Gong H, et al. Electromagnetic wave absorption properties of europium-doped SiCN (Fe) polymer-derived ceramics. J Mater Sci: Mater Electron. 2018;29(14):12496–12502. doi:10.1007/s10854-018-9368-6
[182] Zhang Q, Gou Y, Wang J, et al. Preparation and characterization of polymer-derived Zr/Si/C multiphase ceramics and microspheres with electromagnetic wave absorbing capabilities. J Eur Ceram Soc. 2017;37(5):1909–1916. doi:10.1016/j.jeurceramsoc.2017.01.006
[183] Lusha Z, Zicheng T, Tusiime R, et al. Synthesis and electromagnetic wave absorbing properties of a polymer-derived SiBNC ceramic aerogel. Ceram Int. 2021;47(13):18984–18990. doi:10.1016/j.ceramint.2021.03.242
[184] Saadi M, Maguire A, Pottackal NT, et al. Direct ink writing: a 3D printing technology for diverse materials. Adv Mater. 2022;34(28):2108855. doi:10.1002/adma.202108855
[185] Chen Z, Li Z, Li J, et al. 3D printing of ceramics: a review. J Eur Ceram Soc. 2019;39(4):661–687. doi:10.1016/j.jeurceramsoc.2018.11.013
[186] ISO/ASTM. Additive manufacturing — general principles — fundamentals and vocabulary. In: *ISO/ASTM 52900:2021*. International Organization for Standardization: ISO; 2021. p. 14.
[187] Davoudinejad A, Perez LCD, Quagliotti D, et al. Geometrical and feature of size design effect on direct stereolithography micro additively manufactured components. Procedia Struct Integrity. 2018;13:1250–1255. doi:10.1016/j.prostr.2018.12.256
[188] Ambrosi A, Pumera M. 3D-printing technologies for electrochemical applications. Chem Soc Rev. 2016;45(10):2740–2755. doi:10.1039/C5CS00714C
[189] Herzberger J, Sirrine JM, Williams CB, et al. Polymer design for 3D printing elastomers: recent advances in structure, properties, and printing. Prog Polym Sci. 2019;97:101144. doi:10.1016/j.progpolymsci.2019.101144
[190] Guddati S, Kiran ASK, Leavy M, et al. Recent advancements in additive manufacturing technologies for porous material applications. Int J Adv Manuf Technol. 2019;105(1):193–215. doi:10.1007/s00170-019-04116-z
[191] Wickramasinghe S, Do T, Tran P. FDM-based 3D printing of polymer and associated composite: a review on mechanical properties, defects and treatments. Polymers (Basel). 2020;12(7):1529. doi:10.3390/polym12071529
[192] Pagac M, Hajnys J, Ma Q-P, et al. A review of vat photopolymerization technology: materials, applications, challenges, and future trends of 3d printing. Polymers (Basel). 2021;13(4):598. doi:10.3390/polym13040598
[193] Halloran JW. Ceramic stereolithography: additive manufacturing for ceramics by photopolymerization. Annu Rev Mater Res. 2016;46:19–40. doi:10.1146/annurev-matsci-070115-031841
[194] Truxova V, Safka J, Seidl M, et al. Ceramic 3D printing: comparison of SLA and DLP technologies. MM Sci J. 2020;2020:3905–3911. doi:10.17973/MMSJ.2020_06_2020006
[195] Han J, Liu C, Bradford-Vialva RL, et al. Additive manufacturing of advanced ceramics using preceramic polymers. Materials (Basel). 2023;16(13):4636. doi:10.3390/ma16134636
[196] Magazine R, van Bochove B, Borandeh S, et al. 3D inkjet-printing of photo-crosslinkable resins for microlens fabrication. Addit Manuf. 2022;50:102534. doi:10.1016/j.addma.2021.102534
[197] Lupone F, Padovano E, Casamento F, et al. Process phenomena and material properties in selective laser sintering of polymers: a review. Materials (Basel). 2022;15(1):183. doi:10.3390/ma15010183
[198] Shahzad A, Lazoglu I. Direct ink writing (DIW) of structural and functional ceramics: recent achievements and future challenges. Compos B Eng. 2021;225:109249. doi:10.1016/j.compositesb.2021.109249
[199] del-Mazo-Barbara L, Ginebra M-P. Rheological characterisation of ceramic inks for 3D direct ink writing: a review. J Eur Ceram Soc. 2021;41(16):18–33. doi:10.1016/j.jeurceramsoc.2021.08.031
[200] Martin KL, Street DP, Thompson CM, et al. Impact of the backbone structure on the rheological and thermal properties of preceramic polymer-grafted nanoparticles and derived ceramics. ACS Appl Nano Mater. 2022;5(1):446–454. doi:10.1021/acsanm.1c03278
[201] Xiao B, Zheng X, Zhao Y, et al. Controlling shear rate for designable thermal conductivity in direct ink printing of polydimethylsiloxane/boron nitride composites. Polymers (Basel). 2023;15(16):3489. doi:10.3390/polym15163489
[202] Rau DA, Williams CB, Bortner MJ. Rheology and printability: a survey of critical relationships for direct ink write

materials design. Prog Mater Sci. 2023;140:101188. doi:10.1016/j.pmatsci.2023.101188
[203] Janmey PA, Georges PC, Hvidt S. Basic rheology for biologists. Methods Cell Biol. 2007;83:1–27. doi:10.1016/S0091-679X(07)83001-9
[204] M'Barki A, Bocquet L, Stevenson A. Linking rheology and printability for dense and strong ceramics by direct ink writing. Sci Rep. 2017;7(1):6017. doi:10.1038/s41598-017-06115-0
[205] Schwab A, Levato R, D'Este M, et al. Printability and shape fidelity of bioinks in 3D bioprinting. Chem Rev. 2020;120(19):11028–11055. doi:10.1021/acs.chemrev.0c00084
[206] Polychronopoulos ND, Brouzgou A. Direct Ink writing for electrochemical device fabrication: a review of 3D-printed electrodes and Ink rheology. Catalysts. 2024;14:110. doi:10.3390/catal14020110
[207] Wei P, Cipriani C, Hsieh C-M, et al. Go with the flow: rheological requirements for direct ink write printability. J Appl Phys. 2023;134(10):100701. doi:10.1063/5.0155896
[208] Tu Y, Arrieta-Escobar JA, Hassan A, et al. Optimizing process parameters of direct ink writing for dimensional accuracy of printed layers. 3D Print Addit Manuf. 2023;10(4):816–827. doi:10.1089/3dp.2021.0208
[209] Durão LFC, Barkoczy R, Zancul E, et al. Optimizing additive manufacturing parameters for the fused deposition modeling technology using a design of experiments. Prog Addit Manuf. 2019;4:291–313. doi:10.1007/s40964-019-00075-9
[210] Khalid M, Peng Q. Investigation of printing parameters of additive manufacturing process for sustainability using design of experiments. J Mech Des. 2021;143(3):032001. doi:10.1115/1.4049521
[211] Kaliampakou C, Lagopati N, Charitidis CA. Direct ink writing of alginate–gelatin hydrogel: an optimization of Ink property design and printing process efficacy. Appl Sci. 2023;13(14):8261. doi:10.3390/app13148261
[212] Ebers L-S, Laborie M-P. Direct ink writing of fully bio-based liquid crystalline lignin/hydroxypropyl cellulose aqueous inks: optimization of formulations and printing parameters. ACS Appl Bio Mater. 2020;3(10):6897–6907. doi:10.1021/acsabm.0c00800
[213] Xu C, Quinn B, Lebel LL, et al. Multi-material direct ink writing (DIW) for complex 3D metallic structures with removable supports. ACS Appl Mater Interfaces. 2019;11(8):8499–8506. doi:10.1021/acsami.8b19986
[214] Torre M, Giannitelli SM, Mauri E, et al. Additive manufacturing of biomaterials. In: Magagnin L, Rossi F, editors. Advances in chemical engineering. Elsevier; 2021. p. 233–260.
[215] Roy Barman S, Gavit P, Chowdhury S, et al. 3D-printed materials for wastewater treatment. JACS Au. 2023;3(11):2930–2947. doi:10.1021/jacsau.3c00409
[216] Mubarak S, Dhamodharan D, Byun H-S. Recent advances in 3D printed electrode materials for electrochemical energy storage devices. J Energy Chem. 2023;81:272–312.
[217] DiGregorio SJ, Hildreth OJ. Particle-less reactive inks. In: Gupta RK, Nguyen TA, editors. *Smart multifunctional nano-inks*. Elsevier; 2023. p. 125–158.
[218] Lakhdar Y, Tuck C, Binner J, et al. Additive manufacturing of advanced ceramic materials. Prog Mater Sci. 2021;116:100736. doi:10.1016/j.pmatsci.2020.100736
[219] Freeman TB, Foster KEO, Troxler CJ, et al. Advanced materials and additive manufacturing for phase change thermal energy storage and management: a review. Adv Energy Mater. 2023;13(24):2204208. doi:10.1002/aenm.202204208
[220] Pelanconi M, Zavattoni S, Cornolti L, et al. Application of ceramic lattice structures to design compact, high temperature heat exchangers: material and architecture selection. Materials (Basel). 2021;14:3225. doi:10.3390/ma14123225
[221] Fu Y, Xu L, Zhao F, et al. Ultrafast high-temperature sintering of polymer-derived ceramic thick film sensors. Ceram Int. 2024;50(19, Part B):36908–36918. doi:10.1016/j.ceramint.2024.07.078
[222] Xu L, Zhou X, Zhao F, et al. Rapid laser fabrication of indium tin oxide and polymer-derived ceramic composite thin films for high-temperature sensors. J Colloid Interface Sci. 2024;658:913–922. doi:10.1016/j.jcis.2023.12.119
[223] Seo D, Jung S, Lombardo SJ, et al. Fabrication and electrical properties of polymer-derived ceramic (PDC) thin films for high-temperature heat flux sensors. Sens Actuators, A. 2011;165(2):250–255. doi:10.1016/j.sna.2010.11.013
[224] Wu C, Lin F, Pan X, et al. TiB2-Modified polymer-derived ceramic SiCN double-layer thin films fabricated by direct writing for high-temperature application. Adv Eng Mater. 2022;24(10):2200228. doi:10.1002/adem.202200228
[225] Zocca A, Franchin G, Elsayed H, et al. Direct ink writing of a preceramic polymer and fillers to produce hardystonite ($Ca_2ZnSi_2O_7$) bioceramic scaffolds. J Am Ceram Soc. 2016;99(6):1960–1967. doi:10.1111/jace.14213
[226] Dogrul F, Ożóg P, Michálek M, et al. Polymer-derived biosilicate®-like glass-ceramics: engineering of formulations and additive manufacturing of three-dimensional scaffolds. Materials (Basel). 2021;14:5170. doi:10.3390/ma14185170
[227] Yang J, Li B, Liu J, et al. Application of additive manufacturing in the automobile industry: a mini review. Processes. 2024;12:1101. doi:10.3390/pr12061101
[228] Xiong H, Chen H, Zhao L, et al. Sicw/SiCp reinforced 3D-SiC ceramics using direct ink writing of polycarbosilane-based solution: microstructure, composition and mechanical properties. J Eur Ceram Soc. 2019;39(8):2648–2657. doi:10.1016/j.jeurceramsoc.2019.02.045
[229] Kemp JW, Reed JL, Compton BG. Size effects in 3D-printed polymer-derived, zirconium diboride-reinforced ceramic composites. J Am Ceram Soc. 2024;107(3):1557–1570. doi:10.1111/jace.19516
[230] Croom BP, Abbott A, Kemp JW, et al. Mechanics of nozzle clogging during direct ink writing of fiber-reinforced composites. Addit Manuf. 2021;37:101701. doi:10.1016/j.addma.2020.101701
[231] Jin H-Y, Xu H, Qiao G-J, et al. Study of machinable silicon carbide–boron nitride ceramic composites. Mater Sci Eng A. 2008;483–484:214–217. doi:10.1016/j.msea.2006.12.165
[232] Widgeon S, Sen S, Mera G, et al. 29Si and 13C solid-state NMR spectroscopic study of nanometer-scale structure and mass fractal characteristics of amorphous polymer derived silicon oxycarbide ceramics. Chem Mater. 2010;22(23):6221–6228. doi:10.1021/cm1021432

[233] Yang N, Lu K. Effects of transition metals on the evolution of polymer-derived SiOC ceramics. Carbon N Y. 2021;171:88–95. doi:10.1016/j.carbon.2020.08.072
[234] Liu C, Pan R, Hong C, et al. Effects of Zr on the precursor architecture and high-temperature nanostructure evolution of SiOC polymer-derived ceramics. J Eur Ceram Soc. 2016;36(3):395–402. doi:10.1016/j.jeurceramsoc.2015.09.009
[235] Yang N, Lu K. Phase content prediction in polymer-derived ceramics with metal additives. J Am Ceram Soc. 2021;104(10):5379–5391. doi:10.1111/jace.17769
[236] Biasetto L, Franchin G, Elsayed H, et al. Direct ink writing of cylindrical lattice structures: a proof of concept. Open Ceram. 2021;7:100139. doi:10.1016/j.oceram.2021.100139
[237] Suda H, Yamauchi H, Uchimaru Y, et al. Preparation and gas permeation properties of silicon carbide-based inorganic membranes for hydrogen separation. Desalination. 2006;193(1–3):252–255. doi:10.1016/j.desal.2005.04.143
[238] Konegger T, Tsai C-C, Peterlik H, et al. Asymmetric polysilazane-derived ceramic structures with multiscalar porosity for membrane applications. Microporous Mesoporous Mater. 2016;232:196–204. doi:10.1016/j.micromeso.2016.06.027
[239] Pelanconi M, Colombo P, Ortona A. Additive manufacturing of silicon carbide by selective laser sintering of PA12 powders and polymer infiltration and pyrolysis. J Eur Ceram Soc. 2021;41(10):5056–5065. doi:10.1016/j.jeurceramsoc.2021.04.014
[240] El Chawich G, El Hayek J, Rouessac V, et al. Design and manufacturing of Si-based Non-oxide cellular ceramic structures through indirect 3D printing. Materials (Basel). 2022;15:471. doi:10.3390/ma15020471
[241] Kulkarni A, Pearce J, Yang Y, et al. SiOC(N) cellular structures with dense struts by integrating fused filament fabrication 3D printing with polymer-derived ceramics. Adv Eng Mater. 2021;23(12):2100535. doi:10.1002/adem.202100535
[242] Sarraf F, Churakov SV, Clemens F. Preceramic polymers for additive manufacturing of silicate ceramics. Polymers (Basel). 2023;15:4360. doi:10.3390/polym15224360
[243] Barroso GS, Krenkel W, Motz G. Low thermal conductivity coating system for application up to 1000°C by simple PDC processing with active and passive fillers. J Eur Ceram Soc. 2015;35(12):3339–3348. doi:10.1016/j.jeurceramsoc.2015.02.006
[244] Schütz A, Günthner M, Motz G, et al. Characterisation of novel precursor-derived ceramic coatings with glass filler particles on steel substrates. Surf Coat Technol. 2012;207:319–327. doi:10.1016/j.surfcoat.2012.07.013
[245] Li S, Ye F, Cheng L, et al. Porous silicon carbide ceramics with directional pore structures by CVI combined with sacrificial template method. Ceram Int. 2023;49(5):8331–8338. doi:10.1016/j.ceramint.2022.10.360
[246] Chen H, Wang X, Xue F, et al. 3D printing of SiC ceramic: direct ink writing with a solution of preceramic polymers. J Eur Ceram Soc. 2018;38(16):5294–5300. doi:10.1016/j.jeurceramsoc.2018.08.009
[247] Clarkson CM, Wyckoff C, Parvulescu MJS, et al. UV-assisted direct ink writing of Si_3N_4/SiC preceramic polymer suspensions. J Eur Ceram Soc. 2022;42(8):3374–3382. doi:10.1016/j.jeurceramsoc.2022.03.001
[248] Fiocco L, Elsayed H, Badocco D, et al. Direct ink writing of silica-bonded calcite scaffolds from preceramic polymers and fillers. Biofabrication. 2017;9(2):025012. doi:10.1088/1758-5090/aa6c37
[249] Elsayed H, Gardin C, Ferroni L, et al. Highly porous Sr/Mg-doped hardystonite bioceramics from preceramic polymers and reactive fillers: direct foaming and direct ink writing. Adv Eng Mater. 2019;21(6):1800900. doi:10.1002/adem.201800900
[250] Elsayed H, Rebesan P, Crovace MC, et al. Biosilicate® scaffolds produced by 3D-printing and direct foaming using preceramic polymers. J Am Ceram Soc. 2019;102(3):1010–1020. doi:10.1111/jace.15948
[251] Katsuda Y, Gerstel P, Narayanan J, et al. Reinforcement of precursor-derived Si–C–N ceramics with carbon nanotubes. J Eur Ceram Soc. 2006;26(15):3399–3405. doi:10.1016/j.jeurceramsoc.2005.10.014
[252] Rahman A, Singh A, Harimkar SP, et al. Spark plasma sintering and characterization of graphene reinforced silicon carbide nanocomposites. In: Composite Materials and Joining Technologies for Composites, Volume 7: Proceedings of the 2012 Annual Conference on Experimental and Applied Mechanics; Springer; 2013.
[253] Liu H, Li Y, Tang R, et al. 3D printing of polymer-derived graphene/SiCp/SiC composite by direct ink writing. Crystals (Basel). 2025;15:11. doi:10.3390/cryst15010011
[254] Huang K, Elsayed H, Franchin G, et al. 3D printing of polymer-derived SiOC with hierarchical and tunable porosity. Addit Manuf. 2020;36:101549. doi:10.1016/j.addma.2020.101549
[255] Mazo MA, Rubio J. Novel silicon oxycarbide/spodumene glass-ceramic composites with tailored thermal expansion coefficient. J Non-Cryst Solids. 2023;604:122155. doi:10.1016/j.jnoncrysol.2023.122155
[256] Huang S, Zhang J, Fu H, et al. Irradiation performance of high entropy ceramics: a comprehensive comparison with conventional ceramics and high entropy alloys. Prog Mater Sci. 2024;143:101250. doi:10.1016/j.pmatsci.2024.101250
[257] Wang Y, Liu H, Mei D, et al. Direct ink writing of 3D SiC scaffold as catalyst support for thermally autonomous methanol steam reforming microreactor. Renewable Energy. 2022;187:923–932. doi:10.1016/j.renene.2022.02.004
[258] Solís Pinargote NW, Smirnov A, Peretyagin N, et al. Direct ink writing technology (3D printing) of graphene-based ceramic nanocomposites: a review. Nanomaterials. 2020;10:1300. doi:10.3390/nano10071300
[259] Moyano JJ, Mosa J, Aparicio M, et al. Strong and light cellular silicon carbonitride – reduced graphene oxide material with enhanced electrical conductivity and capacitive response. Addit Manuf. 2019;30:100849. doi:10.1016/j.addma.2019.100849
[260] Zhao Y, Zhu J, He W, et al. 3D printing of unsupported multi-scale and large-span ceramic via near-infrared assisted direct ink writing. Nat Commun. 2023;14(1):2381. doi:10.1038/s41467-023-38082-8
[261] Zhao Y, Shi G, Miao J-T, et al. UV assisted 3D fabrication of hollow ceramic with single-channel direct ink writing.

J Eur Ceram Soc. 2024;44(12):7398–7404. doi:10.1016/j.jeurceramsoc.2024.04.069

[262] He X, Wang R, Qi S, et al. Vat photopolymerization 3D printing of polymer-derived SiOC ceramics with high precision and high strength. Addit Manuf. 2023;78:103889. doi:10.1016/j.addma.2023.103889

[263] He R, Ding G, Zhang K, et al. Fabrication of SiC ceramic architectures using stereolithography combined with precursor infiltration and pyrolysis. Ceram Int. 2019;45(11):14006–14014. doi:10.1016/j.ceramint.2019.04.100

[264] Xiong S, Liu J, Cao J, et al. 3D printing of crack-free dense polymer-derived ceramic monoliths and lattice skeletons with improved thickness and mechanical performance. Addit Manuf. 2022;57:102964. doi:10.1016/j.addma.2022.102964

[265] Schmidt J, Brigo L, Gandin A, et al. Multiscale ceramic components from preceramic polymers by hybridization of vat polymerization-based technologies. Addit Manuf. 2019;30:100913. doi:10.1016/j.addma.2019.100913

[266] Yazdani Sarvestani H, Lacelle T, Sohrabi-Kashani A, et al. 3D-printed polymer-derived ceramics with tunable cellular architectures. Appl Mater Today. 2024;39:102327. doi:10.1016/j.apmt.2024.102327

[267] Kim S, Biju C, Karunarathna MS, et al. Tuning crosslinking of hybrid preceramic polymers in vat photopolymerization toward controlled ceramic yields. Chem Eng J. 2024;499:156585. doi:10.1016/j.cej.2024.156585

[268] Young JC, Brinckmann SA, Fertig RS, III, et al. Influence of layer thickness and exposure on mechanical properties of additively manufactured polymer-derived SiOC ceramics. Open Ceram. 2024;19:100652. doi:10.1016/j.oceram.2024.100652

[269] Su R, Chen J, Zhang X, et al. 3D printed SiOC architecture towards terahertz electromagnetic interference shielding and absorption. Chem Eng J. 2024;498:155689. doi:10.1016/j.cej.2024.155689

[270] Wyatt BC, Nemani SK, Hilmas GE, et al. Ultra-high temperature ceramics for extreme environments. Nat Rev Mater. 2024;9(11):773–789. doi:10.1038/s41578-023-00619-0

[271] Feilden E, Glymond D, Saiz E, et al. High temperature strength of an ultra high temperature ceramic produced by additive manufacturing. Ceram Int. 2019;45(15):18210–18214. doi:10.1016/j.ceramint.2019.05.032

[272] Chen H, Liu Y, Balabani S, et al. Machine learning in predicting printable biomaterial formulations for direct ink writing. Research. 2023;6:0197. doi:10.34133/research.0197

[273] Shi X, Sun Y, Tian H, et al. Evaluation of direct ink write processing parameter window via machine learning. Mater Today Commun. 2024;38:108185. doi:10.1016/j.mtcomm.2024.108185

[274] Thummalapalli SV, Patil D, Ramanathan A, et al. Machine learning–enabled direct ink writing of conductive polymer composites for enhanced performance in thermal management and current protection. Energy Storage Mater. 2024;71:103670. doi:10.1016/j.ensm.2024.103670

[275] Erb D, Lu K. Effect of additive structure and size on SiO_2 formation in polymer-derived SiOC ceramics. J Am Ceram Soc. 2018;101(12):5378–5388. doi:10.1111/jace.15876

[276] Jia Y, Yang N, Xu S, et al. Polymer-derived SiOC reinforced with core–shell nanophase structure of ZrB_2/ZrO_2 for excellent and stable high-temperature microwave absorption (up to 900°C). Sci Rep. 2023;13(1):267. doi:10.1038/s41598-023-27541-3

[277] Key TS, Wilks GB, Parthasarathy TA, et al. Process modeling of the low-temperature evolution and yield of polycarbosilanes for ceramic matrix composites. J Am Ceram Soc. 2018;101(7):2809–2818. doi:10.1111/jace.15463

[278] Jana P, Santoliquido O, Ortona A, et al. Polymer-derived SiCN cellular structures from replica of 3D printed lattices. J Am Ceram Soc. 2018;101(7):2732–2738. doi:10.1111/jace.15533

[279] Altun AA, Ertl F, Marechal M, et al. Additive manufacturing of lunar regolith structures. Open Ceram. 2021;5:100058. doi:10.1016/j.oceram.2021.100058

[280] Cesaretti G, Dini E, De Kestelier X, et al. Building components for an outpost on the lunar soil by means of a novel 3D printing technology. Acta Astronaut. 2014;93:430–450. doi:10.1016/j.actaastro.2013.07.034

[281] Jakus AE, Koube KD, Geisendorfer NR, et al. Robust and elastic lunar and martian structures from 3D-printed regolith inks. Sci Rep. 2017;7(1):44931. doi:10.1038/srep44931

[282] Ma S, Fu S, Wang Q, et al. 3D printing of damage-tolerant martian regolith simulant-based geopolymer composites. Addit Manuf. 2022;58:103025. doi:10.1016/j.addma.2022.103025

[283] Ma S, Jiang Y, Fu S, et al. 3D-printed lunar regolith simulant-based geopolymer composites with bio-inspired sandwich architectures. J Adv Ceram. 2023;12(3):510–525. doi:10.26599/JAC.2023.9220700

[284] Toklu YC, Akpinar P. Lunar soils, simulants and lunar construction materials: an overview. Adv Space Res. 2022;70(3):762–779. doi:10.1016/j.asr.2022.05.017